EXPERIMENTAL INVESTIGATION OF ROTARY TURNING PROCESSES FOR
METAL ALLOYS

by

UTKU OLGUN

Submitted to the Graduate School of Engineering and Natural Sciences

in partial fulfillment of the requirements for the degree of
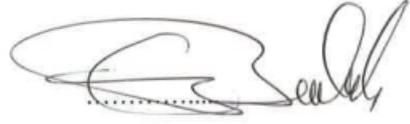
Master of Science

Sabancı University

August 2013

EXPERIMENTAL INVESTIGATION OF ROTARY TURNING PROCESSES FOR METAL ALLOYS

APPROVED BY:

Prof.Dr. Erhan Budak

(Thesis Advisor)

Assoc.Prof.Dr. Barış Balcıoğlu

Assoc.Prof.Dr. Volkan Patoğlu

Assoc.Prof. Dr. Güvenç Şahin

Assoc.Prof.Dr. Mehmet Yıldız

DATE OF APPROVAL   13.08.2013

ABSTRACT

The demand of aerospace, defence, medical and chemical industries to special alloys have been increasing recently in application requiring high performance. Ability to retain their high mechanical and chemical properties even at elevated temperatures makes superalloys such as ni-base, ti-base, co-base, ideal for use in these industries. Even though machining is one of the important production methods of these alloys, these alloys show formidable challenges to cutting tools. Due to their unique inherent properties, cutting tools expose to higher cutting temperatures and higher stresses during process resulting premature failure, hence these alloys are called difficult to machine alloys. As a result, machining of these alloys with conventional processes is unproductive, time consuming and costly. Rotary turning processes can be a good solution for machining these superalloys. Rotational motion of cutting insert around its axis during process provides fresh portion of cutting edge to cutting region continuously. As a result, generated heat is dissipated around cutting edge and heating of a particular portion of tool is prevented. This reduces the thermally activated wear mechanism on cutting edge resulting prolonged tool life and increasing machinability of these alloys.

The main aim of this thesis is to understand the performance of self-propelled rotary turning (SPRT) and actively driven rotary turning (ADRT) tools on metals especially for difficult to cut alloys. Tool life, generated forces, surface roughness and circularity of workpiece are analyzed for various cutting and cooling conditions for rotary turning processes. The effects of tool inclination angle, tool velocity and cooling conditions on tool wear behavior are examined for ADRT process. Then these results are compared with conventional turning process results to see the process advantages. Tool rake face temperature measurements are conducted for ADRT process for various materials in order to correlate the tool life results with cutting temperature. In addition, the difference in performance of SPRT and ADRT is analyzed for the same testing materials and cutting conditions.

Key Words: Machining, Self-Propelled Rotary Turning, Actively Driven Rotary Turning, Tool Life, Tool Temperature Measurement.

ÖZET

Havacılık, savunma, medikal ve kimyasal endüstrilerin yüksek performans gerektiren uygulamaları için özel alaşımlara ihtiyaçları son yıllarda artış göstermektedir. Mekanik ve kimyasal özelliklerini yüksek sıcaklıklarda bile korumaları bu malzemelerin popularitesini artırmıştır. Talaşlı imalat bu alaşımlar için önemli işleme süreçlerinden biri olsa da bu alaşımların üstün özelliklerinden ötürü kesici takımlar yüksek sıcaklıklara ve yüksek gerilmelere maruz kalmaktadır. Bu durum takımların zamansız işgörmesine sebep olduğu gibi verimin düşmesine, kesme zamanının ve maliyetin artmasına sebep olmaktadır. Dönel tornalama süreçleri bu alaşımların işlenebilirliğini arttırması açısından güzel bir çözüm olabilir. Kesici takım dönme hareketi, kesici takımın hep aynı bölgesinin kesme işlemine maruz kalmasını engeller ve oluşan ısının tüm kesme kenarına yayılmasını sağlar. Bu sayede termal olarak aktif olan takım aşınması azalırken takım ömrü ve malzeme işlenebilirliği artar.

Bu tezin en önemli amacı Kendiliğinden Hareketli Dönel Tornalama (KHDT) ve Tahrikli Dönel Tornalama (TDT) takımlarının değişik malzemeler ve değişik koşullar üzerinde performanslarının karşılaştırılmasıdır. Takım ömrü, kesme kuvvetleri, yüzey kalitesi ve iş parçası yuvarlaklığı dataları değişik kesme koşulları ve değişik soğutma koşulları için toplanmış ve konvensiyonel tornalama sonuçlarıyla kıyaslanmıştır. TDT için, takım eğikliğinin, takım hızının ve soğutma koşullarının takım ömrüne etkisi incelenmiştir. Aynı şekilde, TDT için, takım talaş akma yüzeyi üzerinde oluşan sıcaklık dağılımı ölçülmüş ve takım aşınması sonuçlarıyla karşılaştırılmıştır. KHDT ve TDT takımlarının performansları ayrıca değişik test malzemeleri ve değişik kesme koşulları üzerinde incelenmiş ve ilginç sonuçlara ulaşılmıştır.

Anahtar Kelimeler: Talaşlı İmalat, Kendiliğinden Hareketli Dönel Tornalama, Tahrikli Dönel Tornalama, Takım Ömrü, Takım Sıcaklık Ölçümü.

To my family...

ACKNOWLEDGEMENTS

First of all, I would like to express my sincere gratitude to my research supervisor Prof. Dr. Erhan Budak for his guidance, support, encouragement and helpful advice throughout the course of this research.

I would also like to announce my intimate appreciation to Manufacturing Research Laboratory (MRL) for the use of their manufacturing facilities and resources. I would like to thank to Dr. Emre Özlü, Dr. Lütfi Taner Tunç and Ömer Mehmet Özkırımlı for the academic and technical discussions, without their help and support, it was impossible to finish this thesis. My colleques Deniz Aslan, Esma Baytok, Umut Karagüzel, Ceren Çelebi, Emre Uysal and Mehmet Emre Kara were always together with me during my master study. Warm and funny conversations during coffee breaks and their moral supports helped me to finish this thesis on time. I also appreciate Mehmet Güler and Süleyman Tutkun for helping preparations of the experiments.

I am also obliged to sweet Nurşen Aydın, Canan Çapa, Ayşe Melis Deniz, İlke Gören, Gözde Çobanoğlu, Mehmet Ali Araz, Ali Macit Mercan and Ahmet Mavuş for always being with me during my research. Their emotional support, inspiration and encouragements were very special to me and helped me to finish this thesis.

I deeply appreciate my friends in FENS 1021 office, Umman Mahir Yıldırım, Gülnur Kocapınar, Semih Atakan, Ceyda Sol, Selma Yılmaz, Fardin Dashty Saridarq, Gülfidan Karataş, Merve Keskin, Ezgi Aylı, Özge Arabacı, Saime Burçe Özler and Birgül Salihoğlu for always being with me during my research and for all the things and time we shared together.

The last but not the least, I cannot come close to expressing my sincere gratitude to my family. My father İlhan Olgun and my mother Figen Olgun always encouraged and supported me during my whole life. Their pray, motivations and sacrifices were very important to me in completing my studies in my hardest times. Their hearts and souls have enlightened my path all along the way to my righteousness and being an improved man.

TABLE OF CONTENTS

LIST OF FIGURES

LIST OF TABLES

CHAPTER 1 INTRODUCTION

Manufacturing, combination of two Latin origin words "Manus" meaning "Hand" and "Factus" meaning "Made/Fashioned", is the process of converting raw materials, components or parts into finished goods on large scale for use or sale using labor and machine, tools, chemical and/or biological processing and/or formulation. Manufacturing started some 6000 years ago and up to now several different processes and operations such as casting, forming, machining, welding, powder metallurgy, heat treatment were invented to produce valuable goods.

Machining is one of the significant methods in today's manufacturing world. It is material removal process to shape raw materials or near net shape parts to desired geometry where tight tolerances and finishes are required by using chip formation. Chips are produced by shearing mechanism by using cutting tool that is harder and stronger than work piece material. The biggest part of industry belongs to metal cutting that is the subject of this thesis. Conventional operations, turning, milling, broaching, drilling, grinding, etc. and non-traditional operations, EDM, LBM, EBM, etc are the basic metal cutting operations.

The demand within aerospace and defence industries towards lighter, stronger and more heat resisting materials has resulted in that traditional materials, steel, cast iron, are replaced by high performance materials, metal matrix composites, super alloys [1-3]. Due to better mechanical and low thermal properties, to machine these newly developed materials is problematic; such that it is very difficult, time consuming, costly and most significantly unproductive. The reasons behind the scene are the generated high temperatures and high pressure during the operation [2-5].

Almost %95 of mechanical energy coming from shearing and friction mechanisms is converted into heat during operation. A significant portion of generated heat flows into the chip, the rest of it dissipates into the tool and workpiece. This results in an increase in temperature of tool and work piece. High process temperature causes thermal softening of workpiece material with less generated forces that is desirable. On the

other hand, excessive temperatures also soften the cutting edge of tool leading to permanent deformation at the contact zone. This situation is very critical especially for materials with unfavorable thermal properties, since due to low conduction properties, most of the heat goes into the cutting tool on behalf of chip. This accelerates thermally active wear on tool. Tool wear adversely affects the accuracy and integrity of generated surface. Hence, cost of tooling and load/unload time increase, productivity decreases as a consequence of excessive temperatures at tool tip.

Many investigations about tool materials and cooling techniques have been made in order to reduce tool tip temperature. Hot hardness, lubricious, thermal and chemical stability even at elevated temperatures are the features for cutting tool materials used for machining aerospace alloys. Coated carbides, ceramics, CBN/PCBN tools are generally used to machine these alloys [2, 4, 6-8]. In addition to cutting tools, coolants are helpful to decrease tool tip temperature by moving heat from cutting zone. However, at high cutting speeds, penetration of coolants to cutting zone is limited and the usage of coolants cause environmental and health problems. Minimum quantity of liquid (MQL) can be a solution with application of small amount of oil and water with compressed air directed tool edge with a nozzle [9]. On the other hand, mist generation inspires hazardous health problems to operators. In cryogenic cooling, liquid nitrogen (LN2) is used as coolant, yet the ice formation on surface can lead damage on surface and ruin surface integrity [10].

The last but not the least rotary cutting tools can be a solution for generated excessive cutting temperatures. Rotary turning is specialized turning process such that round insert rotates continuously about its own axis during metal cutting. Each portion of cutting edge is in contact with the workpiece for a short period of time, followed by a longer period of time for cooling. Cutting edge cools down and fresh portion of edge is engaged with the work piece continuously. Insert rotation distributes the generated thermal energy to whole cutting edge resulting lowered cutting temperatures and uniformly distributed flank wear without crater wear. Rotary turning process provides a large effective rake angle without sacrificing tool tip strength. These tools transport cutting fluids to cutting region effectively. Moreover, without increasing cutting velocity, chip flow velocity can be enhanced. It is expected that this process increases machinability and productivity of alloys especially difficult to machine alloys. There are two types of rotary turning tools which are Self-Propelled Rotary Turning (SPRT)

tool and Actively Driven Rotary Turning (ADRT) tool as seen in Figure **1**-**1**a and Figure **1**-**1**b, respectively. In SPRT, tool rotation is caused by the action of workpiece with cutting tool. Tool should be inclined at an angle with respect to workpiece so generated cutting force propels cutting tool. However, rigidity of tool is a big problem for this process such that it is difficult to maintain a stable cutting with these tools. Moreover, tool velocity cannot be adjusted freely and it is dependent to tool inclination angle and workpiece velocity.
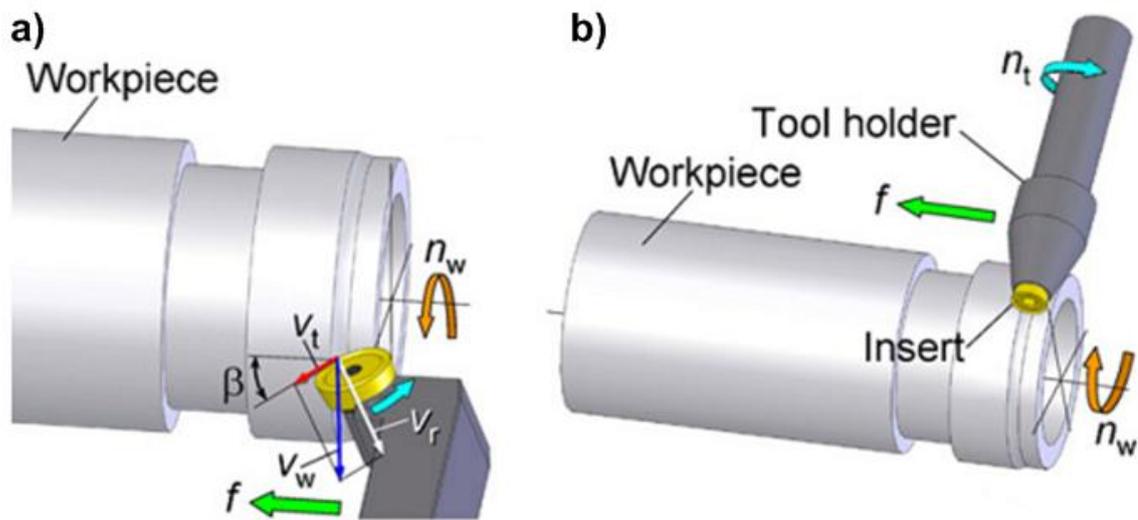
Figure 1-1: Types of rotary turning tools a) SPRT b) ADRT [35].

In ADRT process, an external power source is utilized to propel round insert such that tool circumferential velocity and tool position can be adjusted freely from workpiece velocity and geometry. Despite its potentialities on machinability of difficult to cut machine this process could not be applied to real production process due to some reasons. In first researches, conventional turning centers lack in stiffness and rigidity were utilized to apply this process. Numerical control systems were not sophisticated to provide tool velocity, tool inclination angle and tool position with respect to workpiece. However, with the development of multi-tasking machining centers, the application of ADRT process to real production processes is possible. These machining centers are rigid and their milling head can be positioned with developed software.

1.1 Literature Survey

Even though the rotary turning process is not a novel issue, the publications were limited up to a few decades. First articles were about self-propelled rotary turning

process since in order to study actively driven rotary turning tools effectively and experimentally, specialized machining centers were required.

The history of rotary turning process dates back to 1866 when James Napier foresaw the advantages of process in the manner of tool life and productivity. After his invention, there were a few studies in Soviet Russia, yet the details could not be reached.

Studying kinematics and mechanics of this process is a key factor to gain deep understanding of this operation. Shaw [11] showed the equivalency between rotary turning process and classical oblique cutting process kinematically and mechanically. It is also stated that reduction of required power with lowered cutting temperature can be achieved with increasing tool inclination angle. Armarego et. al. [12, 13] modeled and simulated the rotary cutting processes based on thin shear zone cutting model. Operation is represented as equivalent classical oblique cutting process with chip transportation with no additional energy due to tool rotational motion. In order to predict forces, power and chip flow properties, data from orthogonal tests are required. Venuvinod et al. [14] studied the kinematics and mechanics of ADRT tools. It is stated that at higher tool rotational velocities, shear angle achieves and chip thickness ratio reduces due to eased friction conditions. Venuvinod and Rubenstein [15] used a cutting data taken from conventional oblique cutting tests with a tool having same rake as that of the rotary tool in order to find out chip flow angles and cutting force components of ADRT process by applying a general principle of equivalent obliquity. Choi and Dornfeld [16] indicated that the rotary turning process and classical cutting processes are kinematically equivalent, on the other hand, chip formation mechanisms differ from each other due to friction conditions. According to their hypothesis, chip flow angle for rotary cutting operation is a function of that for classical cutting operation found experimentally such that force components, shear and friction angles can be estimated depending on that function. Armarego and Katta [17] modeled the forces, power and chip flow angle of SPRT tool in turning operations based on "Unified Mechanics of Cutting Approach". Basic data of tool-work piece couple such as shear angle, friction angle, force coefficients should be known from orthogonal cutting tests to predict the forces, power and chip flow angle. Li and Kishawy [18] extended the force model for orthogonal cutting to model the generated cutting forces for SPRT process using Oxley's analysis for tube-end cutting. Hao et al. [19] estimated cutting forces of SPRT

tools using artificial neural networks using two algorithms; back propagation (BP) and hybrid of genetic algorithm (GA). Even though the rotary turning process is complicated mechanically and kinematically due to tool motion, their approach reduces the complexness of operation. Kishawy et al. [20] modeled the chip flow angle for SPRT tools during tube cutting by dividing the undeformed chip into finite elements. After each element's chip flow direction is calculated, absolute chip flow angle is estimated using transformation matrices. Chang et al. [21] modeled a tool rotary velocity and feed rate equation using geometric relations in order to achieve good surface quality. Harun et al. [22] studied the effects of tool holder inclination angle and tool offset height on cutting mechanics of turning with ADRT tools.

Tool wear is one of the challenging parameters in machining operations that limits the machinability of materials and productivity directly. In rotary turning operations whole cutting edge is in cutting zone with uniformly distributed wear on cutting edge. There are lots of studies about the advantages of rotary turning tools in tool wear compared to stationary turning operations for various materials. Kishawy et al. [23] modeled the SPRT tool wear for hard turning processes implementing Dawson and Kurfess's wear model using genetic algorithm with various cutting tests. It is concluded from model that cutting speed and feed have almost the same influence on tool wear. Joshi et al. [24]modeled the rotary tool wear on intermittent machining utilizing Taguchi method to understand the effects of feed rate, cutting velocity, and tool inclination angle. Chen [25] evaluated the performance of SPRT tools on Al/SiC-MMC and compared with conventional fixed round and square tools. Test results show that rotary cutting tools exhibit longer tool life, less tool wear rate and distributed flank wear over entire cutting edge compared to fixed tools. Tool inclination angle affects the tool life in a positive way. Wang et al. [26] and Ezugwu et al. [27] evaluated the SPRT tools with IMI318 and Inconel alloys. Extended tool life by more than 60 times compared to fixed tools with lowered cutting temperatures is obtained from cutting tests for SPRT tools. Thermal fluctuation and thermal fatigue cause excessive chipping, cracks and welding in SPRT process. Tool wear is statistically modeled and it was found that 97% of tool wear is related with cutting speed, feed and inclination angle of tool Kuroda et al. [28] investigated the efficiency of SPRT tools in Inconel and SUS304. Longer tool life is achieved with reduced cutting forces and temperatures. Due to stability problems, surface quality is not at a required level. Manna and Bhattacharyya [29] evaluated the

SPRT tool and compared with fixed rhombic, circular and square tools for Al/SiC-MMC tests. SPRT tooling system gives best tool wear results with no built-up edge on tool. On the other hand, poorest surface roughness values were observed in cutting tests. This is because of large nose radius, greater radial force component and less stiffness of tooling system. Kishawy et al. [30] investigated the performance of SPRT tool in Waspaloy and titanium alloys. Uniformly distributed flank wear is the main tool failure phenomena in SPRT process. Surface scratches (grooves) obtained SPRT process are in direction of effective cutting velocity. Ezugwu [31] studied the machining of aero-engine alloys using SPRT tools. He implies that oxide films that prevent adhesion and diffusion are produced in SPRT process due to short tool engagement time with workpiece. Smearing action between tool and work piece reduces the feed rate effect on surface quality. Kossakowska and Jemielniak [32] evaluated the performance of SPRT tools for turning of difficult to cut materials. Tool run-out, work piece chatter and chip adhesion are the main parameters affecting machined surface quality. Lei and Lui [33] investigated the effects of ADRT process for tool wear and cutting forces in titanium cutting. It is stated that tool strength, rigidity, and dynamic run-out problems directly affect the surface quality and vibration. There is an optimum tool speed in the manner of cutting temperature due to heating and cooling time problems of tool. Nakajima et al. [34] examined the effects of ADRT tools compared with SPRT tools during SUS304 stainless steel cutting. It is stated that ADRT tools are more suitable than SPRT tools for high speed cutting due to wear rates on tools. Hosokawa et al. [35] investigated the ADRT tools in stainless steels and Inconel with dry and MQL cutting. Small and uniform wear without chipping on tool edge was observed in both cooling conditions.

In metal cutting, the generated heat is directly affects the workpiece and tool mechanically and physically. At that point studies about heat generation and temperature measurement for rotary turning process are very significant to understand this mechanism ant its effects. Chen [36] modeled the heat generation for SPRT process using moving heat source approach. Cutting tests results show that SPRT tools provide lower cutting temperatures in both MMCs and Ti alloy compared to fixed tools. Both model and experimental results reveal that contact zone temperature is cooled down to neighborhood of ambient temperature. Dessoly et al. [37] modeled the chip and tool temperature on SPRT process by adding the convective flux term for tool rotation to the conduction term. An IR camera is utilized to measure the chip and tool temperatures.

6

Predicted and measured results show good correlation for heating and cooling behavior of tool during operation. Sasahara et al. [38] investigated the effects of tool inclination angles of ADRT tools in Inconel and SUS304 steel. It was found that higher cutting speed with lower tool inclination angle can be the optimum for lower cutting temperatures due to lower heat partitioning and lower cutting forces. Harun et al. [39]modeled thermal behavior of ADRT process using one-dimensional unsteady heat transfer theory. It is concluded that there should be an optimum rotary tool velocity for heating and cooling time of tool. Higher tool inclination angle enhances cutting temperature reduction during cutting. Yamamoto et al. [40] investigated the thermal behavior of ADRT process. It is found that heat capacity and velocity of tool have influence on thermal behavior of process. Larger tools provide lower cutting temperatures due to higher heat capacity. Hosokawa et al. [35] stated that a raise in tool rotational speed reduces temperature due to intermittent heat cycle. However, at higher cutting velocities, the heat caused by the friction between tool and chip seems to be significant causing tool temperature to increase.

1.2 Objective

The objective of this master thesis is to enhance the knowledge and understanding of rotary turning processes. Rotary turning process can be a remedy to machine difficult to cut alloys. Investigation of tool wear and tool life compared to conventional turning, especially for difficult to cut alloys, is one of the main objective of this thesis. Effects of tool inclination angle and tool velocity on tool life are investigated. Analyzing the effect of cooling types on tool life for various processes is one of the main purposes of thesis. Surface quality is one of the essential parameters in industry defining productivity. In this thesis, surface quality and circularity of machined parts for various cutting processes are examined, especially, for tool velocity and tool inclination angle of ADRT process. Generated component forces for various processes are monitored to see the effect of processes on forces. Cutting temperatures and temperature variations on tool rake face are investigated to understand the effects of tool inclination angle and tool velocity on generated temperatures during cutting.

1.3 Organization of Thesis

This thesis is divided into 6 chapters. After this introductory Chapter 1, kinematics and mechanics of conventional and rotary turning processes is presented in Chapter 2. Experimental procedure about cutting tests is explained in Chapter 3 with machining centers, cutting tools, testing materials and measurement devices. Chapter 4 includes the cutting test results of SPRT process and conventional turning process. In Chapter 5, ADRT process results are presented. Temperature measurements of cutting tool of ADRT process is given in Chapter 6. In Chapter 7, cutting tests and temperature results are discussed and conclusions obtained from this study are presented. Conclusions and future works about rotary turning are given in Chapter 8.

CHAPTER 2 KINEMATICS AND MECHANICS OF ROTARY TURNING PROCESSES

2.1 Fundamentals of Rotary Cutting Process and Equivalence with Classical Cutting Processes

When rotary turning is taken into consideration, it is pretty obvious that this process is more complex compared to classical cutting processes, since both workpiece and cutting tool rotate about their own axes during cutting. In studying this process, machining a tube shape workpiece is utilized in order to understand the fundamentals of this process and to provide a correlation between classical cutting processes. Figure 2-1 presents the rotary tool cutting processes for the tube cutting.
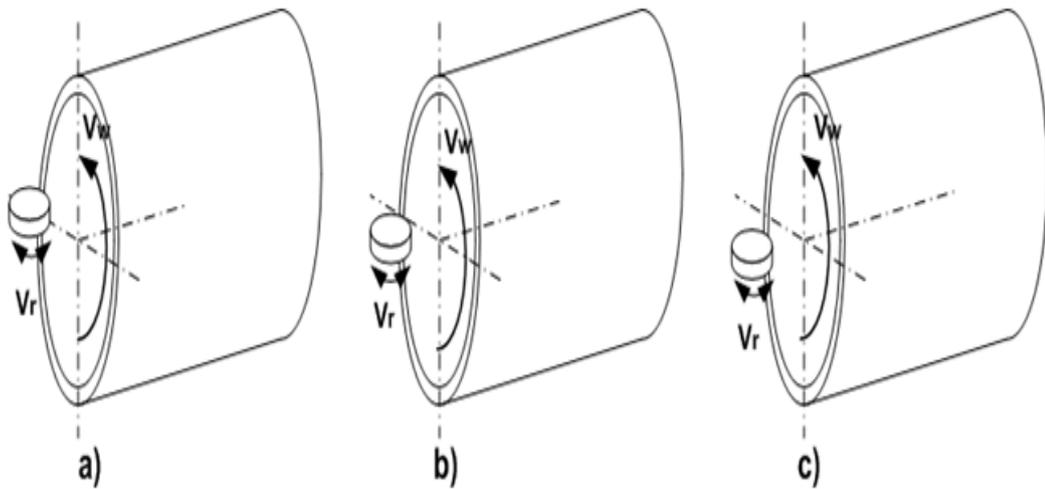
Figure 2-1: Rotary tool cutting processes on tube cutting.

In order to gain understanding of fundamentals of rotary cutting process, some assumptions are made [12];

- Tool and workpiece diameters are large compared to workpiece thickness so that the curvature of tool insert can be neglected.
- Feed velocity, V_f, is negligible compared to workpiece velocity, V_w.
- Since the tube thickness is undersize, V_w is taken as constant across tube thickness.
- Orientation of V_w with respect to plane normal to tool cutting edge is dependent on tool position on workpiece rotation axis.

When the rotary tool is set as in Figure 2-1a and the tool rotates by an action of motor power, the process is called as driven oblique rotary tool cutting and it can be simulated as in Figure 2-2.
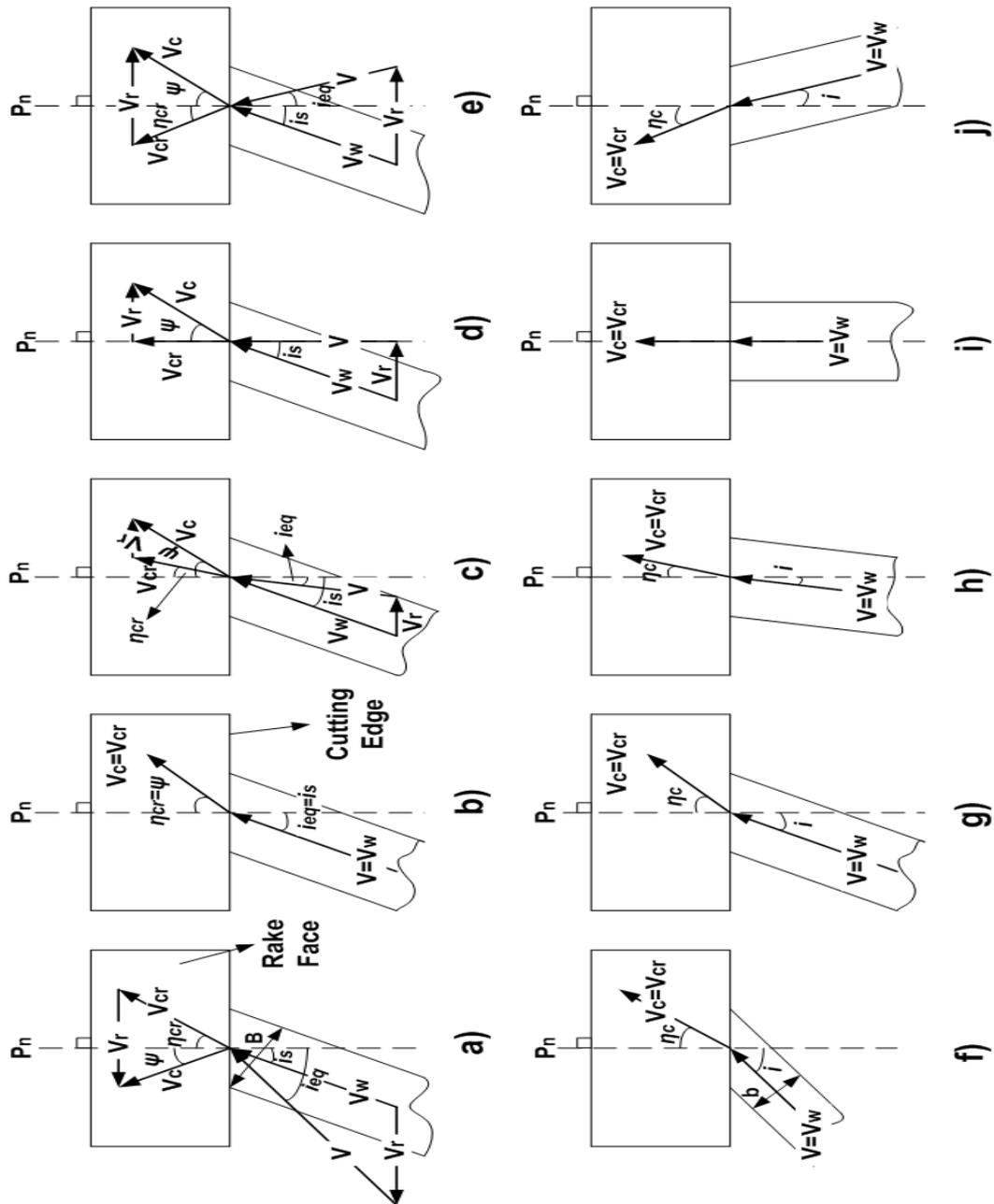
Figure 2-2: Simulation of actively driven oblique rotary tool cutting and equivalent classical processes.

If the rotary tool is set as in Figure 2-1b and an external power source provides tool motion, the process is called as driven orthogonal rotary tool cutting and it can be simulated as in Figure 2-3.
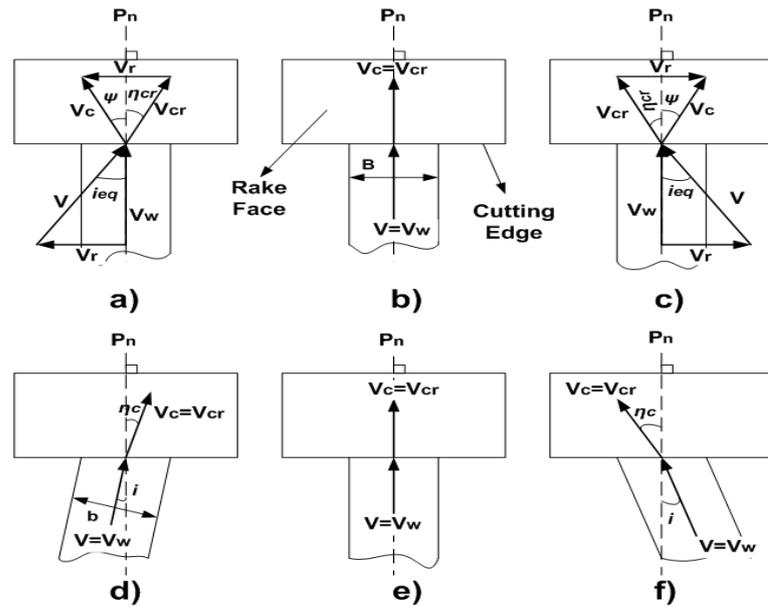
Figure 2-3: Simulation of actively driven orthogonal rotary tool cutting and equivalent classical processes.

When tool is set as in Figure 2-1a or Figure 2-1c and tool rotates by the action between tool and workpiece, the process is called self-propelled rotary tool cutting and it can be simulated as in Figure 2-4.
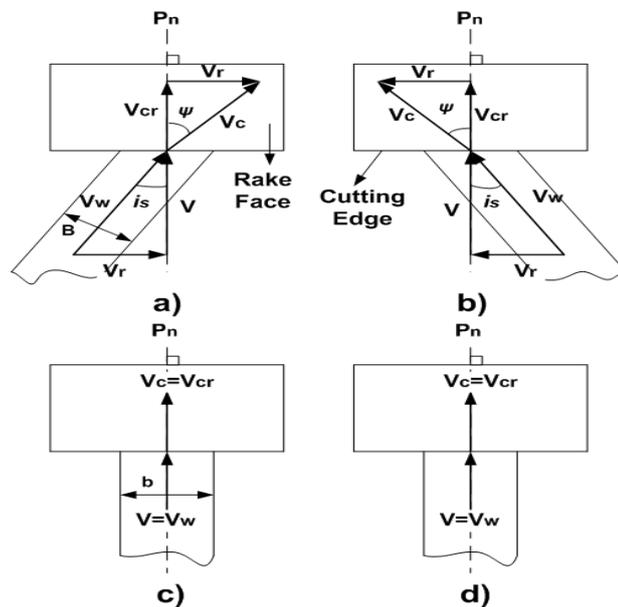
Figure 2-4: Simulation of self propelled rotary tool cutting and equivalent classical processes.

In Figure 2-2, Figure 2-3 and Figure 2-4, P_n, V_w, V, V_r, V_{cr}, V_{cr}, i_s, i_{eq}, η_c, η_{cr}, ψ represent the plane normal to the cutting edge, workpiece velocity, resultant (equivalent) velocity, rotary tool velocity, relative chip flow velocity, absolute chip

flow velocity, static inclination angle (angle between V_w and P_n), equivalent inclination angle (angle between V and P_n), chip flow angle, relative chip flow angle and absolute chip flow angle, respectively. From figures, V and i_{eq} can be found by using simple geometric relations [12];

$$V = \sqrt{(V_w * \cos i_s)^2 + (V_r + V_w * \sin i_s)^2} \qquad (2\text{-}1)$$

$$\tan i_{eq} = \frac{V_r + V_w * \sin i_s}{V_w * \cos i_s} \qquad (2\text{-}2)$$

Then, these relations between $V_w - V$ and $V_c - V$ can be seen easily;

$$V_w * \cos i_s = V * \cos i_{eq} \qquad (2\text{-}3)$$

$$\frac{V_r}{\sin(i_{eq} - i_s)} = \frac{V}{\sin(90 + i_s)} = \frac{V}{\cos i_s} \qquad (2\text{-}4)$$

The major variable in rotary tool cutting is rotary tool velocity. The effect of rotary tool velocity on kinematics of process can be understood from figures shown above. Without alteration the magnitude and direction of V_w, just changing the magnitude and/or direction of V_r results changes in magnitudes and directions in V, V_{cr}, V_c and obviously related cutting angles.

For actively driven rotary tool, V_r is controlled by a power source and obviously its direction and magnitude can be adjusted freely from V_w and i_s. On the other hand, for self-propelled rotary tool, V_r is achieved by the relation between tool and workpiece. Direction and magnitude of V_r are function of V_w and i_s.

In Figure 2-2, tool is positioned above the workpiece axis as a result V_w and B are inclined to the P_n by static inclination angle i_s. Addition of tool rotary velocity, V_r, introduces resultant velocity, V, at an angle i_{eq} to the P_n. In Figure 2-2a, tool and workpiece rotate in different directions, CW and CCW respectively. Addition of rotary tool velocity, V_r to process increases V and i_{eq}, such that process becomes more oblique. As a result, relative chip flow velocity, V_{cr} and relative chip flow angle, η_{cr} can be estimated as in Figure 2-2a due to tool obliquity. However, from an observer's point of view chip emerges with absolute chip flow velocity, V_c and absolute chip flow angle, ψ, this is likely due to chip transportation by moving tool in the direction of V_r.

Interestingly, V and V_c are in same side of P_n. Figure 2-2f is expressed as the equivalent classical oblique cutting of Figure 2-2a.

In Figure 2-2b, tool rotation is considered as 0 meaning that tool is stationary. In that case driven oblique tool cutting process is well identical to classical oblique cutting process, as seen in Figure 2-2g, since there is no effect of V_r on process.

In Figure 2-2c-d-e, tool and workpiece rotate in the same direction, CCW, only the magnitude of V_r differs for these cases. In Figure 2-2c, V_r reduces the V and i_{eq}, such that $i_s > i_{eq} > 0$. In that case, the direction of V_c also changes due to reversed V_r. Figure 2-2h shows the equivalent classical oblique cutting of Figure 2-2c. In Figure 2-2d, V_r is increased such that it makes the process orthogonal cutting, V is reduced to a minimum value and i_{eq} is equated to 0. However, as seen in figure, V_c and ψ increase due to different magnitude of V_r compared to Figure 2-2c. A more increase in V_r changes the direction of V as seen in Figure 2-2e. i_s-i_{eq} and η_{cr}-ψ become in different signs. It can be again considered as classical oblique cutting as seen in Figure 2-2j.

In Figure 2-3, rotary tool is set on the centre of workpiece axis as a result, V_w is normal to the cutting edge on the P_n. In that case i_s is 0 and process is called as actively driven orthogonal rotary tool cutting. In Figure 2-3a, tool and workpiece rotate in different directions, CW and CCW respectively. Addition of V_r to process introduces V with an equivalent inclination angle, i_{eq} to the P_n. Since process resembles classical oblique cutting as seen in Figure 2-3d, V_{cr} and η_{cr} can be estimated. In Figure 2-3b, rotary tool is considered as stationary due to the fact that velocity of tool is set 0. In that case, process is completely equivalent to orthogonal cutting process as seen in Figure 2-3e. In that case, V is equal to V_w and η_{cr} and ψ are 0. In Figure 2-3c, tool and workpiece rotate in the same direction, CCW. This case is the complete symmetry of Figure 2-3a to the P_n.

In Figure 2-4, tool is set above and below the centre of workpiece axis and it is free to rotate. Generated force due to initial cutting action propels and rotates rotary tool about its own axis. In that case process is called as self propelled rotary tool cutting. In Figure 2-4a, tool set above workpiece axis such that V_w is inclined to the P_n at an angle of i_s. The cutting force accelerates the tool in the same direction with workpiece velocity and when V_r reaches its equilibrium, it is anticipated that V is in direction normal to cutting

edge, as a result i_{eq} is equal to 0. Moreover, V_{cr} is on the P_n with relative chip flow angle of 0. So, this process is equivalent to classical orthogonal cutting process. In that case the direction and magnitude of V_c is strongly dependent to V_w rather than V_r.

In order to consider a equivalency between rotary tool cutting and classical cutting processes, volume metal removal rate should be same for same V and chip thickness, t. The relation is shown as;

$$V_w * B * t = V * b * t = V * B * \frac{\cos i_{eq}}{\cos i_s} * t \qquad (2\text{-}5)$$

$$b = B * \frac{\cos i_{eq}}{\cos i_s} \qquad (2\text{-}6)$$

where B is chip width in rotary tool process, b is equivalent width of cut in classical cutting process.

Modified thin shear zone model is applied to rotary tool cutting process in order to develop cutting analysis. Process is considered as a deformation process with respect to fixed tool to obtain forces and relative chip flow velocity with chip transportation due to the effect of rotary tool velocity. There are some assumptions to associate rotary tool cutting with classical cutting processes [11, 12]:

- Chip formation is continuous and straight.
- Chip is formed by shearing in a thin shear plane.
- Chip is in equilibrium under the action of equal, opposite and collinear forces acting at shear plane and rake face of tool.
- Relative chip flow velocity and friction force on rake face are collinear, shear flow velocity and shear force on shear plane are coincident.
- No additional energy is required for chip transportation due to rotary tool velocity.
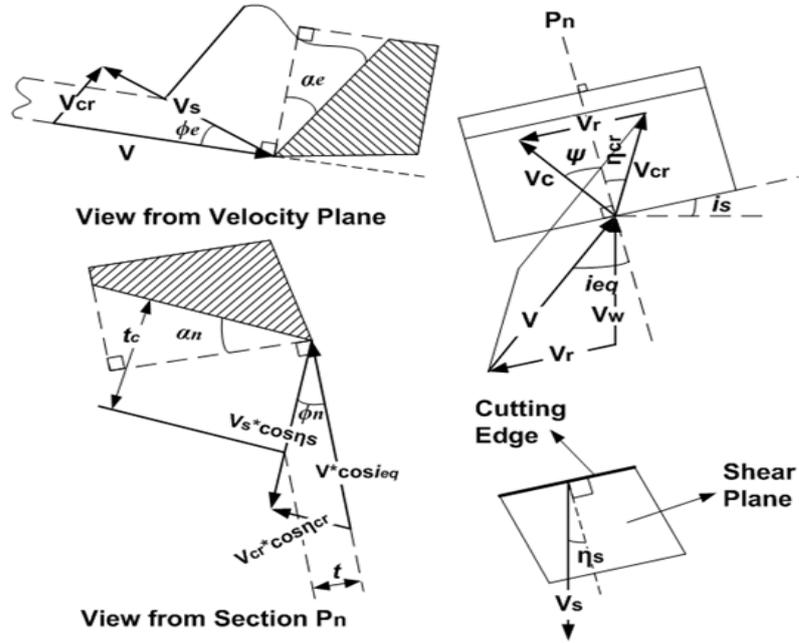
Figure 2-5: Velocity relations, shear and rake angles in rotary turning process.

Figure 2-5 exhibits the deformation geometry and cutting velocities of rotary tool cutting process. From Figure 2-5, using the continuity and incompressibility conditions of chip formation, the following relations can be correlated [12];

$$\frac{B_c}{\cos\psi} = \frac{B}{\cos i_s} = \frac{b}{\cos i_{eq}} \tag{2-7}$$

where B_c is chip width in rotary tool process. Chip length ratio, r_l, the ratio of length of chip, l_c, produced in V_c direction to length of workpiece cut, l, in V_w direction is found by [12];

$$r_l = \frac{l_c}{l} = \frac{V_c}{V_w} \tag{2-8}$$

Then, chip thickness ratio is expressed as [12];

$$r_c = r_l * \frac{\cos\psi}{\cos i_s} \tag{2-9}$$

The effective rake angle, α_e, in the plane of V - V_{cr} as in classical oblique cutting is found by [11];

$$\sin\alpha_e = \sin\eta_{cr} * \sin i_{eq} + \cos\eta_{cr} * \cos i_{eq} * \sin\alpha_n \tag{2-10}$$

The normal shear angle, ϕ_n, on P_n, is defined [11, 12];

$$\tan\phi_n = \frac{r_c * \cos\alpha_n}{1 - r_c * \sin\alpha_n} = \frac{r_l * \left(\frac{\cos\psi}{\cos i_s}\right) * \cos\alpha_n}{1 - r_l * \left(\frac{\cos\psi}{\cos i_s}\right) * \sin\alpha_n} \tag{2-11}$$

15

The effective shear angle, ϕ_e, in the plane of V - V_{cr} as in classical oblique cutting is expressed as [11,12];

$$\tan \phi_e = \frac{V_{cr}/V * \cos \alpha_e}{1 - V_{cr}/V * \sin \alpha_e} \qquad (2\text{-}12)$$

$$\sin \phi_e = \frac{\cos \eta_s * \cos \alpha_e}{\cos \eta_{cr} * \cos \alpha_n} * \sin \phi_n \qquad (2\text{-}13)$$

The relative chip flow angle, η_{cr}, on tool rake face is found by using geometric relations [12];

$$\tan \eta_{cr} = \frac{\sin(i_{eq} - i_s)}{r_t * \cos i_{eq} * \cos i_s} - \tan \psi \qquad (2\text{-}14)$$

On the other hand, V, V_{cr} and V_s lie in velocity plane as discussed above and they are in balance. These velocity vectors can be defined by Cartesian coordinates;

$$V = (V * \cos i_{eq} \qquad\qquad V * \sin i_{eq} \qquad\qquad 0)$$
$$V_{cr} = (V_{cr} * \cos \eta_{cr} * \sin \alpha_n \qquad V_{cr} * \sin \eta_{cr} \qquad V_{cr} * \cos \eta_{cr} * \cos \alpha_n)$$
$$V_s = (-V_s * \cos \eta_s * \cos \phi_n \qquad - V_s * \sin \eta_s \qquad V_s * \cos \eta_s * \sin \phi_n)$$

After balancing each coordinate axis these relations can be found in terms of normal shear and rake angle as in classical oblique cutting;

$$\frac{V_{cr}}{V} = \frac{\sin \phi_n * \cos i_{eq}}{\cos(\phi_n - \alpha_n) * \cos \eta_{cr}} \qquad (2\text{-}15)$$

$$\frac{V_s}{V} = \frac{\cos i_{eq} * \cos \alpha_n}{\cos \eta_s * \cos(\phi_n - \alpha_n)} \qquad (2\text{-}16)$$

Then the shear flow angle, η_s, in shear plane is given by following equation [11];

$$\tan \eta_s = \frac{\tan i_{eq} * \cos(\phi_n - \alpha_n) - \sin \phi_n * \tan \eta_{cr}}{\cos \alpha_n} \qquad (2\text{-}17)$$

16
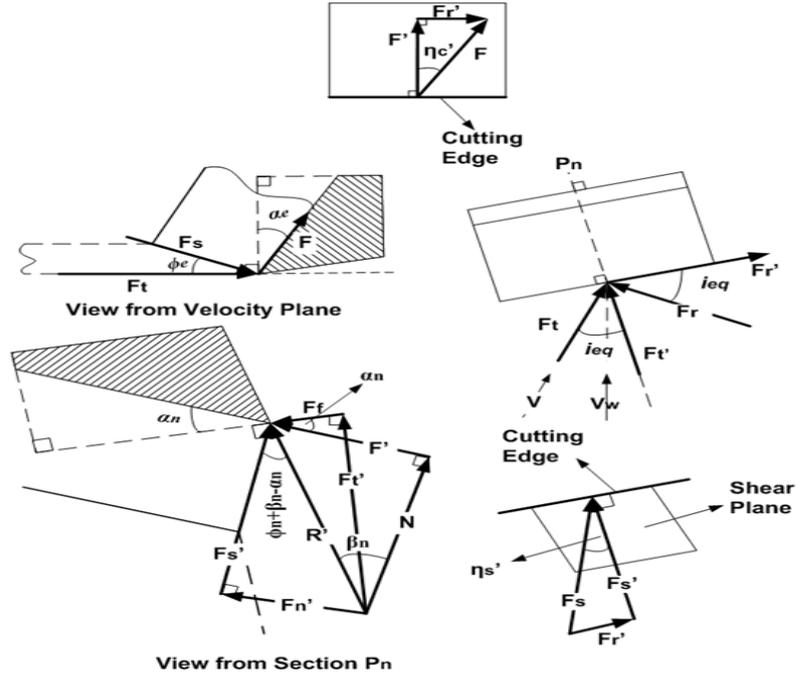
Figure 2-6: Force components in rotary turning process.

Figure 2-6 shows the deformation geometry and relevant forces in tool rake face, shear and normal planes of rotary tool cutting process. Using the assumptions explained above, these relations can be found [11, 12];

$$\eta'_{cr} = \eta_{cr}$$

$$\eta'_s = \eta_s$$

(2-18)

According to Figure 2-6, using these assumptions, resultant force, R, is expressed as;

$$R = \sqrt{(R')^2 + \left(F'_r\right)^2}$$

$$R = \sqrt{F_t^2 + F_f^2 + F_r^2}$$

(2-19)

The friction angle, β, is expressed as in classical cutting processes. Then the friction angle obtained in P_n, β_n, is found by [12];

$$\tan \beta_n = \frac{F'}{N} = \frac{F * \cos \eta_{cr}}{N} = \tan \beta * \cos \eta_{cr}$$

(2-20)

The direction of shear flow, η_s, from Figure 2-6 on shear plane is given by following equation [12];

$$\tan \eta_s = \frac{F'_r}{F'_s} = \frac{F' * \tan \eta_{cr}}{R' * \cos(\phi_n + \beta_n - \alpha_n)} = \frac{\sin \beta_n * \tan \eta_{cr}}{\cos(\phi_n + \beta_n - \alpha_n)}$$

(2-21)

Assuming the stress distributions on the thin shear plane are uniform, the shear force, F_s, is given by [12];

$$F_s = \tau * A_s = \tau * \frac{B}{\cos i_{eq}} * \frac{t}{\sin \phi_n} \qquad (2\text{-}22)$$

where A_s is the area of shear plane in rotary tool cutting. From Figure 2-6, tangential force, F_t, is found by [12];

$$F_t = F_t' * \cos i_{eq} + F_r' * \sin i_{eq}$$

$$F_t = F_s' * \frac{\cos(\beta_n - \alpha_n) * \cos i_{eq}}{\cos(\phi_n + \beta_n - \alpha_n)} + F_s * \sin \eta_s * \sin i_{eq} \qquad (2\text{-}23)$$

Hence the tangential force for rotary tool cutting is given by [12];

$$F_t = t * \frac{B * \cos i_{eq}}{\cos i_s} * \left[\frac{\tau}{\sin \phi_n} * \frac{\cos(\beta_n - \alpha_n) + \tan i_{eq} * \tan \eta_{cr} * \sin \beta_n}{\sqrt{cos^2(\phi_n + \beta_n - \alpha_n) + tan^2 \eta_{cr} * sin^2 \beta_n}} \right] \qquad (2\text{-}24)$$

Similarly, feed force acting on tool tip, F_f, is found by [12];

$$F_f = R' * \sin(\beta_n - \alpha_n) = \frac{F_s * \cos \eta_s * \sin(\beta_n - \alpha_n)}{\cos(\phi_n + \beta_n - \alpha_n)}$$

$$F_f = t * \frac{B}{\cos i_s} * \left[\frac{\tau}{\sin \phi_n} * \frac{\sin(\beta_n - \alpha_n)}{\sqrt{cos^2(\phi_n + \beta_n - \alpha_n) + tan^2 \eta_{cr} * sin^2 \beta_n}} \right] \qquad (2\text{-}25)$$

The radial force component, F_r, is given by [12];

$$F_r = F_t' * \sin i_{eq} - F_r' * \cos i_{eq}$$

$$F_r = F_s' * \frac{\cos(\beta_n - \alpha_n) * \sin i_{eq}}{\cos(\phi_n + \beta_n - \alpha_n)} - F_s * \sin \eta_s * \cos i_{eq} \qquad (2\text{-}26)$$

Hence, the radial force [12];

$$F_r = t * \frac{B * \cos i_{eq}}{\cos i_s} * \left[\frac{\tau}{\sin \phi_n} * \frac{\cos(\beta_n - \alpha_n) * \tan i_{eq} - \tan \eta_{cr} * \sin \beta_n}{\sqrt{cos^2(\phi_n + \beta_n - \alpha_n) + tan^2 \eta_{cr} * sin^2 \beta_n}} \right] \qquad (2\text{-}27)$$

Using the geometric relations, since F_t, F_f and F_r are known, friction force, F and normal force, N can be found [12].

$$F = \sqrt{\left\{ (F_t * \cos i_{eq} + F_r * \sin i_{eq}) * \sin \alpha_n + F_f * \cos \alpha_n \right\}^2 + (F_t * \sin i_{eq} - F_r * \cos i_{eq})^2} \qquad (2\text{-}28)$$

and,

$$N = [F_t * \cos i_{eq} + F_r * \sin i_{eq}] * \cos \alpha_n - F_f * \sin \alpha_n \qquad (2\text{-}29)$$

The shear force, F_s, and the normal force on shear plane, F_n, are also found using geometric relations [12];

$$F_s = \sqrt{\left\{ (F_t * \cos i_{eq} + F_r * \sin i_{eq}) * \cos \phi_n - F_f * \sin \phi_n \right\}^2 + (F_t * \sin i_{eq} - F_r * \cos i_{eq})^2} \qquad (2\text{-}30)$$

and,

$$F_n = [F_t * \cos i_{eq} + F_r * \sin i_{eq}] * \sin \phi_n + F_f * \cos \phi_n \qquad (2\text{-}31)$$

18

It is seen from equations that if ϕ_n, β, τ are known with additional quantity such as α_n, i_s, V_r generated forces can be predicted. Again by using the collinearity between relative chip flow velocity - friction force and shear flow velocity – shear force, the relation between ϕ_n and β_n can be found [12];

$$\tan(\phi_n + \beta_n) = \frac{\tan i_{eq} * \cos \alpha_n}{\tan \eta_c - \sin \alpha_n * \tan i_{eq}}$$

(2-32)

The formulas can be applicable to all rotary tool cutting processes. For actively driven rotary tool, i_{eq} and i_s are used in equations. For actively driven orthogonal rotary tool, i_s is equated to 0 due to tool position according to workpiece. For self propelled rotary tool, i_{eq} is taken as 0 since tool rotational velocity, V_r makes process classical orthogonal cutting.

Using database taken from orthogonal cutting test results, the rotary turning process is simulated with the aid of MATLAB®. For simulation the tool-workpiece contact zone is divided into segments and cutting parameters for each segment are calculated. The orthogonal cutting parameters are 150 m/min cutting velocity, 0.05 mm/rev feed rate, 2.05 mm depth of cut with 5° rake angle of cutting insert. Moreover, from experimental results, shear strength of material is calculated as 606 MPa, normal friction angle is found as 23° and chip ratio is taken as 0.55. For the simulation i_s is taken as 15° with 13.5 mm cutting insert radius. Depending on these parameters, the simulated results are found in following. The effect of tool velocity on effective rake, effective shear and chip flow angles are seen in Figure 2-7, Figure 2-8 and Figure 2-9, respectively.
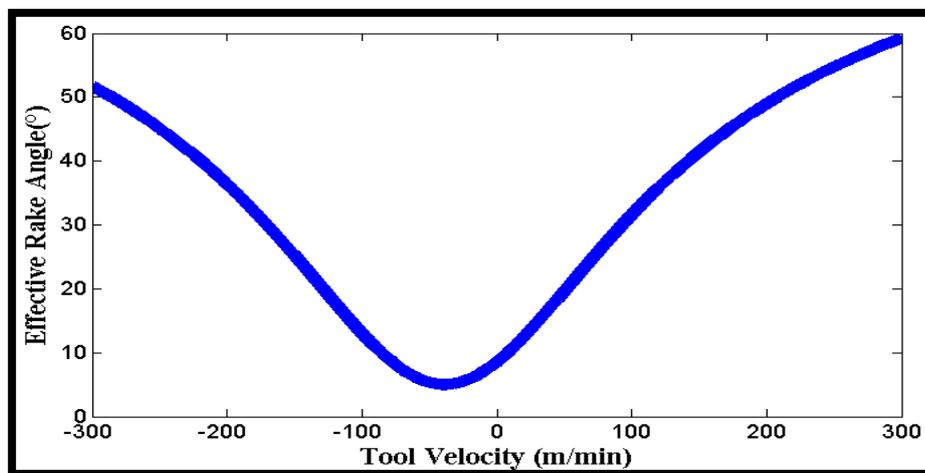
Figure 2-7: Effective rake angle variation with tool velocity.
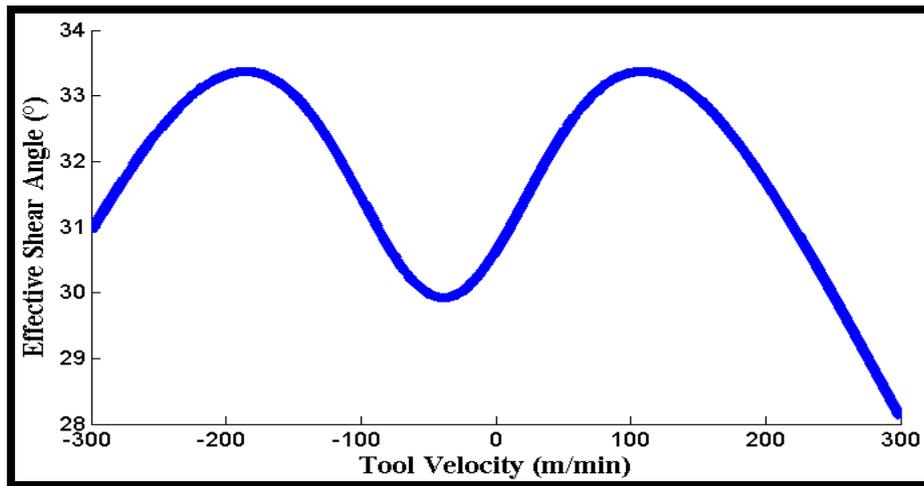
Figure 2-8: Effective shear angle variation with tool velocity.
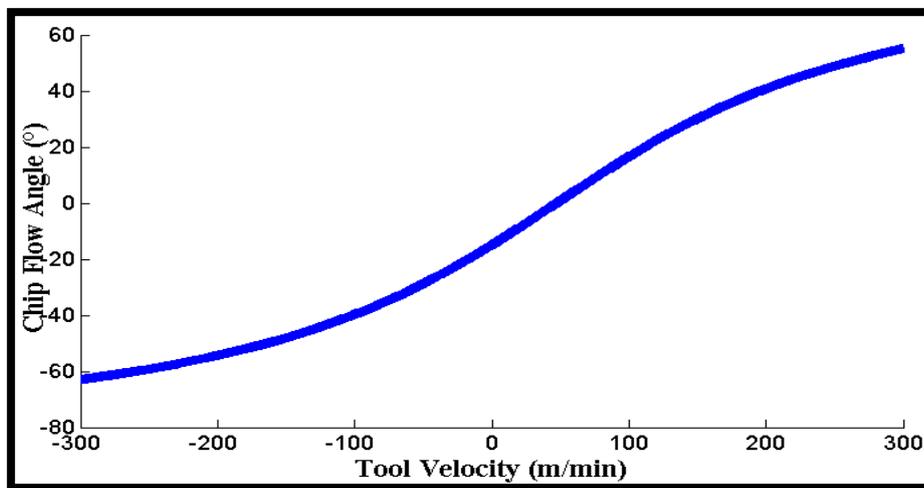
Figure 2-9: Chip flow angle variation with tool velocity.

Also Figure 2-10 shows the component force variation with tool velocity using orthogonal cutting parameters.
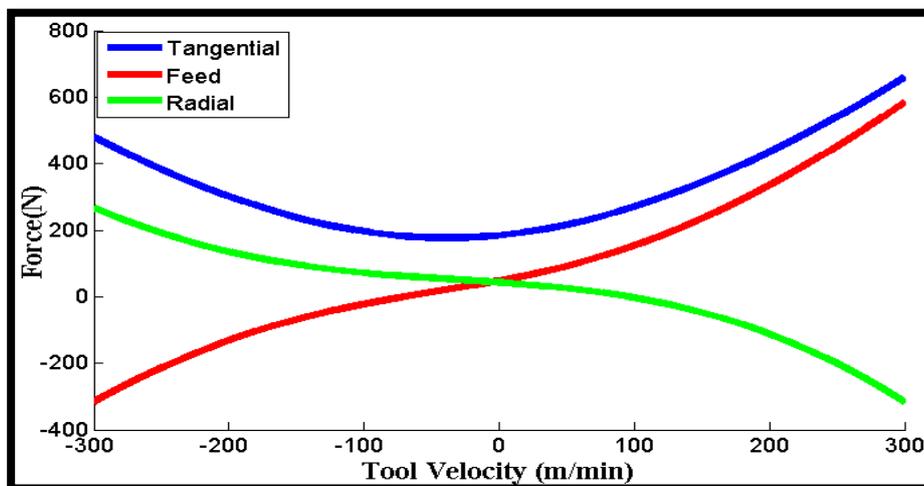
Figure 2-10: Component forces variation with tool velocity.

The effects of tool inclination angle on cutting parameters are also simulated. The effects of tool velocity for different tool inclination angles on effective rake angle, effective shear angle and chip flow angle are seen in Figure 2-11, Figure 2-12, and Figure 2-13, respectively.
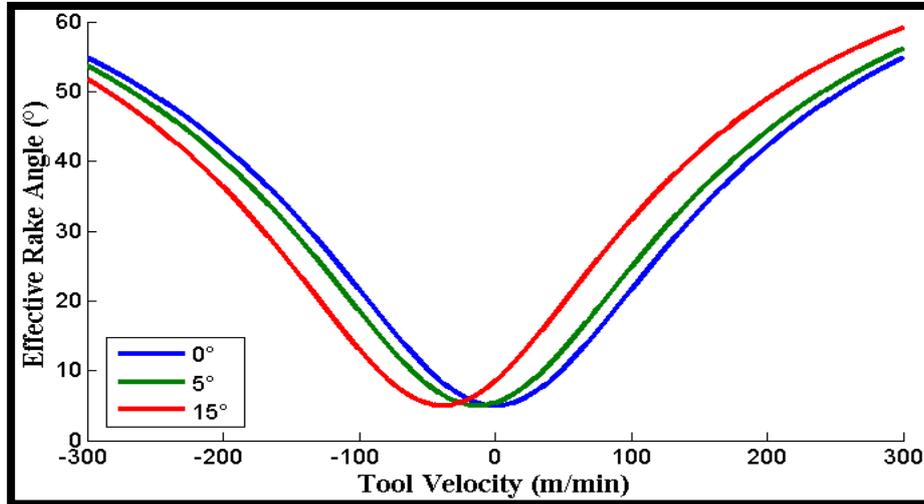
Figure 2-11: Effective rake angle variation with tool velocity for different inclination angles.
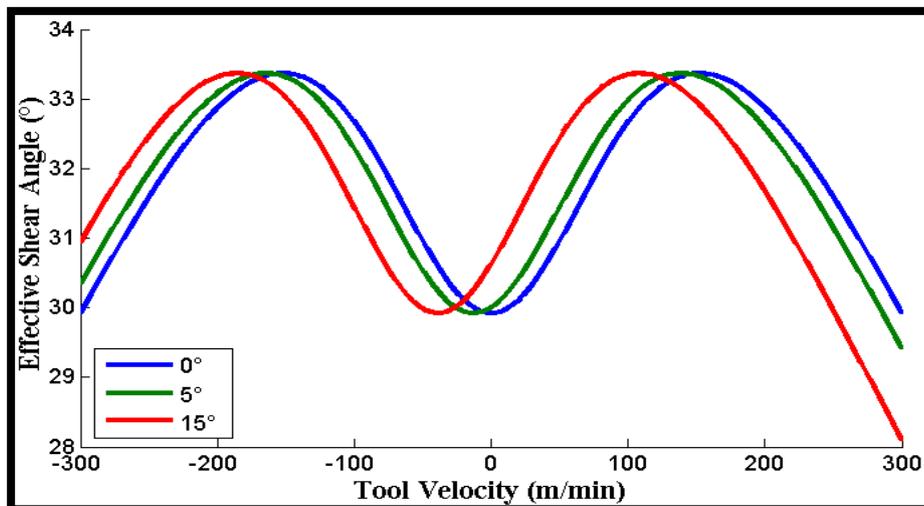
Figure 2-12: Effective shear angle variation with tool velocity for different inclination angles.
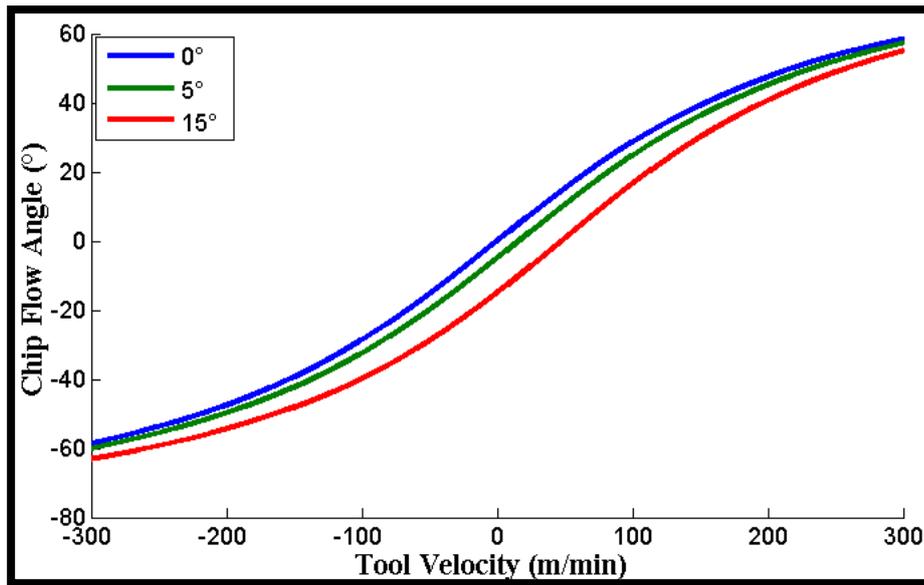
Figure 2-13: Chip flow angle variation with tool velocity for different inclination angles.

The effects of tool inclination angle on component forces are also simulated. Figure 2-14, Figure 2-15 and Figure 2-16 show the force variations in tangential, feed and radial directions, respectively.
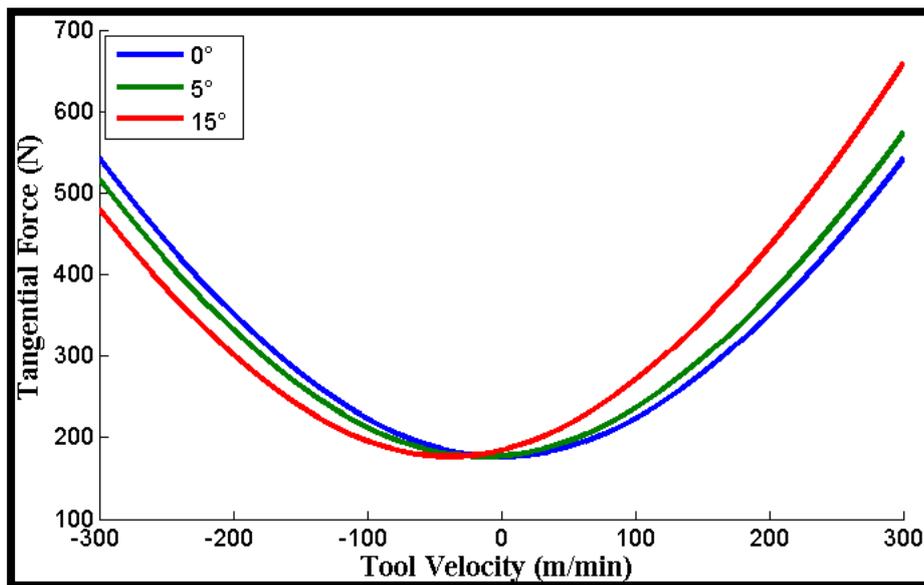
Figure 2-14: Tangential force variation with tool velocity for different inclination angles.
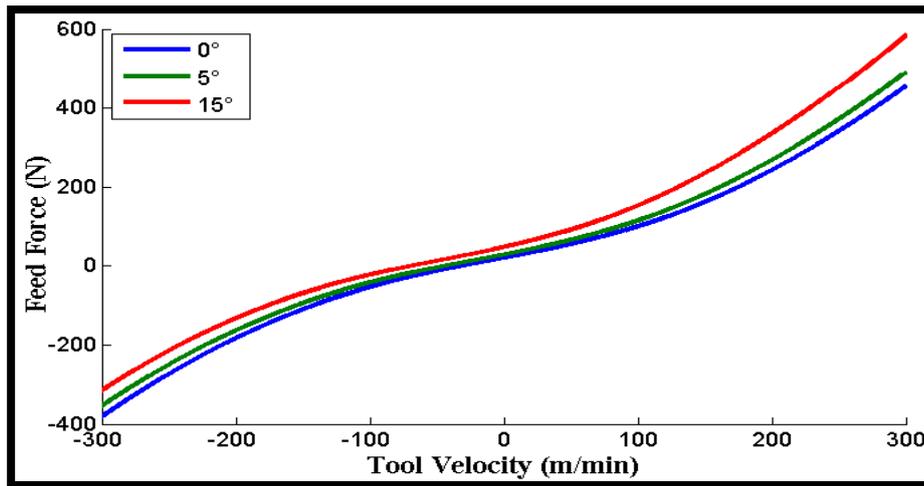
Figure 2-15: Feed force variation with tool velocity for different inclination angles.
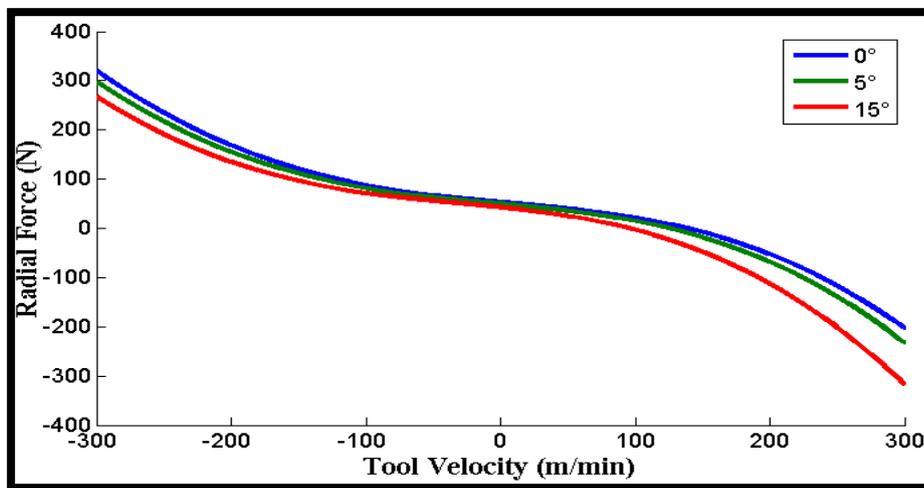
Figure 2-16: Radial force variation with tool velocity for different inclination angles.

It is seen from graphs that without increasing cutting velocity, effective rake angle can be increased by changing tool velocity. As tool velocity increases in both CW and CCW directions, effective rake angle changes. Changing the tool inclination angle affects the position of minimum value of effective rake angle. Furthermore, a variation in tool velocity changes the effective shear angle during process. In a range of tool velocity in both CW and CCW directions, the value of effective shear angle becomes maximum and easy chip formation takes place. Variation in inclination angle affects only the tool velocity range in which the effective shear angle shows maximum values. Tool velocity also directly changes the chip flow angle. Obviously, including the effect of tool velocity makes the process oblique compared to conventional fixed one, as a result, increasing tool velocity in both CW and CCW directions rises chip flow angle. Change in tool inclination angle exhibits different behaviors on chip flow angle

depending on tool rotation direction. Change in tool velocity also affects the component forces due to variations in cutting angles. Tangential force shows its minimum at around 40 m/min tool velocity. As tool velocity increases in CW or CCW directions, freely from tool rotation direction tangential force rises in positive direction. However, forces in feed and radial directions show different behaviors depending on tool rotation direction. When workpiece and tool rotate at the same direction, feed force rises in positive direction, yet increase in radial force is observed in negative direction. When tool rotation direction is changed and as tool velocity is increased, feed force increases in negative direction, but radial force becomes positive and increases in that direction. Increasing inclination angle, when workpiece and tool rotate at the same direction, causes an increase for tangential and feed forces in positive direction, yet an increase in radial force in negative direction is observed. Reductions in tangential and radial forces in positive direction are found when tool rotation direction changes compared to workpiece. Similarly, feed force decreases as inclination angle increases when tool and workpiece rotate in different directions.

2.2   Summary

In this chapter, the kinematics and mechanics of rotary turning process are examined. It is observed that ADRT processes are similar to classical oblique cutting process while SPRT process is almost equivalent to classical orthogonal cutting process. Modified thin shear zone model is applied to develop cutting analysis. Rotary turning process is assumed to be a deformation process equivalent to classical cutting processes including the effect of tool velocity. Using equivalent cutting parameters, generated formulas are found to be similar to ones used in classical cutting processes. Simulation results show the effects of tool velocity and inclination angle on cutting parameters and forces during rotary cutting.

CHAPTER 3 EXPERIMENTAL PROCEDURE

In this study, the effects of rotary turning tools on tool life, surface quality of machined parts and generated cutting temperatures are investigated. The tests are applied in a wide range of cutting conditions in order to have better and various data cutting with rotary turning tools. Tool wear, cutting forces, surface roughness, circularity of machined parts and tool rake face temperature are inspected during cutting tests.

Cutting tests are performed in three different machining processes, conventional turning, SPRT and ADRT. These tests are applied for different testing materials especially difficult to cut materials in order to clarify the advantages of rotary turning processes on tool wear, cutting forces and surface quality. Different cooling conditions are used for these processes to explain the effects of coolants on tool life and cutting forces. For ADRT process, various rotary tool velocities and rotary tool inclination angles are utilized in order to gain understanding the effects of them on tool life, surface quality and generated cutting temperatures.

3.1 Workpiece Materials

3.1.1 AISI 1050

Even though AISI 1050 steel is not a superalloy, cutting tests were conducted using this alloy for rotary turning and stationary turning process to discuss the tool performances. AISI 1050 is a high quality structural plain carbon steel and it is very commonly used in manufacturing. This alloy is used in parts of ships, automobiles, aircrafts, weapons, railways, pressure vessels. The metallurgical properties of AISI 1050 are seen in Table 3-1.

Element	C	Mn	P	S	Fe
Content (%)	0.47-0.55	0.6-0.9	0.04	0.05	Balance

Table 3-1: Metallurgical properties of AISI 1050 steel.

Density of AISI 1050 alloy is 7850 kg/m^3. The mechanical properties and thermal properties are found in Table 3-2 and Table 3-3, respectively.

Property	Metric Unit
Tensile Strength	635 MPa
Yield Strength	515 MPa
Shear Modulus	80 GPa
Bulk Modulus	140 GPa
Elastic Modulus	190-210 GPa
Poisson's Ratio	0.27-0.3
Elongation at Break	10-15 %
Reduction of Area	30-40 %
Hardness, Brinell	187-197 HB
Impact Strength	16.9 J

Table 3-2: Mechanical properties of AISI 1050 steel.

Property	Metric Unit
Specific Heat Capacity	0.486 J/kg*°C
Thermal Conductivity	49.8 W/m*K
Coefficient of Thermal Expansion	$11.3*10^{-6}/°C$

Table 3-3: Thermal properties of AISI 1050 steel.

Plain carbon steels have the best machinability properties compared to other steel types. Carbon content is the main affecting parameter of machinability. High carbon steels are difficult to cut since they are strong and they may contain carbide particles. On the other hand, low carbon steels are very soft such that these alloys are gummy and stick to cutting tool causing BUE at the tool tip with shortened tool life.

3.1.2 Waspaloy

Waspaloy, a registered trademark of United Technologies Corp, is a wrought age-hardenable austenitic nickel base superalloy. It has excellent high-temperature strength, hot hardness and good corrosion resistance, notably to oxidation, at service temperatures up to 650°C for critical applications and up to 870°C for less demanding applications.

Solid solution strengthening elements, Mo, Co and Cr and age hardening elements Al and Ti provide high temperature strength to Waspaloy. The metallurgical properties of Waspaloy are seen in Table 3-4.

Element	Cr	Mo	Co	Al	Ti	Fe	C	Mn	Si	Cu	Ni
Content %	21	5	15	1.6	3.25	2	0.1	0.1	0.15	0.1	Balance

Table 3-4: Metallurgical properties of Waspaloy.

Due to high strength and resistance to corrosion properties even at elevated temperatures, this alloy is preferable for high technology application areas such as gas

turbine engine components, miscellaneous jet engine hardware, space shuttle turbo pump seals, airframe assemblies and missile systems. The physical properties can be found in Table 3-5.

Property	Metric Unit
Density	8190 kg/m^3
Melting Point	1330°C

Table 3-5: Physical properties of Waspaloy.

The mechanical properties and thermal properties of Waspaloy are found in Table 3-6 and Table 3-7, respectively.

Property	Metric Unit
Tensile Strength	1276 MPa
Yield Strength	897 MPa
Elastic Modulus	211 GPa
Elongation at Break	26.6 %
Reduction of Area	25%
Hardness, Brinell	351 HB

Table 3-6: Mechanical properties of Waspaloy.

Property	Metric Unit
Specific Heat Capacity	0.52 J/kg*°C
Thermal Conductivity	11 W/m*K
Coefficient of Thermal Expansion	12.2*10^{-6}/°C

Table 3-7: Thermal properties of Waspaloy.

Waspaloy, like Nickel base super alloys, has bad reputation about their machinability properties. Due to its inherent properties, Waspaloy maintains its strength at high temperatures. Poor thermal diffusivity, high thermal gradients are generated in cutting tool. Austenitic matrix of alloy results in work hardening rapidly during machining. Abrasive wear on cutting tools is a result of presence of hard carbide particles in microstructure and tendency of Waspaloy to form BUE. At high cutting temperatures, chemical reaction occurs between tool and workpiece leading to high diffusion wear rate. Localization of shear in chip produces abrasive saw toothed chips that makes difficult to handle. Furthermore, forming of tough and continuous chip contributes for degradation of tool by seizure and cratering.

3.1.3 Ti6Al4V

Ti6Al4V, Grade 5 titanium, is the most commonly used titanium alloys such that over 70% of all alloy grades melted are sub-grade of Ti6Al4V. It is stronger than pure

titanium having the same stiffness and thermal properties. It has high strength-to-weight ratio and high corrosion resistance. It is an α+β alloy that is heat treatable to achieve required strength values. The metallurgical properties of Ti6Al4V can be seen in Table 3-8.

Element	Al	V	C	N	O	H	Fe	Y	Ti
Content %	6	4	0.1	0.05	0.02	0.02	0.4	0.01	Balance

Table 3-8: Metallurgical properties of Ti6Al4V.

The addition of palladium, ruthenium and nickel increase corrosion resistance in acidic environments. Due to the combination of high strength and light weight with an excellent corrosion resistance, Ti6Al4V can be operable to any engineering applications. This alloy is mainly used in turbine engine components, structural components, aircraft fasteners, marine applications and sports equipments. Since it has superior biocompatibility, it can be used in medical industry especially when direct contact with tissue and bone is required. The physical properties can be found in Table 3-9.

Property	Metric Unit
Density	4430 kg/m^3
Melting Point	1649°C

Table 3-9: physical properties of Ti6Al4V.

The mechanical properties and thermal properties are found in Table 3-10 and Table 3-11 respectively.

Property	Metric Unit
Tensile Strength	950 MPa
Yield Strength	880 MPa
Shear Strength	550 MPa
Elastic Modulus	114 GPa
Poisson's Ratio	0.342
Elongation at Break	14%
Reduction of Area	36%
Hardness, Brinell	334 HB
Impact Strength	17J

Table 3-10: Mechanical properties of Ti6Al4V.

Property	Metric Unit
Specific Heat Capacity	0.53 J/kg*°C
Thermal Conductivity	7.2 W/m*K
Coefficient of Thermal Expansion	8.6*10^{-6}/°C

Table 3-11: Thermal properties of Ti6Al4V.

Ti6Al4V alloys are well known as extremely difficult to machine alloys due to inherent properties. Low thermal conductivity prevents heat flow through chip. Maintaining its high strength even at elevated temperatures opposes the plastic deformation to form chip. Strong chemical reactivity of Ti6Al4V with almost all tooling materials contributes partially hardening of outer surface layer of workpiece with a high tool wear rate.

3.1.4   Inconel 718

Inconel 718, trademark of Special Metals Corporation, is an austenitic nickel-chromium based superalloy. Due to solid solution strengthening, Inconel 718 keeps its high strength even at elevated temperatures. Inconel 718 is oxidation and corrosion resistant material applicable for extreme environments such as high pressure and high heat. An oxide layer is formed on the surface of this alloy to protect material from further attack. Moreover, this alloy is preferable for high temperature engineering applications owing to high fatigue, creep and rupture strength values. The metallurgical properties of Inconel 718 are seen Table 3-12.

Element	Ni	Cr	Nb	Mo	Co	Ti	Si	Al	C	Mn	Fe
Content %	55	21	5.5	3.3	1	0.3	0.35	1.15	0.08	0.35	Balance

Table 3-12: Metallurgical properties of Inconel 718.

Due to keeping its mechanical properties even at elevated temperatures, Inconel 718 has wide range of application areas. This alloy can be used in components for liquid fueled rockets, ring and casing parts for aircrafts, land-based gas turbine engines, and cryogenic tanks. The physical properties of Inconel 718 can be found in Table 3-13.

Property	Metric Unit
Density	8190 kg/m^3
Melting Point	1336°C

Table 3-13: Physical properties of Inconel 718.

The mechanical properties and thermal properties of Inconel 718 are seen in Table 3-14 and Table 3-15, respectively.

Property	Metric Unit
Tensile Strength	1375 MPa
Yield Strength	1100 MPa
Bulk Modulus	150 GPa
Shear Modulus	100 GPa
Elastic Modulus	200 GPa
Poisson's Ratio	0.29
Elongation at Break	12%
Reduction of Area	15%

Table 3-14: Mechanical properties of Inconel 718.

Property	Metric Unit
Specific Heat Capacity	435 J/kg*°C
Thermal Conductivity	11.4 W/m*K
Coefficient of Thermal Expansion	13/°C

Table 3-15: Thermal properties of Inconel 718.

Inconel shows the similar behavior with Waspaloy during machining operations. Their tendency to galling and welding on tool rake face, forming built-up edge on tool and presence of hard particles in microstructure increase tool wear rate. Relatively low thermal conductivity of these alloys causes heat piling up in front of tool tip.

3.2 Cutting Tools and Holders

The tool holder used in conventional turning tests is a TaeguTec PRGNR 2525 M12 as shown in Figure 3-1. It is a screw clamp holder for round inserts. The cutting insert used in conventional turning tests is TaeguTec RNMG 43 TT3500. The insert can be seen in Figure 3-2. The insert is a carbide insert with CVD coating with TiN. It has a chip breaker on rake face with 15 mm diameter and 0° of rake and clearance angles.

Figure 3-1: Tool holder for conventional turning tests.

Figure 3-2: The cutting insert used for conventional turning cutting tests.

The holder used for SPRT cutting tests is patented design of Rotary Technologies Corporation, CLT-15/RH as shown in Figure 3-3. The inserts are coated carbide with a diameter of 27 mm with 0º of rake and clearance angles as shown in Figure 3-4. Insert cartridge and tool holder together provide -15° of rake and 5° of effective clearance to cutting edge.

Figure 3-3: The tool holder for SPRT cutting tests.

Figure 3-4: The cutting insert used for SPRT cutting tests.

ADRT tool is composed of a round insert and a specified holder shaft. A holder shaft is simply designed as shown in Figure 3-5 and it is produced by a tool supplier in order to minimize the error in concentricity of the insert to the center of holder shaft within 30 μm.
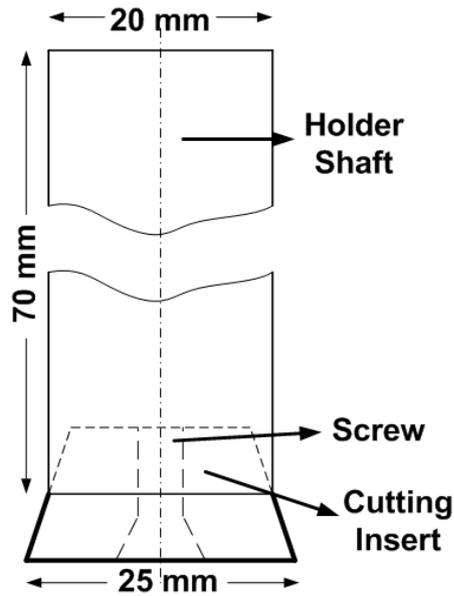
Figure 3-5: Designed ADRT holder shaft with half cone shaped cutting insert.

The cutting insert used for ADRT process is SandvikCoromant RCMT 25 07 M0 4225 as shown in Figure 3-6. It is a carbide insert with multi-layer CVD coating of MT-Ti(C,N)+Al_2O_3+TiN. It has 25 mm diameter with a chip breaker and 7° clearance angle.
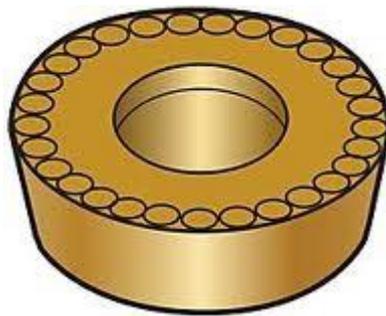
Figure 3-6: The cutting insert used for ADRT cutting tests.

3.3 Machine Tools

For SPRT and conventional turning processes, Mori Seiki NL 1500 CNC lathe is used as shown in Figure 3-7. It is a 3-axis turning center with maximum 6000 rpm spindle speed. The machine tool has a maximum capacity of 260 mm diameter and 515 mm workpiece length.

Figure 3-7: Mori Seiki NL1500 CNC lathe.

All ADRT process and temperature measurement tests are conducted in Mori Seiki NTX2000 Mill-Turn machining center as shown in Figure 3-8. This machine includes 9 axes with two chucks, a milling spindle and a turning turret. Milling spindle moves along X-, Y- and Z- axes and rotates around B- axis. Turning turret moves in X- and Z- directions with maximum 10 cutting tools.

Figure 3-8: Mori Seiki NTX2000 Mill-Turn center.

3.4 Measurement Equipments

The three generated cutting forces during SPRT and conventional turning tests are measured using Kistler 9257BA dynamometer as shown in Figure 3-9. The forces are

measured in every cutting tests under different cutting conditions. A program written in LabView amplifies the gathered force signals coming from dynamometer.

Figure 3-9: Kistler 9257BA 3-Component Dynamometer.

During SPRT cutting tests, the insert rotation velocity is measured by Keyence LK 031 laser displacement sensor. The laser sensor is placed on a sliding fixture as shown in Figure 3-10. The small hole in the middle of rotary tool shaft is used as a reference point for velocity measurement.
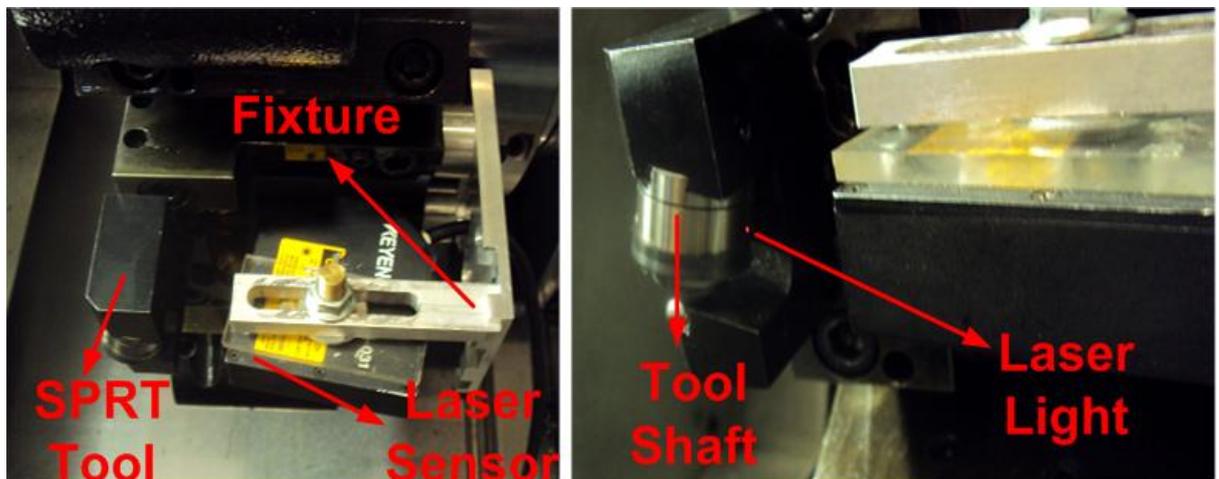
Figure 3-10: Configuration of SPRT tool and laser system in Mori Seiki NL1500.

Tool flank wear is measured by using NanoFocusµsurf surface metrology system as shown in Figure 3-11. Measurements are conducted at four different locations for rotary turning tools. These locations are approximately equidistant along the perimeter of cutting insert. The obtained values are averaged to attain tool wear. For conventional turning tool, standard tool edge examination is performed to find out tool wear value.
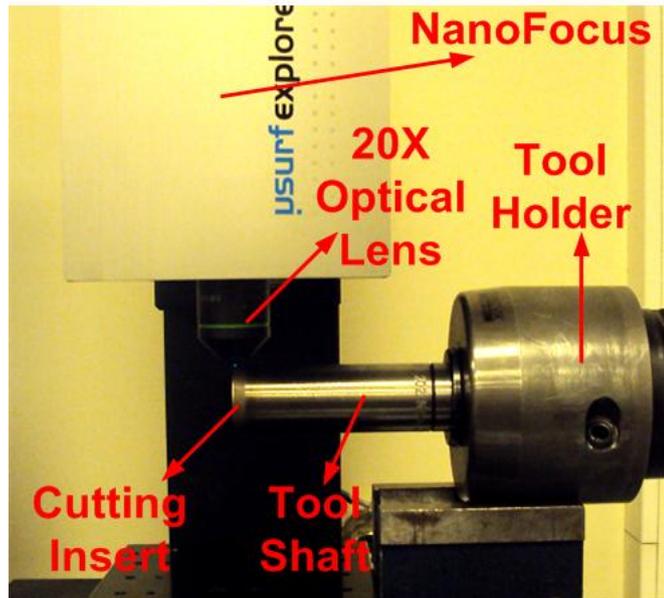
Figure 3-11: Tool flank wear measurement using NanoFocusµsurf surface metrology system.

A scanning electron microscope (SEM) is used for revealing information of a sample's texture, chemical composition and crystalline structure. The worn ADRT cutting inserts for different cutting conditions are inspected by LEO Supra 35VP as shown in Figure 3-12. The magnifying rate for SEM images varies between 200 and 1500 times greater than the original size.

Figure 3-12: SEM for detailed inspection of ADRT cutting inserts.

Surface roughness of machined parts is accessed using NanoFocusµsurf metrology system. Ten measurements are performed in both feed direction of tool and circumferential direction of workpiece, the obtained values are averaged to attain surface roughness value. Mitutoyo Euro-C-A544 Coordinate Measuring System is utilized to measure the roundness of machined parts as shown in Figure 3-13. Measurements are conducted at four different height locations for machined workpieces. 0.005 mm is taken as tolerance while measuring roundness.

Figure 3-13: Roundness measurement by using Mitutoyo Euro-C-A544 CMM.

ADRT tool temperature measurements are made with FLIR A325 SC infrared thermal imaging camera as shown in Figure 3-14. This camera has ability to visually record and display in real time temperature distribution of the tool.

Figure 3-14: FLIR A325 SC infrared thermal camera.

Using ThermaCAM software, the camera can be fully controlled from the PC. Its spectral range is 7.5-13 μm with 320*240 resolution. It can be focused to the target automatically or manually. Since the standard temperature range is not well enough for our testing conditions, camera is calibrated to high temperature (1200ºC).

Thermal camera is positioned as close as possible to cutting insert in order to obtain exact temperature results in Mori Seiki NTX2000 Mill-Turn center. During measurements, chip motion obstructs the thermal measurement and its motion is almost unpredictable. Due to thermal camera position, chip generally moves between tool and thermal camera. A protective window is designed and produced to prevent chip flow through thermal camera lens. The protective window is made of ZnSe glass having thermal properties and there is no change in the quality and resolution of thermal image due to this protection.

3.5 Cutting Conditions

In this thesis, cutting velocity, feed rate and depth of cut are kept constant for SPRT, ADRT and conventional turning processes.

3.5.1 SPRT and Conventional Turning Processes

The cutting conditions for AISI 1050 steel, Waspaloy and Ti6Al4V with tooling system and cooling conditions are summarized in Table 3-16, Table 3-17, and Table 3-18 respectively for tool wear and tool life tests.

Test No	Workpiece	Tooling System	Cooling System	Cutting Velocity (m/min)	Feed Rate (mm/rev)	Depth of Cut (mm)
1	AISI 1050	Conventional	Dry	400	0.2	1
2	AISI 1050	SPRT	Dry	400	0.2	1
3	AISI 1050	SPRT	Coolant	400	0.2	1

Table 3-16: Experimental conditions for SPRT and conventional turning cutting tests for tool wear and tool life measurements for AISI 1050 steel cutting tests.

Test No	Workpiece	Tooling System	Cooling System	Cutting Velocity (m/min)	Feed Rate (mm/rev)	Depth of Cut (mm)
1	Waspaloy	Conventional	Dry	45	0.1	0.2
2	Waspaloy	SPRT	Dry	45	0.1	0.2
3	Waspaloy	SPRT	Coolant	45	0.1	0.2
4	Waspaloy	SPRT	MQL	45	0.1	0.2

Table 3-17: Experimental conditions for SPRT and conventional turning cutting tests for tool wear and tool life measurements for Waspaloy cutting tests.

Test No	Workpiece	Tooling System	Cooling System	Cutting Velocity (m/min)	Feed Rate (mm/rev)	Depth of Cut (mm)
1	Ti6Al4V	Conventional	Dry	45	0.1	0.2
2	Ti6Al4V	Conventional	Coolant	45	0.1	0.2
3	Ti6Al4V	SPRT	Dry	45	0.1	0.2
4	Ti6Al4V	SPRT	Coolant	45	0.1	0.2
5	Ti6Al4V	SPRT	MQL	45	0.1	0.2

Table 3-18: Experimental conditions for SPRT and conventional turning cutting tests for tool wear and tool life measurements for Ti6Al4V cutting tests.

Cutting tests in order to find out the behavior of rotary tool velocity are performed using AISI 1050 steel. All tests are conducted under dry cutting conditions using 0.2 mm/rev feed rate and 1 mm depth of cut. Cutting velocities range from 50 m/min to 400 m/min to gain understanding of the effects of workpiece velocity on tool velocity.

3.5.2   ADRT Process

For ADRT cutting tests, cutting velocity, feed rate and depth of cut for all testing materials are kept constant as in SPRT and conventional turning process. 400 m/min cutting velocity with 0.2 mm/rev feed rate and 1 mm depth of cut are the cutting parameters for AISI 1050 steel. However, for Waspaloy, Ti6Al4V and Inconel 718 alloys, 45 m/min cutting velocity, 0.1 mm/rev feed rate and 0.2 mm depth of cut are used for cutting tests. Different rotary tool velocities and different rotary tool inclination angles are tested under various cooling conditions for each testing materials. The cutting conditions for AISI 1050 steel, Waspaloy, Ti6Al4V and Inconel 718 are summarized in Table 3-19, Table 3-20, Table 3-21 and Table 3-22, respectively.

Test No	Workpiece	Cooling Type	Tool Velocity (m/min)	Tool Inclination Angle (°)
1	AISI 1050	Dry	50	0
2	AISI 1050	Dry	250	0
3	AISI 1050	Dry	400	0
4	AISI 1050	Dry	50	5
5	AISI 1050	Dry	250	5
6	AISI 1050	Dry	400	5
7	AISI 1050	Coolant	50	0
8	AISI 1050	Coolant	250	0
9	AISI 1050	Coolant	400	0
10	AISI 1050	Coolant	50	5
11	AISI 1050	Coolant	250	5
12	AISI 1050	Coolant	400	5
13	AISI 1050	MQL	50	0
14	AISI 1050	MQL	250	0
15	AISI 1050	MQL	50	5
16	AISI 1050	MQL	250	5

Table 3-19: Experimental conditions for ADRT turning cutting tests for tool wear and tool life measurements for AISI 1050 steel cutting tests.

Test No	Workpiece	Cooling Type	Tool Velocity (m/min)	Tool Inclination Angle (°)
1	Waspaloy	Dry	10	0
2	Waspaloy	Dry	20	0
3	Waspaloy	Dry	45	0
4	Waspaloy	Dry	10	5
5	Waspaloy	Dry	20	5
6	Waspaloy	Dry	10	15
7	Waspaloy	Coolant	0	0
8	Waspaloy	Coolant	10	0
9	Waspaloy	Coolant	20	0
10	Waspaloy	Coolant	45	0
11	Waspaloy	Coolant	10	5
12	Waspaloy	Coolant	20	5
13	Waspaloy	Coolant	10	15
14	Waspaloy	MQL	10	0
15	Waspaloy	MQL	20	0
16	Waspaloy	MQL	45	0
17	Waspaloy	MQL	10	5
18	Waspaloy	MQL	20	5
19	Waspaloy	MQL	10	15

Table 3-20: Experimental conditions for ADRT turning cutting tests for tool wear and tool life measurements for Waspaloy cutting tests.

Test No	Workpiece	Cooling Type	Tool Velocity (m/min)	Tool Inclination Angle (º)
1	Ti6Al4V	Dry	10	0
2	Ti6Al4V	Dry	20	0
3	Ti6Al4V	Dry	45	0
4	Ti6Al4V	Dry	10	5
5	Ti6Al4V	Dry	20	5
6	Ti6Al4V	Dry	10	15
7	Ti6Al4V	Coolant	0	0
8	Ti6Al4V	Coolant	10	0
9	Ti6Al4V	Coolant	20	0
10	Ti6Al4V	Coolant	45	0
11	Ti6Al4V	Coolant	10	5
12	Ti6Al4V	Coolant	20	5
13	Ti6Al4V	Coolant	10	15
14	Ti6Al4V	MQL	10	0
15	Ti6Al4V	MQL	20	0
16	Ti6Al4V	MQL	45	0
17	Ti6Al4V	MQL	10	5
18	Ti6Al4V	MQL	20	5
19	Ti6Al4V	MQL	10	15

Table 3-21: Experimental conditions for ADRT turning cutting tests for tool wear and tool life measurements for Ti6Al4V cutting tests.

Test No	Workpiece	Cooling Type	Tool Velocity (m/min)	Tool Inclination Angle (º)
1	Inconel 718	Dry	10	0
2	Inconel 718	Dry	20	0
3	Inconel 718	Dry	45	0
4	Inconel 718	Dry	10	5
5	Inconel 718	Dry	20	5
6	Inconel 718	Dry	10	15
7	Inconel 718	Coolant	10	0
8	Inconel 718	Coolant	20	0
9	Inconel 718	Coolant	45	0
10	Inconel 718	Coolant	10	5
11	Inconel 718	Coolant	20	5
12	Inconel 718	Coolant	10	15
13	Inconel 718	MQL	10	0
14	Inconel 718	MQL	20	0
15	Inconel 718	MQL	10	5
16	Inconel 718	MQL	20	5
17	Inconel 718	MQL	10	15

Table 3-22: Experimental conditions for ADRT turning cutting tests for tool wear and tool life measurements for Inconel 718 cutting tests.

The effects of rotary tool velocity and rotary tool inclination angle on surface roughness and circularity of machined parts are also investigated using comprehensive cutting

tests of AISI 1050 steel under coolant cutting conditions. 400 m/min cutting velocity, 0.2 mm/rev feed rate and 1 mm depth of cut are the cutting parameters. Table 3-23 summarizes the tests plan for surface quality and circularity tests.

Test No	Workpiece	Tool Velocity (m/min)	Tool Inclination Angle (°)
1	AISI 1050	50	0
2	AISI 1050	75	0
3	AISI 1050	100	0
4	AISI 1050	125	0
5	AISI 1050	150	0
6	AISI 1050	50	5
7	AISI 1050	75	5
8	AISI 1050	100	5
9	AISI 1050	125	5
10	AISI 1050	150	5

Table 3-23: Experimental conditions for ADRT turning cutting tests for surface roughness and circularity measurements for AISI 1050 steel cutting tests.

Tool rake face temperature measurements are performed for AISI 1050 steel and Ti6Al4V alloy using infrared camera for various rotary tool velocities and for various rotary tool inclination angles. Cutting velocities for these tests are kept low owing to security reasons. All cutting tests are conducted under dry cutting conditions. 100 m/min cutting velocity with 0.2 mm/rev feed rate and 1 mm depth of cut are AISI 1050 steel cutting parameters while Ti6Al4V are tested using 20 m/min cutting velocity, 0.1 mm/rev feed rate, 0.2 mm depth of cut. Table 3-24 and Table 3-25 summarize the cutting conditions for AISI 1050 steel and Ti6Al4V respectively.

Test No	Workpiece	Tool Velocity (m/min)	Tool Inclination Angle (°)
1	AISI 1050	10	0
2	AISI 1050	25	0
3	AISI 1050	50	0
4	AISI 1050	150	0
5	AISI 1050	250	0
6	AISI 1050	25	5
7	AISI 1050	50	5
8	AISI 1050	150	5

Table 3-24: Experimental conditions for ADRT turning cutting tests for tool rake face temperature measurements for AISI 1050 steel cutting tests.

Test No	Workpiece	Tool Velocity (m/min)	Tool Inclination Angle (°)
1	Ti6Al4V	3	0
2	Ti6Al4V	5	0
3	Ti6Al4V	10	0
4	Ti6Al4V	15	0
5	Ti6Al4V	20	0
6	Ti6Al4V	25	0
7	Ti6Al4V	5	5
8	Ti6Al4V	10	5
9	Ti6Al4V	20	5
10	Ti6Al4V	5	10
11	Ti6Al4V	10	10
12	Ti6Al4V	15	10
13	Ti6Al4V	20	10
14	Ti6Al4V	5	15
15	Ti6Al4V	10	15
16	Ti6Al4V	15	15
17	Ti6Al4V	20	15

Table 3-25: Experimental conditions for ADRT turning cutting tests for tool rake face temperature measurements for Ti6Al4V cutting tests.

CHAPTER 4 EXPERIMENTAL RESULTS FOR CONVENTIONAL TURNING AND SPRT PROCESSES

All tests planned in Chapter 3 for conventional turning and SPRT operations for tool life, surface quality and rotary tool velocity were successfully completed. Different data is collected through measurements done during cutting tests. Worn cutting edges and surface roughness of machined parts are analyzed using NanoFocus. Kistler dynamometer is used to collect cutting force data. Mitutoyo CMM is used to measure roundness of workpieces after cutting tests. Keyence laser sensor is utilized to obtain rotary tool velocity data during operation. In this section tool life, cutting forces, surface quality and rotary tool velocity results are presented.

The position of SPRT tool with Kistler dynamometer on Mori Seiki Nl1500 is shown in Figure 4-1.
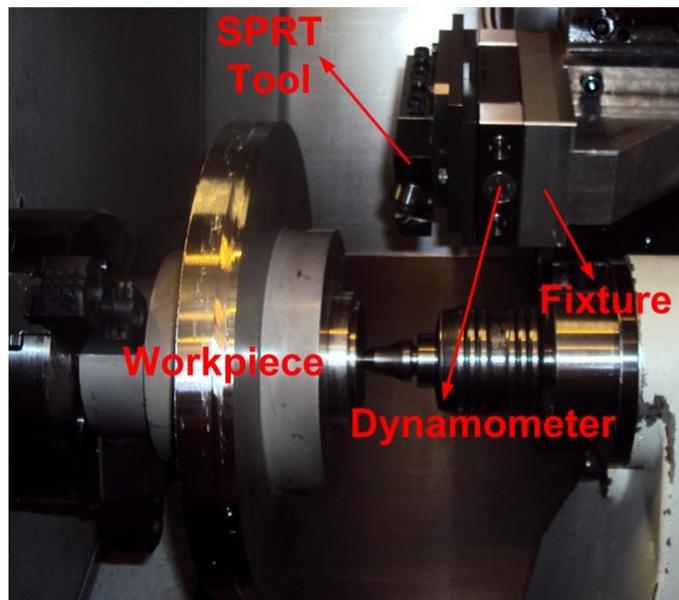
Figure 4-1: Configuration of SPRT tool and workpiece in Mori Seiki NL 1500 turning center.

4.1 AISI 1050 Steel

The AISI 1050 steel cutting test conditions for tool wear, cutting forces, surface quality and rotary tool velocity are explained in Chapter 3 in detail in Table 3-16. The

workpiece material has 120 mm diameter with 110 mm cutting length. The measurement results are presented as follows.

4.1.1 Tool Wear

Tool wear results of conventional turning and SPRT process for AISI 1050 steel cutting tests for different cooling conditions are presented in Figure 4-2.
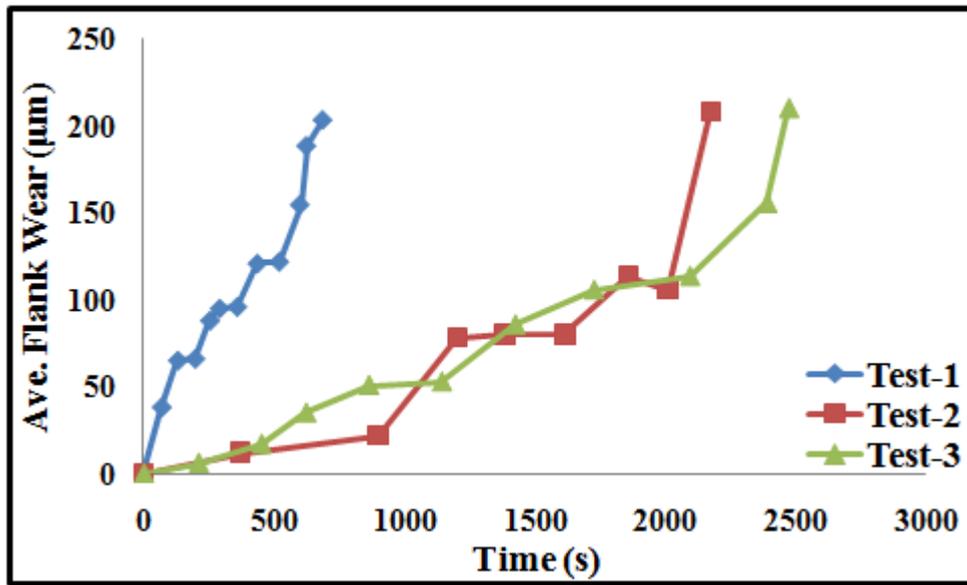
Figure 4-2: Tool flank wear variation with time for different tooling system and cooling conditions for AISI 1050 steel cutting.

It is easily seen from the graph that flank wear rate of SPRT tool is lower than that of conventional turning. Obviously, due to lower tool wear rate higher tool life is attained for SPRT process compared to conventional turning process. In order to compare tool wear results properly, *normalization* of conventional turning insert is required. This insert can be indexed and its unused portions can be used until the whole cutting edge is completely worn. When normalization is done by considering the fact that the conventional turning tool can be indexed four times the tool life results seem to be close to each other for both processes. Flank wear on SPRT tool is the dominant wear mechanism and it is uniformly distributed over the entire circumferential cutting edge. The main reason of uniform flank wear distribution is the use of full circular cutting edge during operation. Little or no crater wear is observed on SPRT cutting edge. This can be attributed to lower heat generation during cutting. However, when conventional turning tool is examined, crater wear on tool rake face with flank wear is observed. This is likely due to heat accumulation on the same contact zone in conventional turning. It

is also noticeable that when SPRT process test are conducted under coolant cutting, tool wear rate slightly reduces compared to dry cutting condition such that 14 % improvement in tool life is achieved. The main reason is the effective transportation of coolant to cutting zone with rotational motion of insert. Moreover, uniform flank wear distribution is also dominant in SPRT process with coolant cutting. Small chipping of cutting edge is also observed.

4.1.2 Cutting Forces

Generated cutting force results of conventional turning and SPRT process for AISI 1050 steel cutting tests for different cooling conditions are presented. Figure 4-3 exhibits the cutting force results for various tooling system and cooling conditions.
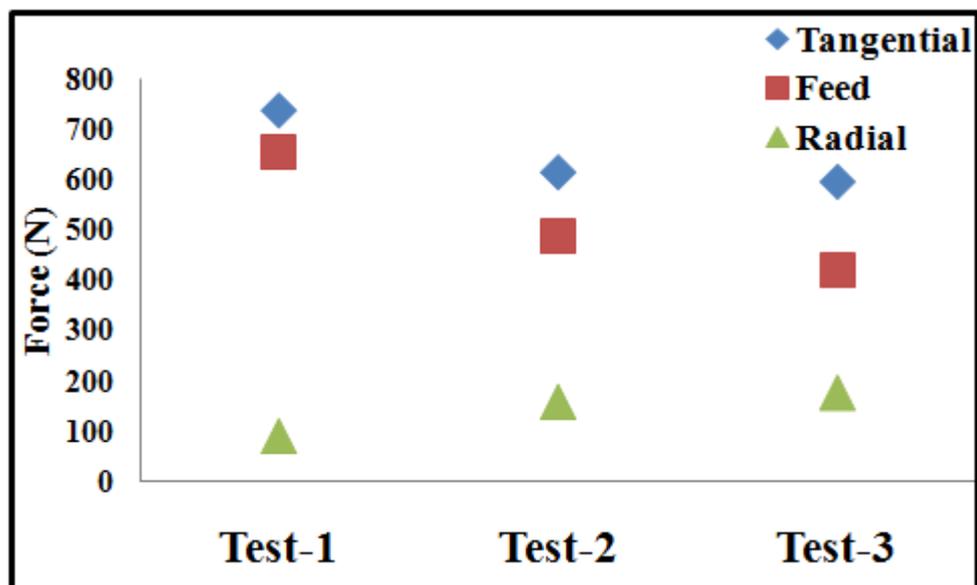
Figure 4-3: Generated cutting force variation for different tooling system and cooling conditions for AISI 1050 steel cutting.

It is seen from graph that component forces except radial force are reduced when machining with SPRT tool compared to stationary tool for different cooling conditions. In machining of AISI 1050 steel, generated tangential and feed forces with SPRT tool are 16.7% and 25.5% lower than those in conventional turning tool, respectively, in dry cutting conditions. Reduction in work done for chip formation, reduction in specific energy and lower friction conditions on tool rake face causes lower forces during operation. An increase in radial force component is observed when machining with SPRT tool compared to conventional turning in dry cutting. The increased effective oblique angle during operation is the main reason for higher radial forces. When

machining with coolant cutting, 3% and 14% reduction in force components are found in tangential and feed directions, respectively, compared to dry cutting condition in SPRT machining. 9% increase in force component in radial direction is found when SPRT tests are conducted with coolant cutting compared to dry cutting.

4.1.3 Surface Roughness and Circularity

In this section, surface roughness and circularity results of conventional turning and SPRT processes for AISI 1050 steel cutting tests for same cutting conditions are presented. Figure 4-4 exhibits the generated surface topography for conventional turning and SPRT processes.
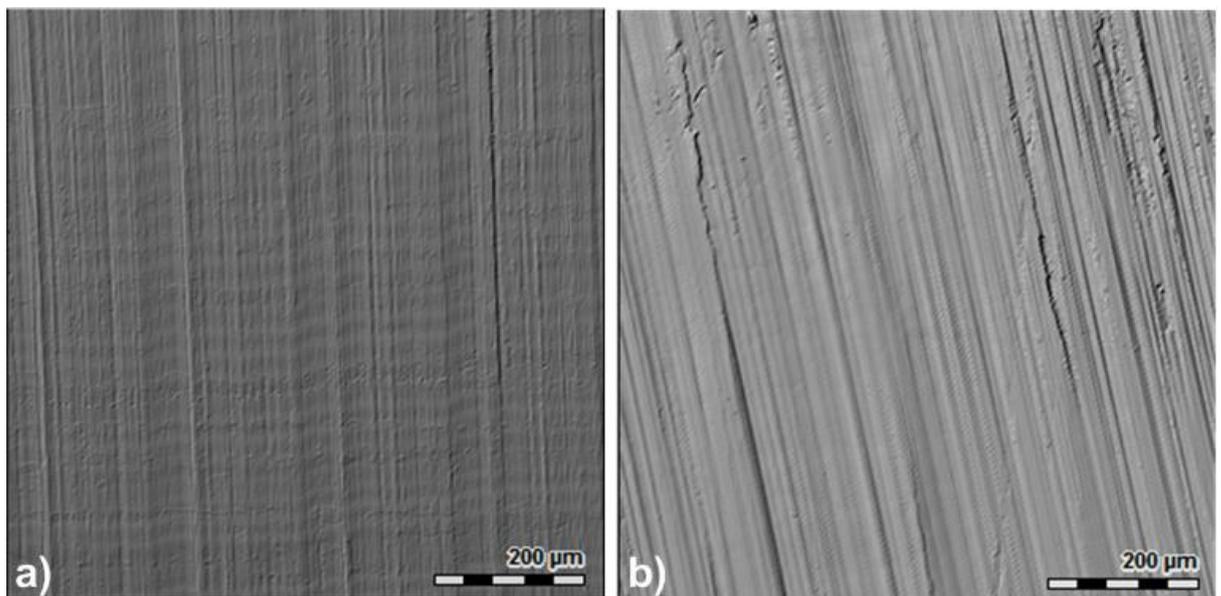

Figure 4-4: Surface topography for a) Test-1 b) Test-2.

The surface grooves for different cutting conditions are easily seen from the figure. The spinning feature of SPRT tool influences the surface topography of machined workpiece. Produced grooves from SPRT tool are found at an angle to the effective cutting velocity direction while the direction of grooves from conventional turning tool is parallel to feed direction. Moreover, the inclination angle of grooves produced by SPRT tool is always smaller than the tool inclination angle owing to friction conditions in SPRT tooling system. Furthermore, chip's swirling action around SPRT tool rake face results pulling under insert and workpiece. This situation causes adhesion of chips, deeper grooves and scratches on workpiece surface reducing the surface quality as shown in Figure 4-5.
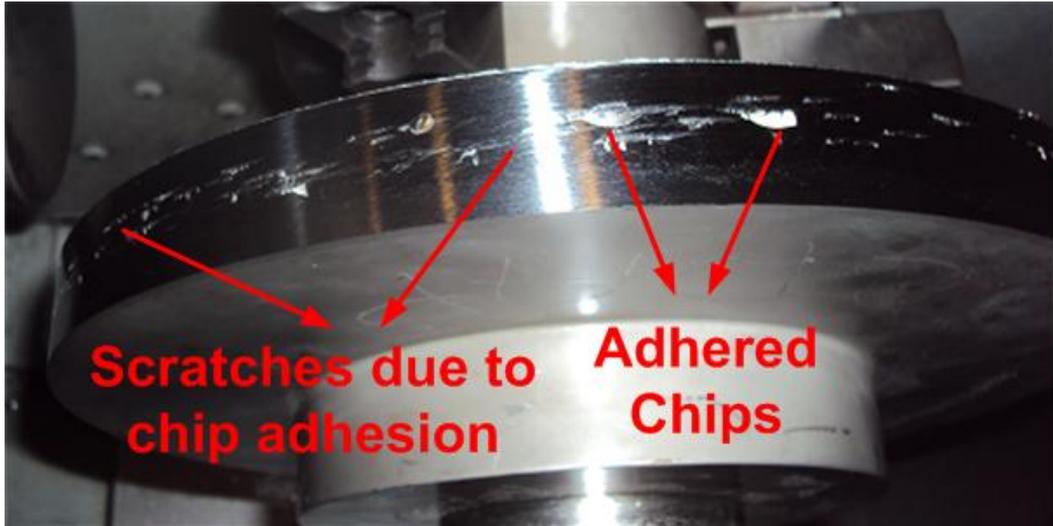
Figure 4-5: Example of machined surface of SPRT process with scratches and adhered chips.

The measured surface roughness values are recorded after one machining pass in order to eliminate any tool wear effect. Table 4-1 summarizes the surface roughness measurements. Even though the differences in roughness values are not remarkable, the roughness in circumferential direction for SPRT tool is better than that of conventional turning tool. However, the roughness in feed direction increased significantly in SPRT process compared to conventional turning.

The circularity is the measure of sharpness of workpiece's corners. It is very essential for machined surface quality for turning operations. The circularity measurements for different tests are shown in Figure 4-6.
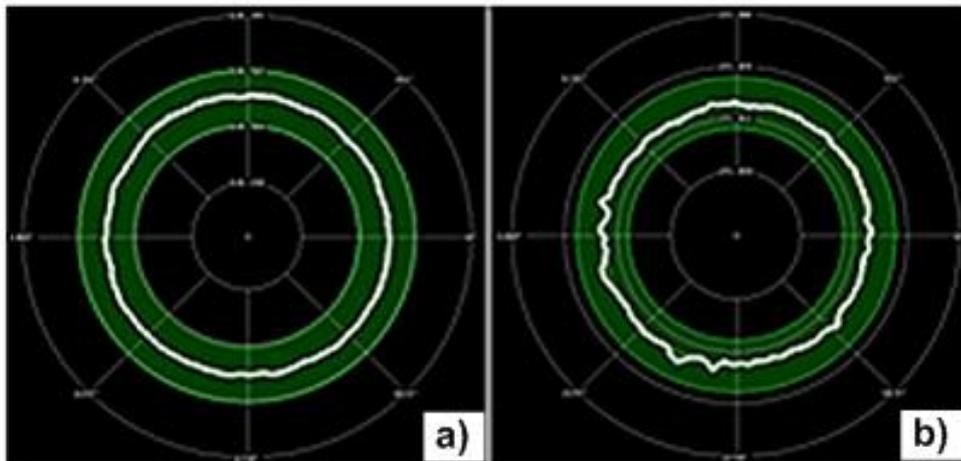
Figure 4-6: Circularity of machined workpieces a) Test-1 b) Test-2.

The difference in the circularities of two processes is not remarkable as seen in Table 4-1. The obtained circularity result with conventional turning tool is slightly better than SPRT process. This situation can be attributed to moving components and rigidity of SPRT tool. Lower rigidity of tool causes run-out of the insert resulting worse circularity of machined surface.

	Test-1	Test-2
Roughness in Feed Direction	0.3 μm	0.65 μm
Roughness in Circumferential Direction	1.16 μm	0.77 μm
Circularity	2-3 μm	4-6 μm

Table 4-1: Surface roughness and circularity measurement results for Test-1 and Test-2.

4.1.4 Rotary Tool Velocity Characteristics

In this section, rotary tool velocity variation with different cutting velocities for AISI 1050 steel is presented. In order to provide rotational motion to SPRT tool, tool axis should be at an inclination angle with respect to cutting velocity. This inclination angle is the most important factor in SPRT process such that it directly affects the performance of rotary tool. Rotary tool velocity is closely related to the inclination of tool edge as shown in Figure 4-7.
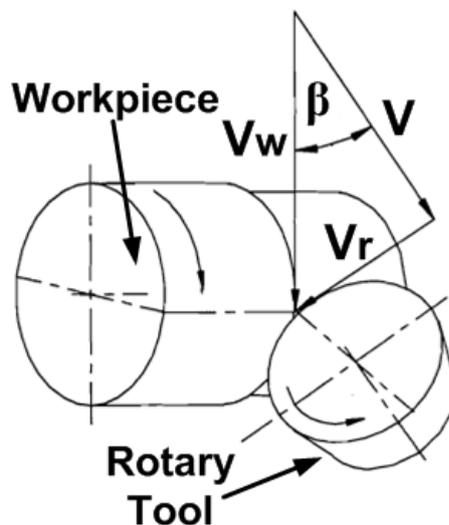
Figure 4-7: The principle of SPRT process.

Using the pure kinematic relations, rotary tool velocity is obtained analytically. The inclination angle of SPRT tool used in cutting tests is 15°. It is apparent from the results collected in Figure 4-8 how the cutting velocity affects the velocity of SPRT tool. Both

analytical and experimental results are seen in graph together. It should be clarified that all experimental tool velocities are measured after tool reaching stable period during cutting.
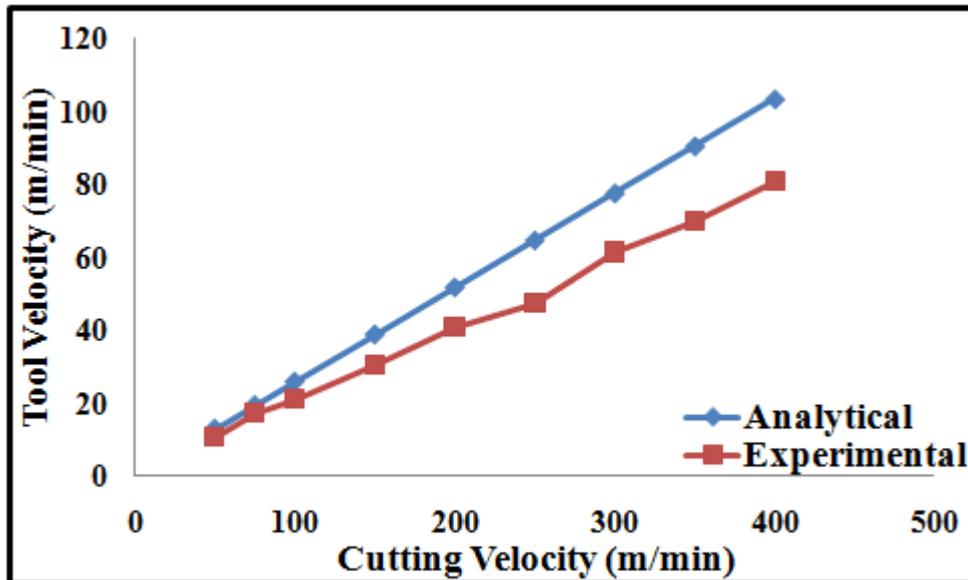
Figure 4-8: Rotary tool velocity variation with different cutting velocities.

It is seen from the graph that experimental results show that there is almost linearity with tool velocity and workpiece velocity. A good agreement between analytical and experimental results of rotary tool is observed up to 100 m/min cutting velocity. After that cutting velocity, the deviation between analytical and experimental results seems to be increased. For instance, 21.3% and 21.9% reductions in tool velocity are observed when cutting tests are performed at 150 m/min and 400 m/min cutting velocities, respectively. Friction conditions of process and tool rotary shaft mechanism can be reason of that deviation, since only the pure kinematic relations are used for analytic results without considering any side effects such as friction in SPRT process. At lower cutting velocities, the effect of friction on insert propelling is higher than at higher cutting velocities. As cutting velocity increases coefficient of friction between chip and tool reduces as a result, friction force acting on tool edge decreases with lowering effect to propel cutting insert. Moreover, a small loss in rotational velocity at lower cutting velocities can also be explained by the friction in bearing system in rotary shaft.

4.2 Waspaloy

The Waspaloy cutting test conditions for tool wear and cutting forces are explained in Chapter 3 in detail in Table 3-17. The used workpiece material has 275 mm diameter with 27 mm cutting length. The obtained results are presented as follows.

4.2.1 Tool Wear

Tool wear results of conventional turning and SPRT process for Waspaloy cutting tests for different cooling conditions are presented. Figure 4-9 shows the tool wear results for different tooling system and cooling conditions.

Figure 4-9: Tool flank wear variation with time for different tooling system and cooling conditions for Waspaloy cutting.

Figure 4-9 shows that extremely low flank wear rate is recorded with SPRT tool when machining Waspaloy for various cooling conditions. Uniformly distributed flank wear over entire cutting edge is the main tool failure mechanism during SPRT process. Due to rotational motion of tool, the whole circular cutting edge is involved to chip shearing causing distributed flank wear on insert edge. There is no evidence of crater wear on tool edge which can be attributed to self-cooling feature of tool with a significant reduction in heat generation. As discussed in previous section, normalization of conventional turning insert life is required to compensate for the unused portions of the tool for proper tool life comparison with SPRT. Even normalization is done, tool life is achieved 8.9 folds when cutting with SPRT compared to conventional turning tool. Using longer effective cutting edge provided by tool motion is the main reason behind

it. Using coolants for SPRT process is also essential to increase the effectiveness of process. Coolant and MQL cutting improve tool life 2.2 folds and 2.4 folds compared to dry cutting conditions. Air pressure used in MQL cooling is also effective to remove chip from tool rake face.

4.2.2 Cutting Forces

Generated cutting force results of conventional turning and SPRT process for Waspaloy cutting tests for different cooling conditions are presented. Figure 4-10 exhibits the cutting force results for various tooling system and cooling conditions.

Figure 4-10: Generated cutting force variation for different tooling system and cooling conditions for Waspaloy cutting.

It is seen from figure that SPRT process reduces component forces compared to conventional turning process except in radial direction in all different cooling conditions. In machining of Waspaloy, generated tangential and feed forces with SPRT tool are 53% and 32% lower than those in conventional turning tool, respectively, in dry cutting conditions. Easy shearing of chip due to reduced work done in SPRT process and lower friction conditions are the reasons for decreased forces. An increase in radial force component is observed when machining with SPRT tool compared to conventional turning in dry cutting. The effective obliquity of tool due to spinning motion is the main reason for higher radial forces. When SPRT tool is tested in MQL cooling condition, a slight decrease in all three component forces are found. The lubrication effect of used oil in MQL decreases friction coefficient in tool rake face

resulting lowered forces. When cutting tests of SPRT tool with coolant cutting, almost similar feed and radial forces are observed compared to dry and MQL cooling condition. During machining with coolant, 14% and 6% reduction in tangential force component are found compared to dry and MQL cooling conditions, respectively.

4.3 Ti6Al4V

The Ti6Al4V cutting test conditions for tool wear and cutting forces are explained in Chapter 2 in detail in Table 3-18. The used workpiece material has 175 mm diameter with 50 mm cutting length. The obtained results are presented as follows.

4.3.1 Tool Wear

Tool wear results of conventional turning and SPRT process for Ti6Al4V cutting tests for different cooling conditions are presented. Figure 4-11 shows the tool wear results for different tooling system and cooling conditions.
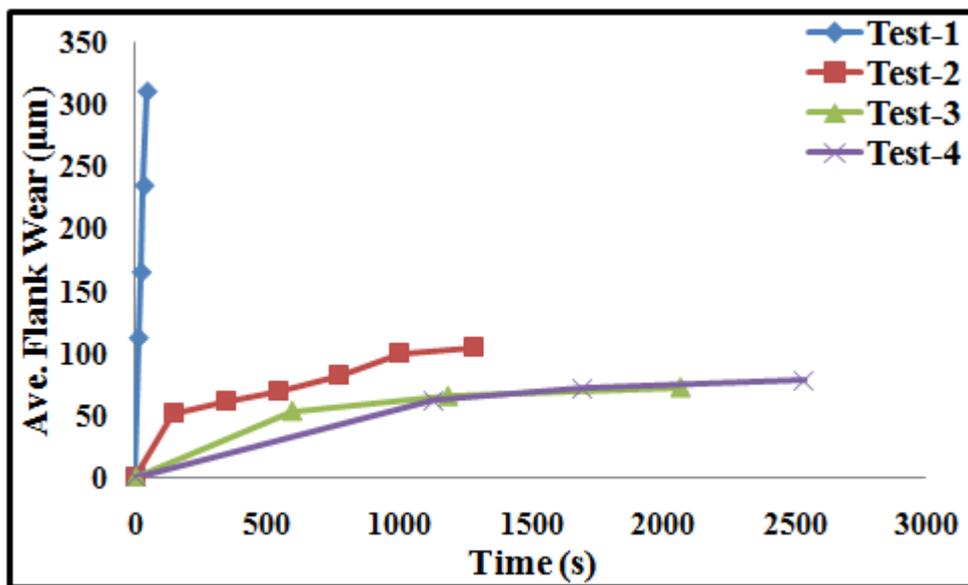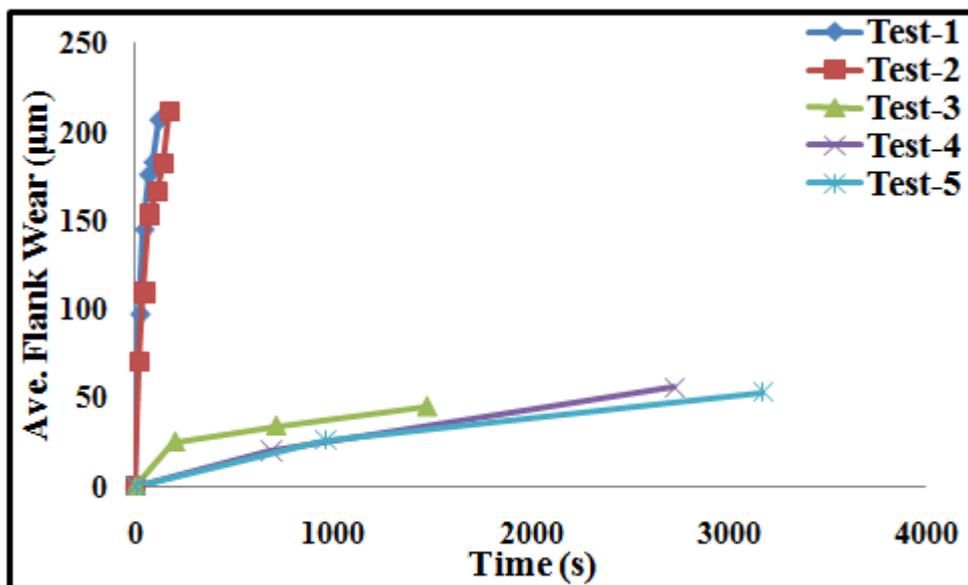

Figure 4-11: Tool flank wear variation with time for different tooling system and cooling conditions for Ti6Al4V cutting.

When Ti6Al4V cutting tests results are considered, similar tool wear and tool life results are observed as in previous sections. SPRT tool shows superior wear resistance hence longer tool life compared to conventional turning. Uniformly distributed flank wear over the whole cutting edge with no crater wear is the main tool failure mode of SPRT process due to rotational motion of tool. However, in conventional turning process, high crater wear and flank wear at cutting zone are observed. It is seen from

figure that cutting with coolant is effective for conventional turning process such that it improves tool life 46% compared to dry cutting condition. Even normalization is performed to conventional turning tool, SPRT process is more effective for achievement of longer tool lives. A tool wear of 145 μm and 153 μm are measured on conventional turning tool after 45 seconds and 74 seconds for dry and coolant cutting respectively, whereas flank wear of 128 μm, 114 μm and 124 μm are measured on SPRT tool for dry, coolant and MQL cutting conditions, respectively. The effect of coolant on tool wear is not much enough as expected compared to dry cutting condition.

4.3.2 Cutting Forces

Generated cutting force results in conventional turning and SPRT process for Ti6Al4V cutting tests for different cooling conditions are presented in Figure 4-12.
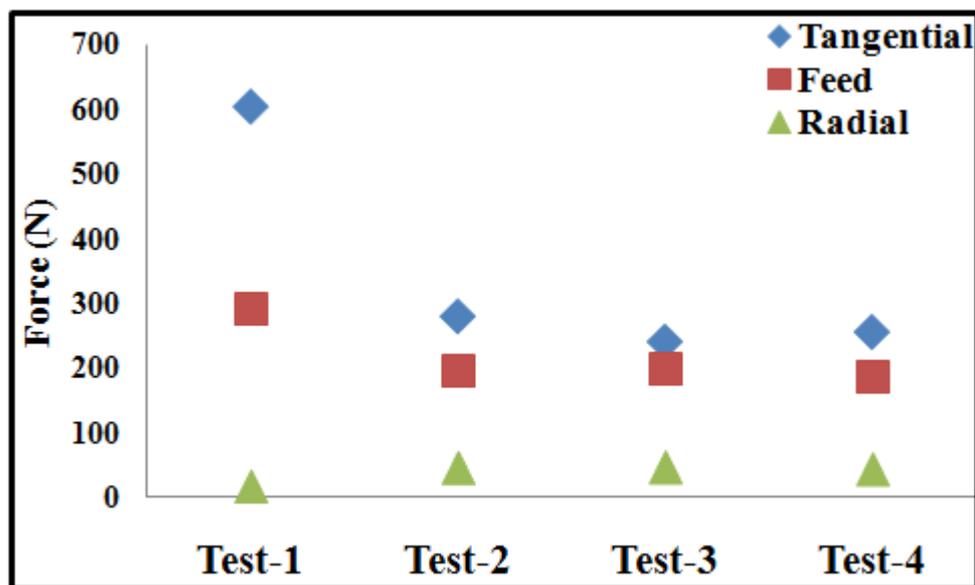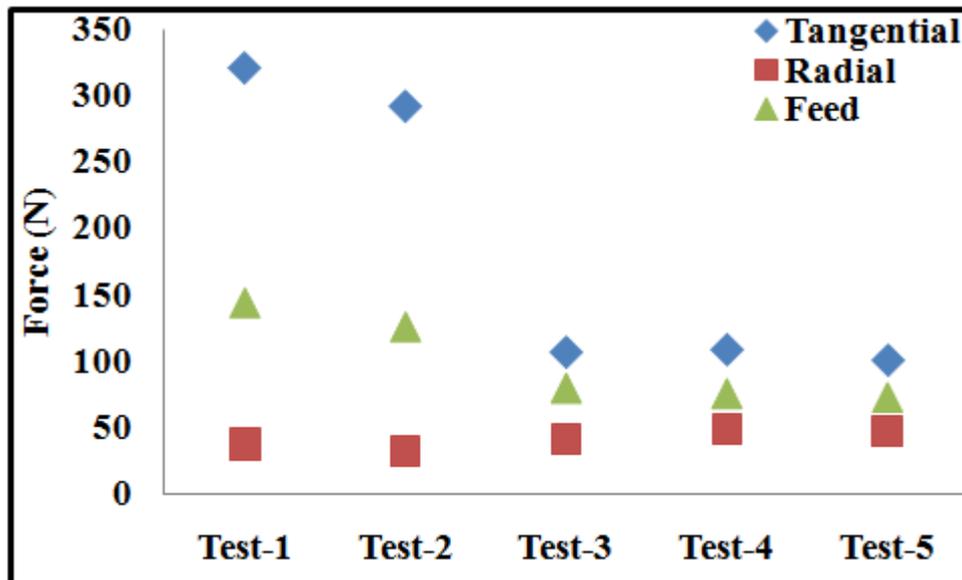

Figure 4-12: Generated cutting force variation for different tooling system and cooling conditions for Ti6Al4V cutting.

Figure 4-12 shows that an improvement in forces is achieved when cutting with SPRT tool compared to conventional turning tool in all cooling conditions. In machining Ti6Al4V, tangential and feed forces obtained in SPRT process decrease 67% and 44% compared to conventional one in dry cutting conditions. Moreover, when SPRT results with coolant cutting are examined, 63% and 39% reductions are found in tangential and feed directions, respectively. Reduction in work done for chip formation with lowered friction conditions is likely to cause lowered component forces. It is also easily seen that in all cooling conditions, SPRT tool causes higher radial force component

compared to conventional one due to larger effective tool obliquity caused by tool rotary motion. Cutting with MQL in SPRT process results lower force components in tangential and feed directions. Minimum radial forces in SPRT process is achieved by dry cutting conditions.

4.4   Summary

Observations of conventional turning and SPRT tests bring some conclusions. SPRT process results in longer tool lives for various materials especially difficult to cut alloys even tool life normalization is applied to conventional turning tool. Lowered component forces except in radial direction are found when cutting tests are conducted in SPRT compared to conventional turning. In SPRT process, surface scratches are in different direction from feed direction due to process kinematic and machined surface roughness in circumferential direction is better compared to conventional turning. Circularity of machined surface with SPRT shows promising results. Tool velocity variation results show that at lower cutting velocities a good agreement between analytical and experimental results of tool velocity.

CHAPTER 5 EXPERIMENTAL RESULTS FOR ADRT PROCESS

All testing plan mentioned in Chapter 3 for ADRT operation for tool life and surface quality is executed and successfully completed. Different data is collected through measurements done during cutting tests. Worn cutting edges and surface roughness of machined parts are analyzed using NanoFocus. SEM analysis makes it possible to take a closer look to worn cutting edge. Mitutoyo CMM measures the roundness of workpieces after cutting tests. In this section tool life and surface quality results are exhibited.

Figure 5-1 shows the position of ADRT tool on Mori Seiki NTX2000 Mill-Turn machining center with rotary tool inclination angle (β).
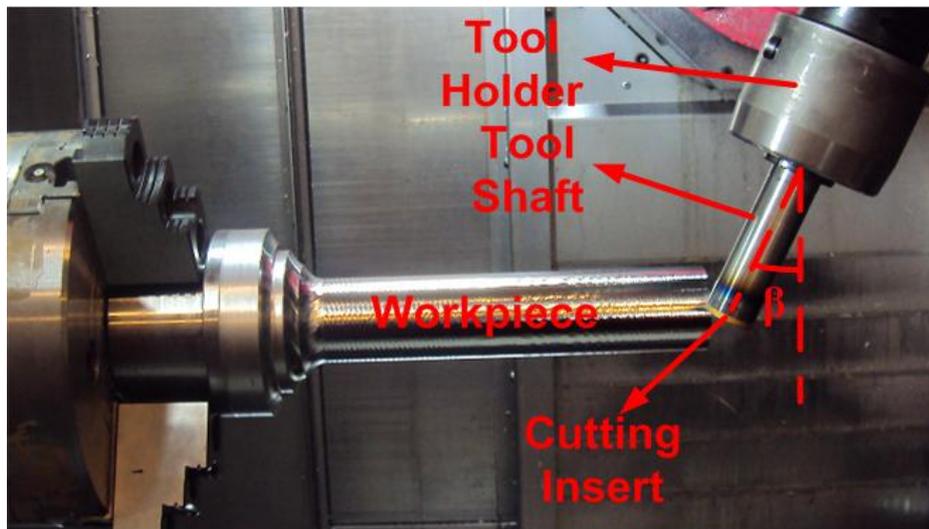
Figure 5-1: Position of ADRT tool and workpiece on Mori Seiki NTX2000 machining center.

5.1   AISI 1050 Steel

The AISI 1050 steel cutting test conditions for tool wear and surface quality are explained in Chapter 3 in detail in Table 3-19 and Table 3-23. The used workpiece material has 100 mm diameter with 150 mm cutting length. The obtained results are presented as follows.

5.1.1 Tool Wear

Tool wear results of ADRT process for AISI 1050 steel cutting tests for different rotary tool velocities, rotary tool inclination angles and cooling conditions are presented. Figure 5-2, Figure 5-3 and Figure 5-4 give the tool life results for different rotary tool velocities and for different inclination angles for dry, coolant and MQL cutting conditions, respectively.
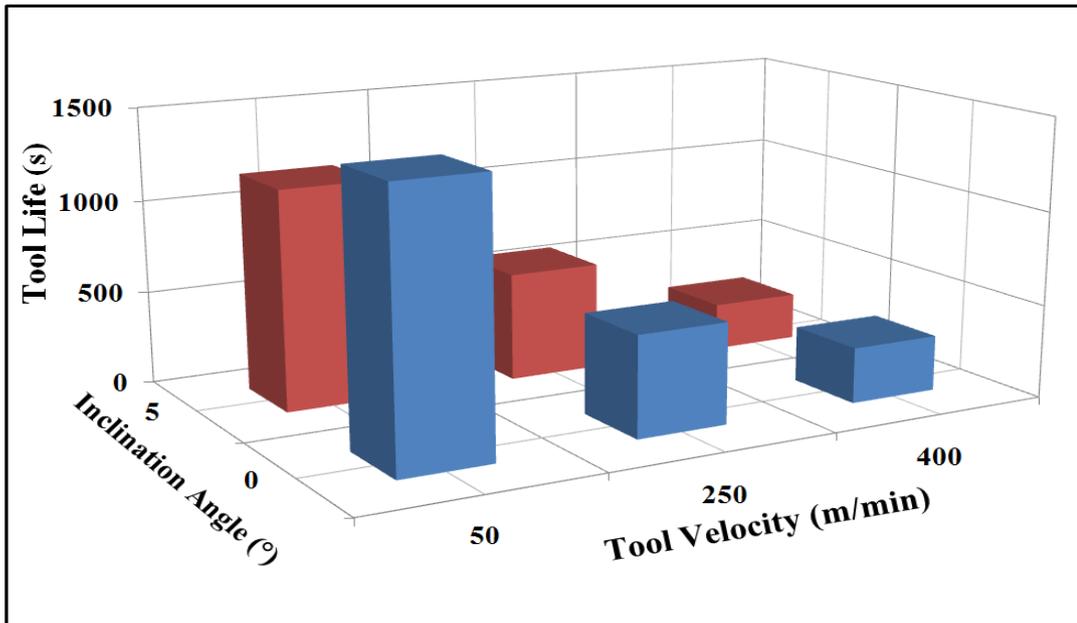
Figure 5-2: Tool life results for different inclination angles and for different tool velocities for dry cutting of 1050 steel.
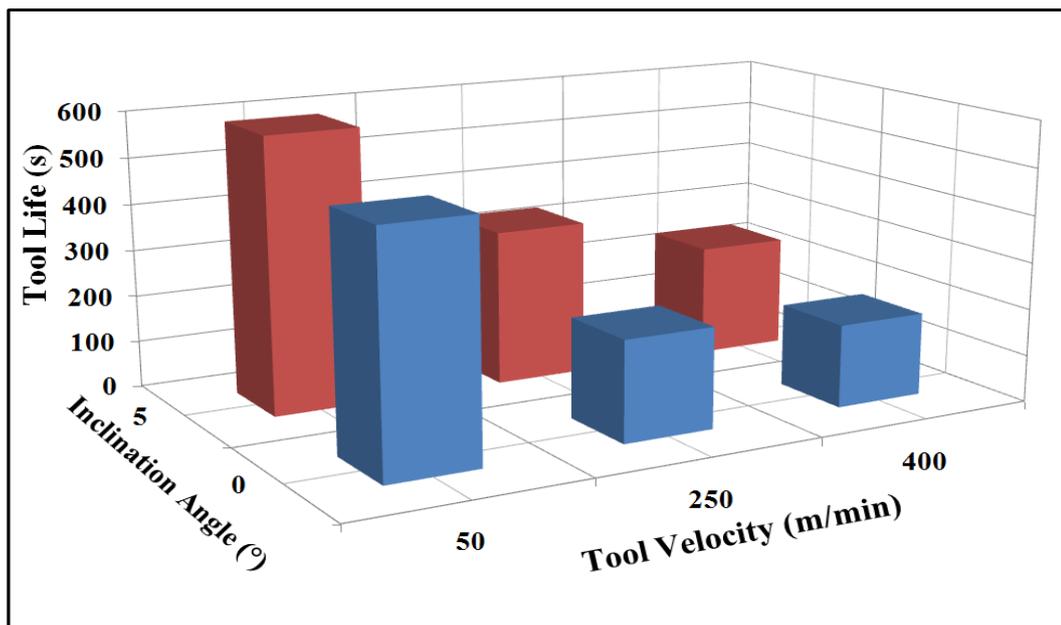
Figure 5-3: Tool life results for different inclination angles and for different tool velocities for coolant cutting of 1050 steel.
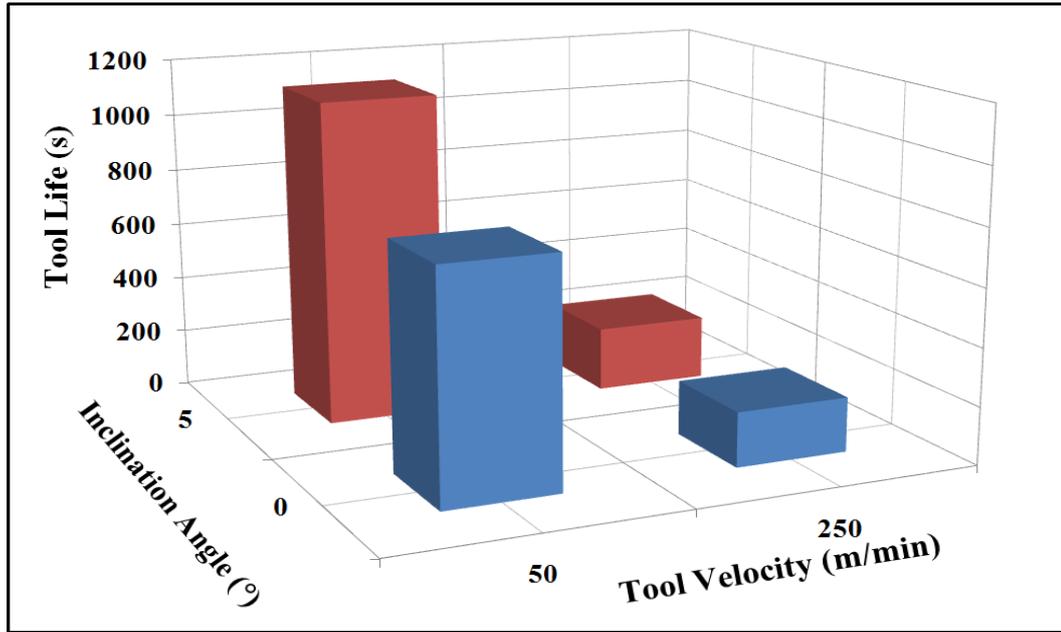
Figure 5-4: Tool life results for different inclination angles and for different tool velocities for MQL cutting of 1050 steel.

Results show that interestingly dry cutting condition gives the best tool life results for AISI 1050 steel. Using coolants, for this tool-workpiece couple, probably increases thermal fatigue action on cutting edge due to tool rotational motion resulting high tool wear rates and low tool lives. It is seen that for both tool inclination angles, reducing tool velocity achieves cutting tool life for all cooling conditions. At 0° inclination angle, 50 m/min tool velocity improves tool life 370% and 180% compared to 400 m/min for dry and coolant cutting conditions, respectively. Moreover, 50 m/min tool velocity prolongs tool life 2.7, 2.3 and 4.2 times compared to 250 m/min tool velocity for dry, coolant and MQL conditions. 250 m/min tool velocity shows more promising tool life results than 400 m/min as seen in figures. At 0° inclination angle, cutting with 250 m/min tool velocity is able to prolong tool life 1.9 and 1.2 times to that of 400 m/min for dry and coolant conditions, respectively. Tool life behavior also seems to be similar at 5° inclination angle such that cutting with 50 m/min improves tool life 2, 2.14 and 5 times compared to 250 m/min for dry, coolant and MQL conditions, respectively. When 400 m/min tool velocity is considered, it is seen that tool wear rate increases. It is found that tool life is one of four and one of three of 50 m/min tool velocity for dry and coolant conditions.

It is seen from figures also that increasing tool inclination angle improves tool life except 50 m/min and 400 m/min for dry cutting condition. At 50 m/min, increasing

inclination angle achieves tool performance 21.8% and 25% for coolant and MQL cutting conditions, respectively. For 250 m/min, the most achievement in tool life is obtained by 18% in MQL cutting condition by increasing inclination angle to 5°. At 400 m/min tool velocity, 5° inclination angle improves tool life 35% compared to 0° when coolant is used. It is also seen that cutting with MQL is the second best alternative after dry cutting for 50 m/min for both inclination angles. When 250 m/min is considered, cutting with coolant improves tool life 13% and 48% in comparison to MQL for 0° and 5° inclination angles, respectively. Although highest tool wear rates are observed in cutting with 400 m/min tool velocity due to shortened cooling time of cutting edge, it is also seen that increasing tool inclination angle results 36% achievement in tool life for coolant condition.

5.1.2   Surface Roughness and Circularity

In this section, surface roughness and circularity results of ADRT process for AISI 1050 steel cutting tests for different rotary tool velocities and rotary tool inclination angles are presented. Figure 5-5 shows the generated surface topography for different cutting conditions.
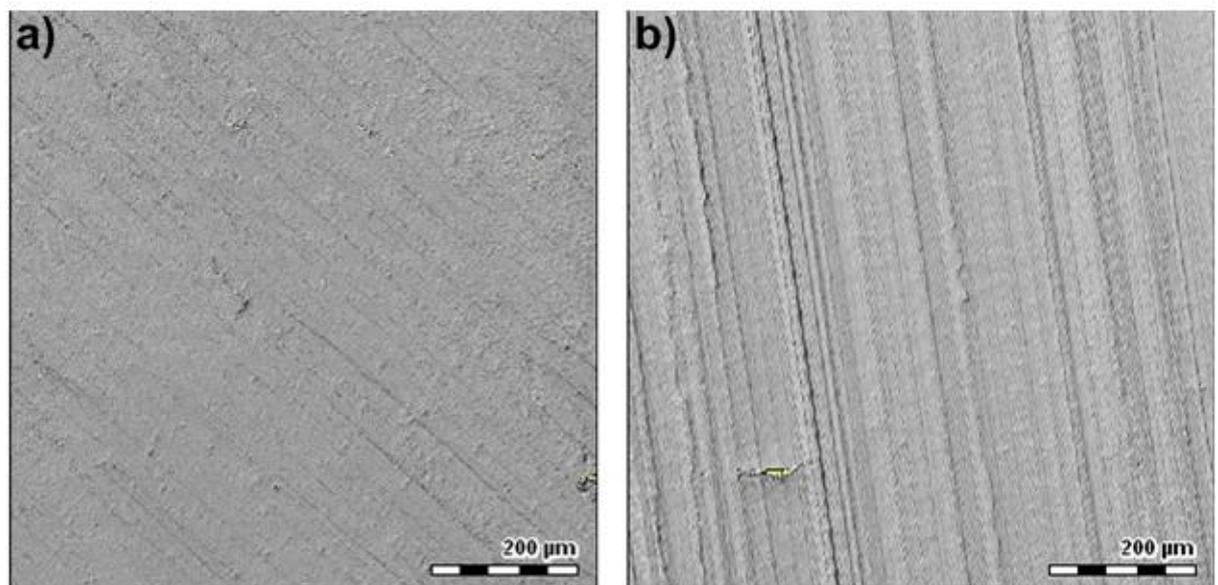
Figure 5-5: Surface topography for a) Test-1 b) Test-6.

Due to the effect of rotary tool spinning action, surface grooves are produced on machined surfaces. However, different tool inclination angles causes surface grooves in different directions. Both surface grooves in Figure 5-5 are found at an angle close to

the effective cutting directions of different cutting tests due to friction conditions of process.

The effects of rotary tool velocities on surface roughness in feed and circumferential directions for 0° and 5° tool inclination angles are presented in Figure 5-6 and Figure 5-7, respectively.
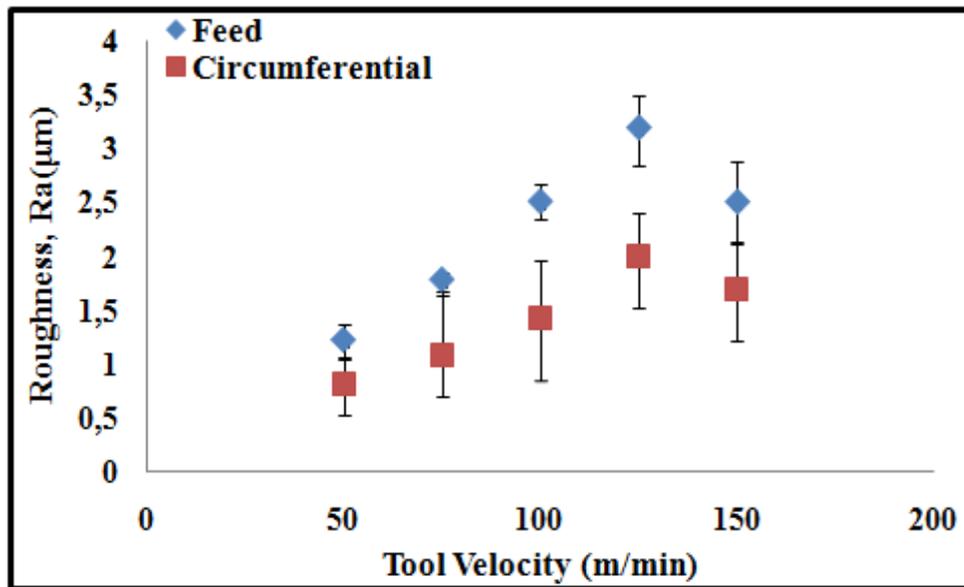
Figure 5-6: Surface roughness variation with tool velocity in feed and circumferential directions for 0º tool inclination angle.
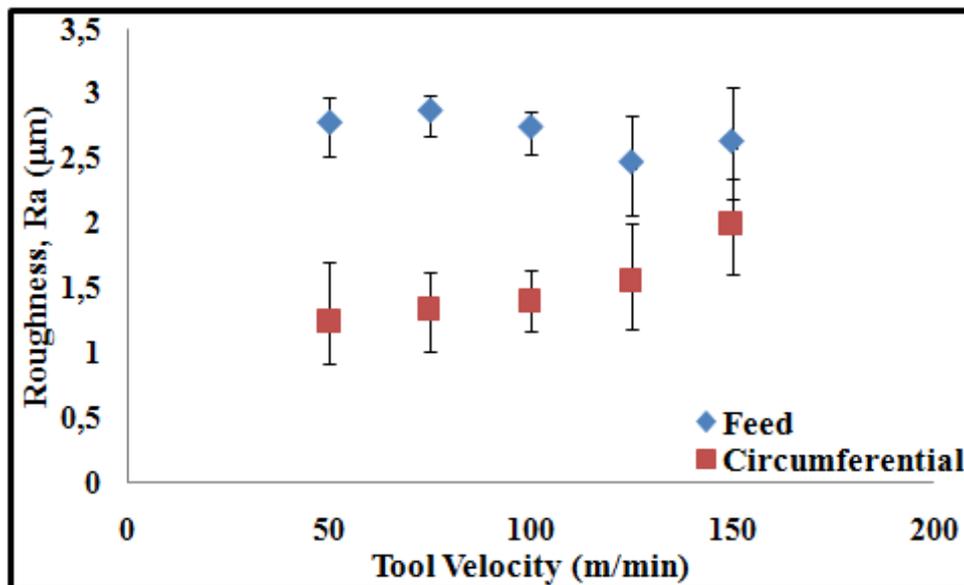
Figure 5-7: Surface roughness variation with tool velocity in feed and circumferential directions 5° of rotary tool inclination angle.

The measured surface roughness values are recorded after one machining pass in order to eliminate any tool wear effect. It is seen from the graphs, surface quality in feed

direction is worse than that in circumferential direction of workpiece. 0° of tool inclination angle with 50 m/min tool velocity shows the minimum surface roughness value in both feed and circumferential directions. In both directions, at 0° of tool inclination angle, change in tool velocity presents the same surface roughness trend such that at 125 m/min tool velocity worst surface quality is attained. At 5° inclination angle, roughness in feed direction is remained relatively constant over different tool velocities, however, in circumferential direction, surface quality deteriorates as tool velocity increases.

The circularity of machined parts is also investigated. The effects of rotary tool inclination angle for different rotary tool velocities on circularity of machined parts are shown in Figure 5-8.
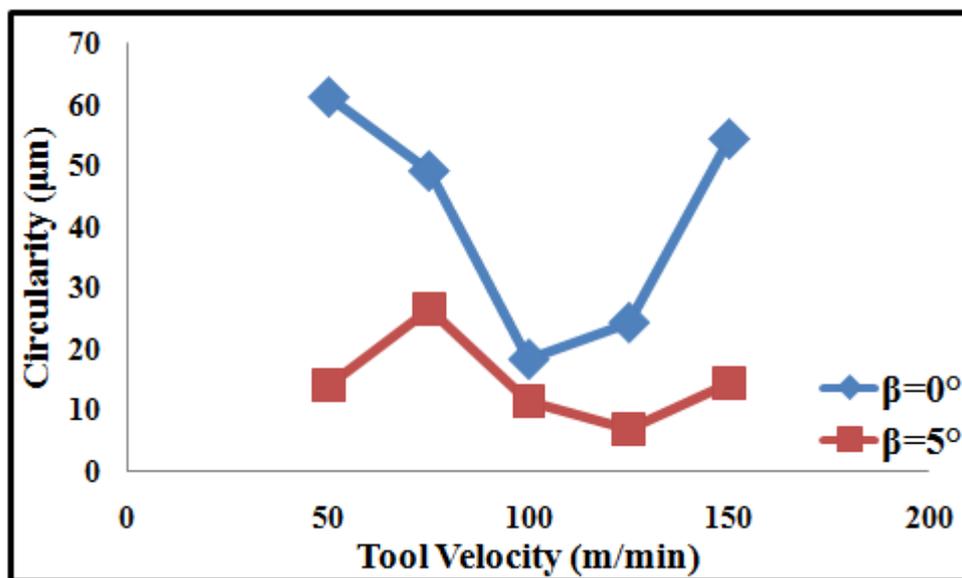
Figure 5-8: Machined workpiece circularity variation with different tool velocities for 0º and 5º of rotary tool inclination angles.

One can see from Figure 5-8 easily that at 5° of tool inclination angle, circularity of machined surface is much better than 0° of that for every single tool velocities. For 0° of tool inclination angle, circularity curve has U shape, such that circularity values decrease as the tool velocity increases up to 100 m/min, then show an increasing behavior when tool velocity reaches up to 150 m/min. Regarding 5° of tool inclination angle, the least circularity value is attained at 125 m/min tool velocity while 75 m/min tool velocity shows highest value.

5.2 Waspaloy

The Waspaloy cutting test conditions for tool wear are explained in Chapter 3 in detail in Table 3-20. The used workpiece material has 215 mm diameter with 27 mm cutting length. The obtained results are presented as follows.

5.2.1 Tool Wear

Tool wear results of ADRT process for Waspaloy cutting tests for different rotary tool velocities, rotary tool inclination angles and cooling conditions are presented. The effects of rotary tool velocities and inclination angles on tool life for dry, coolant and MQL cutting conditions are seen in Figure 5-9, Figure 5-10 and Figure 5-11, respectively.
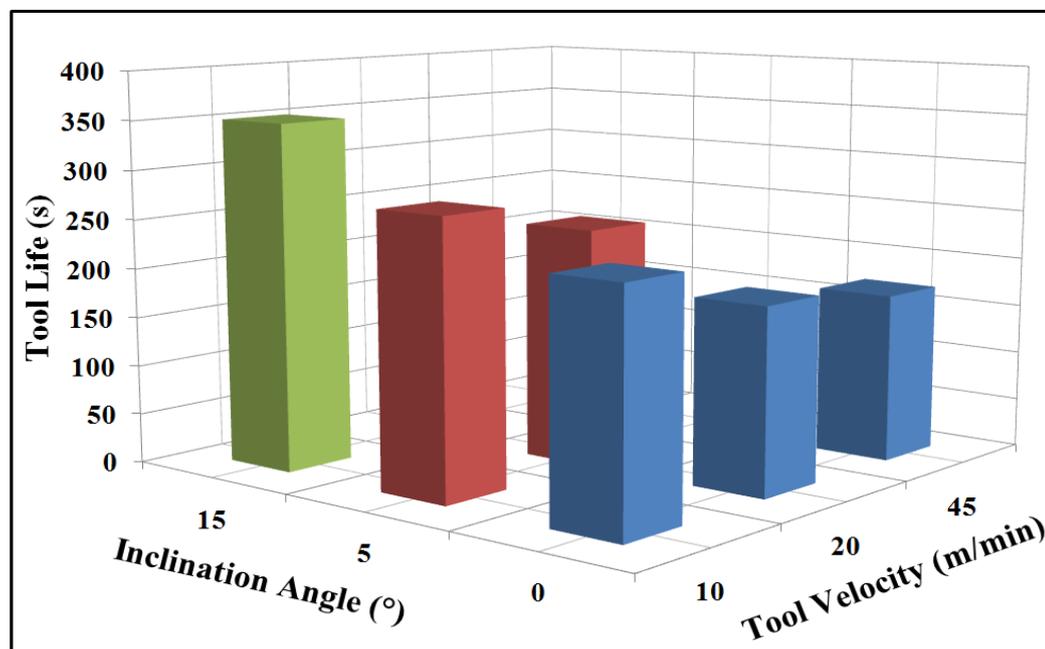
Figure 5-9: Tool life results for different inclination angles and for different tool velocities for dry cutting of Waspaloy.
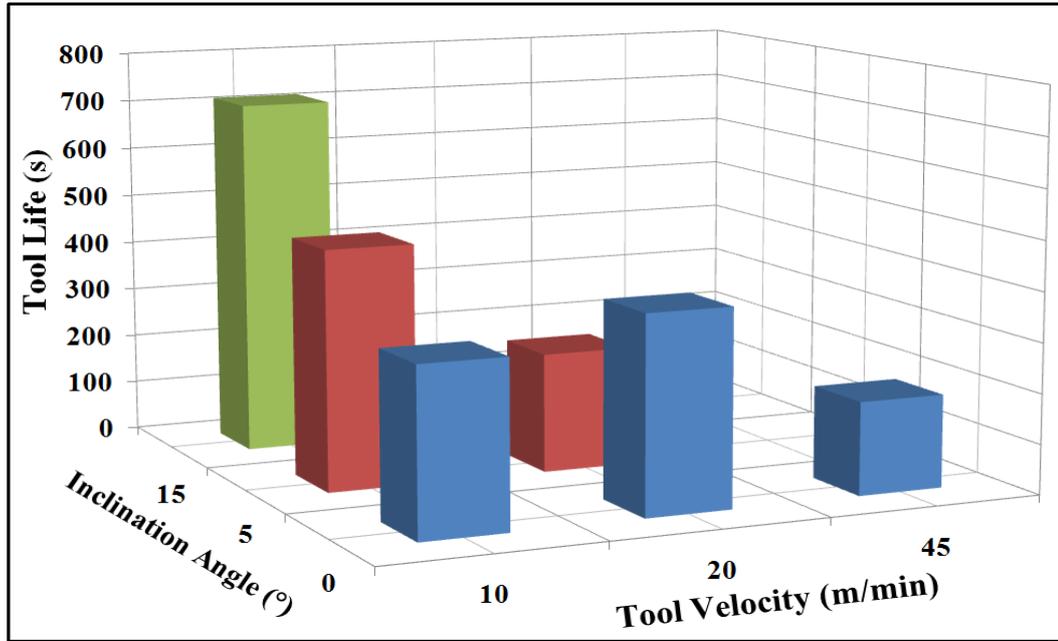
Figure 5-10: Tool life results for different inclination angles and for different tool velocities for coolant cutting of Waspaloy.
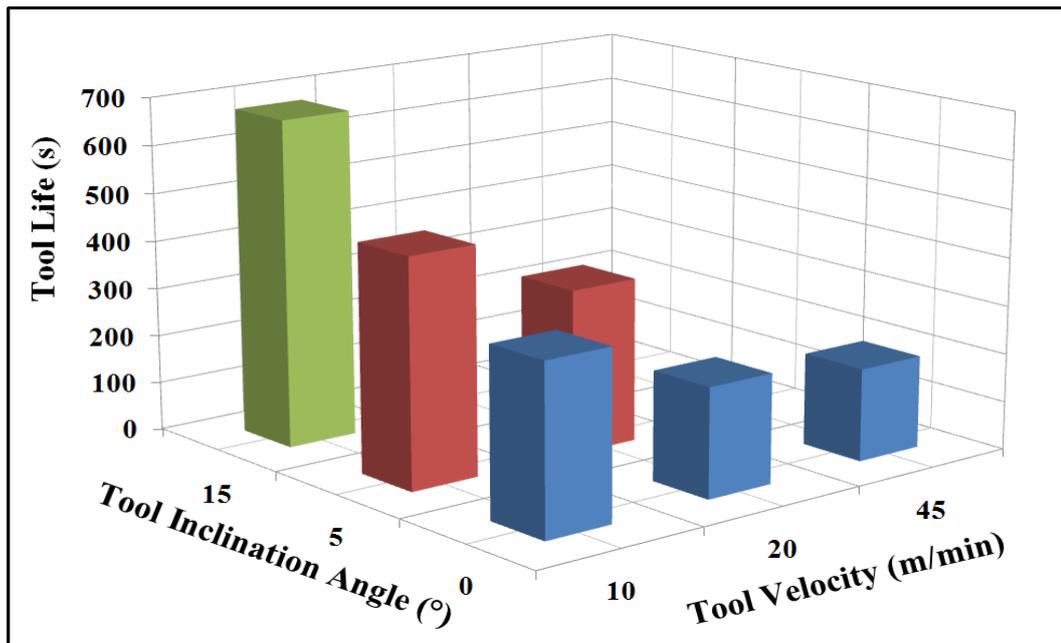
Figure 5-11: Tool life results for different inclination angles and for different tool velocities for MQL cutting of Waspaloy.

It is seen from figures that coolant and MQL conditions give promising tool life results in comparison to dry cutting condition. This can be attributed to effective transportation of cutting fluids to cutting zone by rotational motion of insert resulting efficient cooling of insert. At lower velocities generally higher tool lives are achieved for all cooling conditions. At 0° inclination angle, 10 m/min tool velocity improves tool life 25% and 40% compared to 20 m/min and 45 m/min in dry cutting condition respectively. When

cutting with coolant is taken into consideration, 20 m/min tool velocity is found to be the best choice in the manner of tool life and the tool life is the double of that obtained in 45 m/min tool velocity. As observed in other cooling conditions, 45 m/min tool velocity exhibits the worst tool life results such that 45% and 15% reductions in tool life are found in comparison to 10 m/min and 20 m/min in MQL cutting condition. At 5° inclination angle, lowering tool velocity reduces tool wear rate with prolonged tool life. Cutting with 10 m/min tool velocity improves tool life 15%, 95% and 39% compared to 20 m/min for dry, coolant and MQL cutting conditions, respectively. At 15° inclination angle, when tool reaches its end of life after cutting tests, it is found that tool life for coolant and MQL cutting condition is almost double of that for dry cutting condition.

Increasing tool inclination angle generally prolongs tool life with reducing tool wear rate as observed from figures. For 10 m/min tool velocity, positioning the tool to 15° improves tool life 1.5, 2.15 and 1.94 times in comparison to 0° inclination angle for dry, coolant and MQL cutting conditions, respectively. When tool velocity is doubled, 28% and 50% achievements in tool life are performed by increasing inclination angle to 5° for dry and MQL cutting conditions. However, for coolant cutting condition, it should be pointed out that increasing inclination angle causes almost 40% reduction in tool life. At 45 m/min tool velocity, a significant improvement in tool life could not be achieved in coolant and MQL conditions, yet tool life results are slightly better than dry cutting.
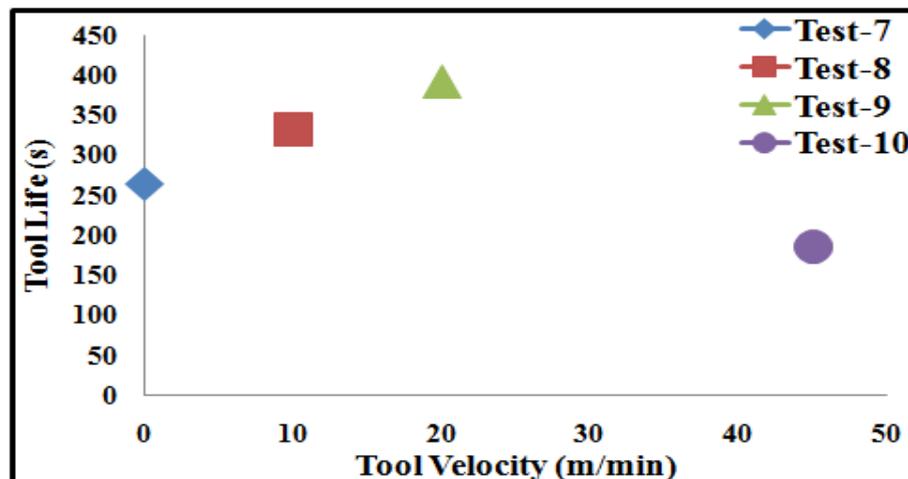
Figure 5-12: Tool Life variation with different tool velocities for 0° tool inclination angle for coolant cutting of Waspaloy.

Figure 5-12 shows comparison of tool lives of conventional turning and rotary turning processes for coolant cutting condition. 0 m/min tool velocity represents fixed tool. In order to compare tool life results properly with conventional one, *normalization* of round insert used in conventional turning test is necessary. Figure 5-12 exhibits the normalized tool life results. 20 m/min tool velocity shows the best tool life. At that tool velocity, tool life increases 43% compared to conventional turning result. At lower and at higher tool velocities, expectation is the reduction of tool life with higher wear rate. At lower tool velocities, due to higher tool workpiece contact time and at higher tool velocities, due to lower cooling time of insert, tool temperature increases resulting lower tool life. Moreover, at 45 m/min tool velocity, tool life reduces 29% compared to conventional turning test result.

5.2.2 SEM Analysis of Worn Tools

In this section, SEM analyses of wear zones on cutting edge for a number of samples are presented in order to inspect the cutting inserts in detail for different cutting conditions of Waspaloy cutting tests. Acceleration voltage used for SEM analyses is 10 kV for each sample. Figure 5-13 shows the SEM image of worn zone of cutting edge of 10 m/min tool velocity for 0º of rotary tool inclination angle for dry cutting.
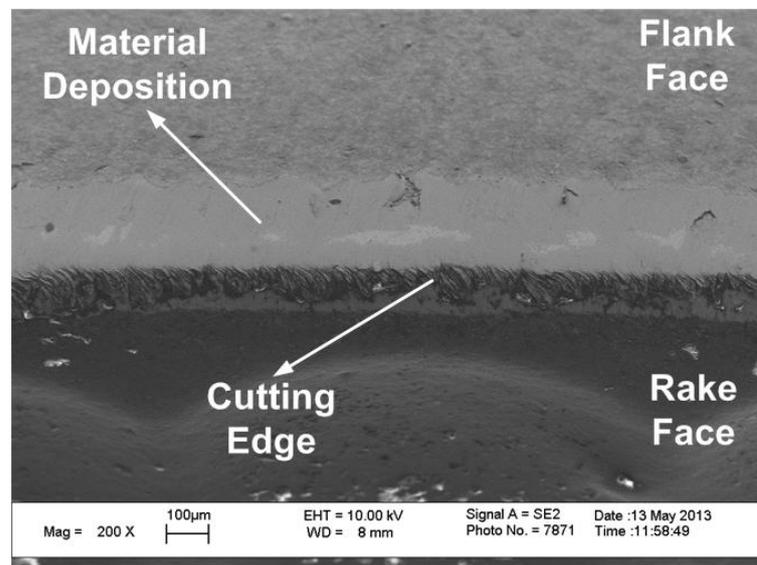
Figure 5-13: SEM image of cutting edge with 200X magnification for 10 m/min rotary tool velocity for 0º of rotary tool inclination angle for dry cutting of Waspaloy.

SEM images of cutting edge for 10 m/min tool velocity for 0º of rotary tool inclination angle for coolant and MQL cooling conditions are shown in Figure 5-14 and Figure 5-15, respectively.

64
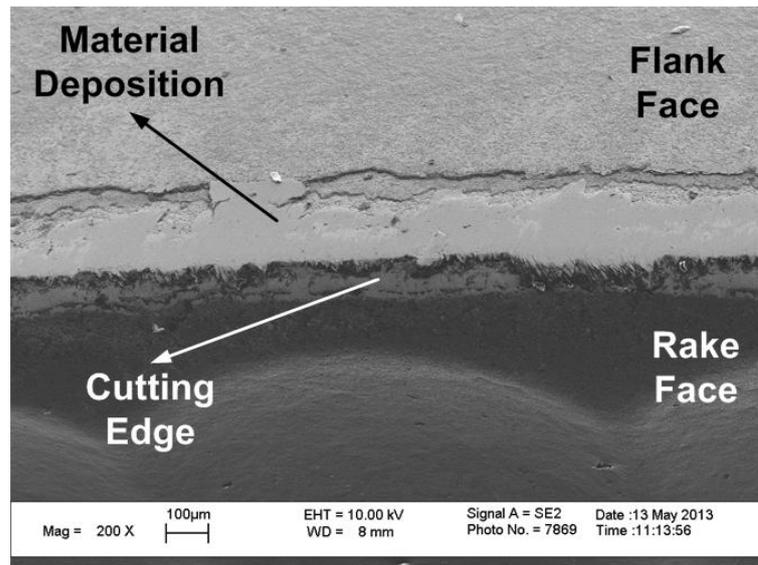
Figure 5-14: SEM image of cutting edge with 200X magnification for 10 m/min rotary tool velocity for 0º of rotary tool inclination angle for coolant cutting of Waspaloy.
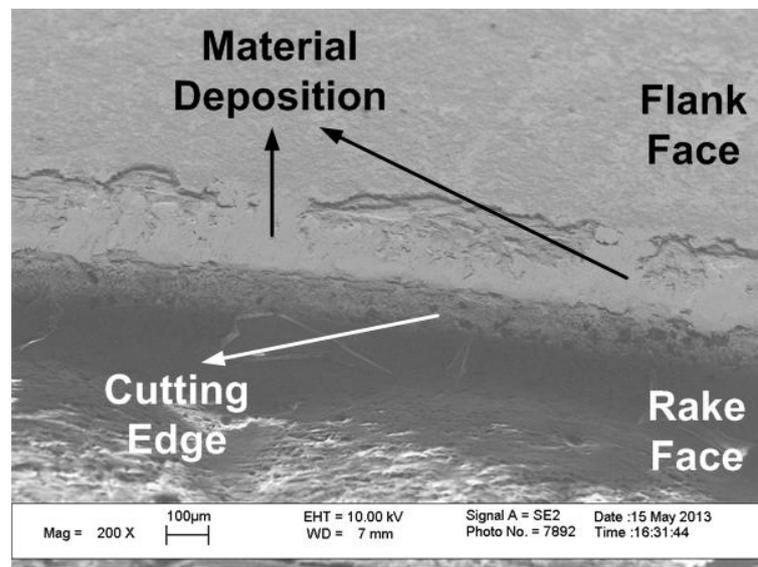
Figure 5-15: SEM image of cutting edge with 200X magnification for 10 m/min rotary tool velocity for 0º of rotary tool inclination angle for MQL cutting of Waspaloy.

Typical wear lands for 10 m/min tool velocity for 0° of tool inclination angle for different cooling conditions at 200X magnifications are presented in figures. For better SEM images, samples are coated with carbon film. It is observed that flank wear is the dominant mode of tool failure. Uniform flank wear distribution over entire circumferential of the tool edge due to tool rotational motion can be seen in figures. Moreover, there is no evidence of formation of crater wear on tool rake face. Workpiece material deposition on worn are on flank face is observed in all samples of cutting

inserts. Highest rate of material deposition on flank wear land is observed in dry cutting.

5.3 Ti6Al4V

The Ti6Al4V cutting test conditions for tool wear are explained in Chapter 3 in detail in Table 3-21. The used workpiece material has 135 mm diameter with 50 mm cutting length. The obtained results are presented as follows.

5.3.1 Tool Wear

Tool wear results of ADRT process for Ti6Al4V cutting tests for different rotary tool velocities, rotary tool inclination angles and cooling conditions are presented. The effects of rotary tool velocities and inclination angles on tool life for dry, coolant and MQL cooling conditions are seen in Figure 5-16, Figure 5-17 and Figure 5-18 respectively.
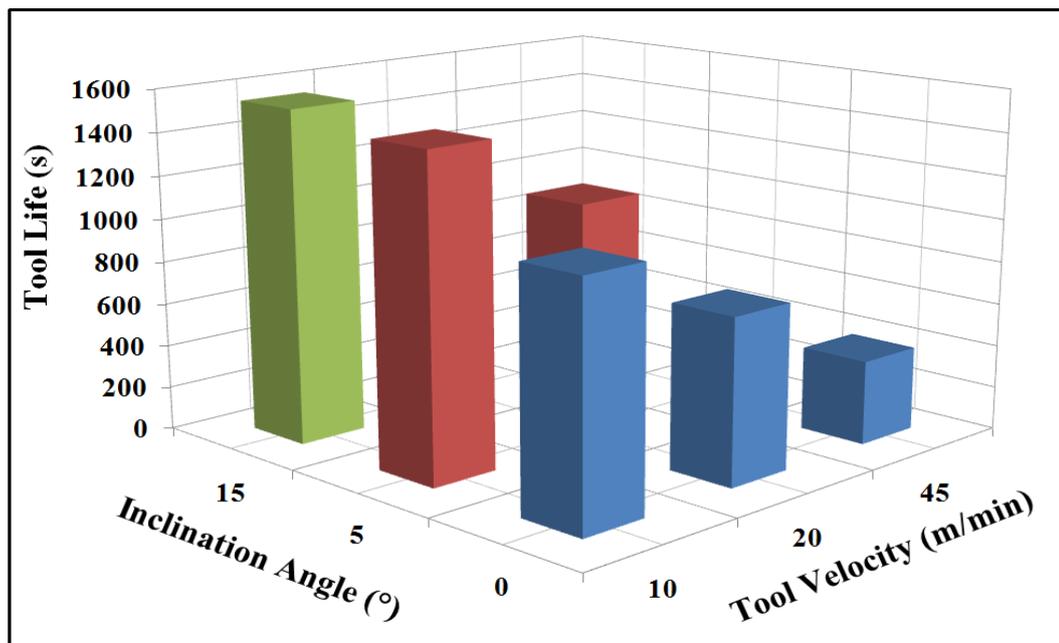
Figure 5-16: Tool life results for different inclination angles and for different tool velocities for dry cutting of Ti6Al4V.
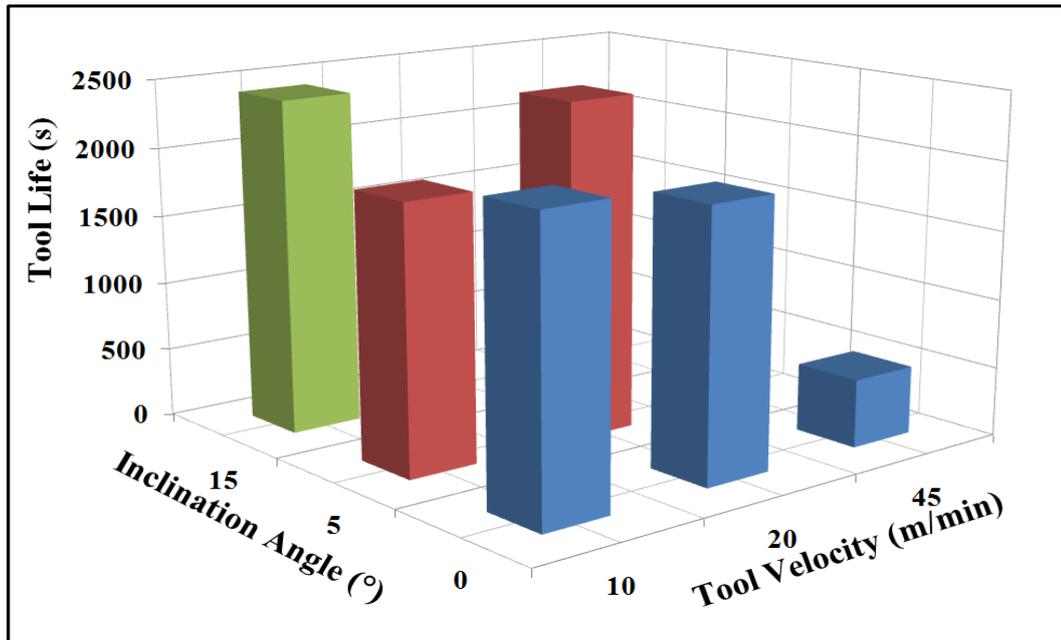
Figure 5-17: Tool life results for different inclination angles and for different tool velocities for coolant cutting of Ti6Al4V.
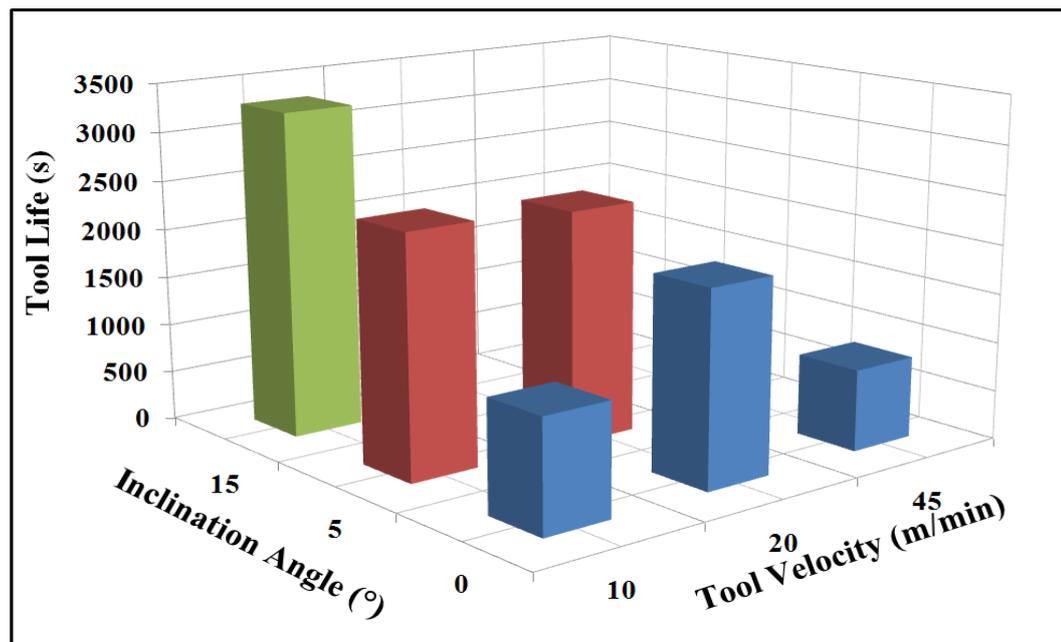
Figure 5-18: Tool life results for different inclination angles and for different tool velocities for MQL cutting of Ti6Al4V.

Cutting with coolant and MQL are more preferable compared to dry cutting conditions for Ti6Al4V cutting tests due to easy penetration of fluids to cutting zone as a result of cutting insert rotational motion. It is also found that lower tool velocities generally show promising tool life results as observed in previous sections. At 0° inclination angle, in dry cutting condition, 43% and 180% improvement in tool life are achieved when cutting with 10 m/min tool velocity compared to 20 m/min and 45 m/min,

respectively. Similarly, at coolant cutting condition, 10 m/min tool velocity improves tool life 4.2 times in comparison to 45 m/min. When MQL cooling condition is considered for 0° inclination angle, 20 m/min tool velocity shows the best tool life result. When 5° inclination angle results are examined, highest tool life results are observed for 10 m/min tool velocity for dry and MQL conditions. In coolant cutting, 20 m/min tool velocity reduces tool wear rate and improves tool life by 27%. At 15° inclination angle, cutting with MQL is more advantageous such that tool life doubled compared to dry cutting.

It is observed from figures that a rise in inclination angle results longer tool life with decreasing tool wear rate. For 10 m/min tool velocity, increasing tool inclination angle from 5° to 15° achieves tool life 41%, 21% and 192% for dry, coolant and MQL conditions, respectively. However, contrary to expectations, increasing inclination angle to 5° causes 10% reduction in tool life compared to 0° in coolant condition. When 20 m/min tool velocity results are examined, tool life is improved by increasing inclination angle to 5°, but the most achievement is observed in dry cutting condition by 46% increase. Obviously, the worst tool life results are observed at 45 m/min tool velocity. In that case even, coolant and MQL improve tool life 27% and 190% compared to dry cutting condition, the observed results are not significant compared to other tool velocities.
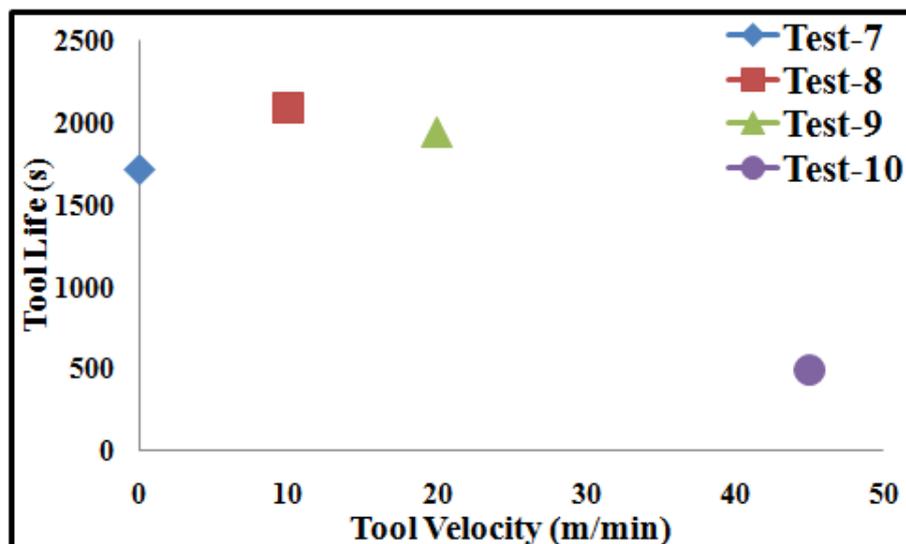
Figure 5-19: Tool flank wear variation with time for different tool velocities for 0° of rotary tool inclination angle for coolant cutting of Ti6Al4V.

Figure 5-19 exhibits the comparison between rotary turning tool and conventional turning tool for coolant cutting condition. 0 m/min tool velocity presents the conventional turning test. *Normalization* of conventional turning insert is required to yield unused portions of tool. It is seen that 10 m/min tool velocity achieves highest tool life result such that tool life increases 22% compared to conventional turning test. Cutting with 45 m/min tool velocity is worthless such that 71% reduction in tool life is observed compared to conventional turning test.

5.3.2 SEM Analysis of Worn Tools

In this section, SEM analyses of wear zones on cutting edge for a number of samples are presented in order to inspect the cutting inserts in detail for different cutting conditions of Ti6Al4V cutting tests. Acceleration voltage used for SEM analyses is 10 kV for each sample. Figure 5-20 shows the SEM image of worn zone of cutting edge of 10 m/min tool velocity for 0º of rotary tool inclination angle for dry cutting.

Figure 5-20: SEM image of cutting edge with 200X magnification for 10 m/min tool velocity for 0º of rotary tool inclination angle for dry cutting of Ti6Al4V.

SEM images of cutting edge for 10 m/min tool velocity for 0º of rotary tool inclination angle for coolant and MQL cooling conditions are shown in Figure 5-21 and Figure 5-22, respectively.

Figure 5-21: SEM image of cutting edge with 200X magnification for 10 m/min tool velocity for 0º of rotary tool inclination angle for coolant cutting of Ti6Al4V.

Figure 5-22: SEM image of cutting edge with 200X magnification for 10 m/min tool velocity for 0º of rotary tool inclination angle for MQL cutting of Ti6Al4V.

Figures exhibit typical wear lands for 10 m/min tool velocity for 0° of tool inclination angle for different cooling condition at 200X magnification. Carbon film coating is applied for better SEM images. Uniformly distributed flank wear on tool edge is observed in all samples with practically no formation of crater wear. Material deposition is not as much as observed in Waspaloy samples. Material deposits slightly on wear land for dry and coolant conditions while almost no material deposition is attained in MQL cutting.

5.4   Inconel 718

The Inconel 718 cutting test conditions for tool wear are explained in Chapter 3 in detail in Table 3-22. The used workpiece material has 180 mm diameter with 30 mm cutting length. The obtained results are presented as follows.

5.4.1   Tool Wear

Tool wear results of ADRT process for Inconel 718 cutting tests for different rotary tool velocities, rotary tool inclination angles and cooling conditions are presented. The effects of rotary tool velocities and inclination angles on tool life for dry, coolant and MQL cooling conditions are seen in Figure 5-23, Figure 5-24 and Figure 5-25 respectively.
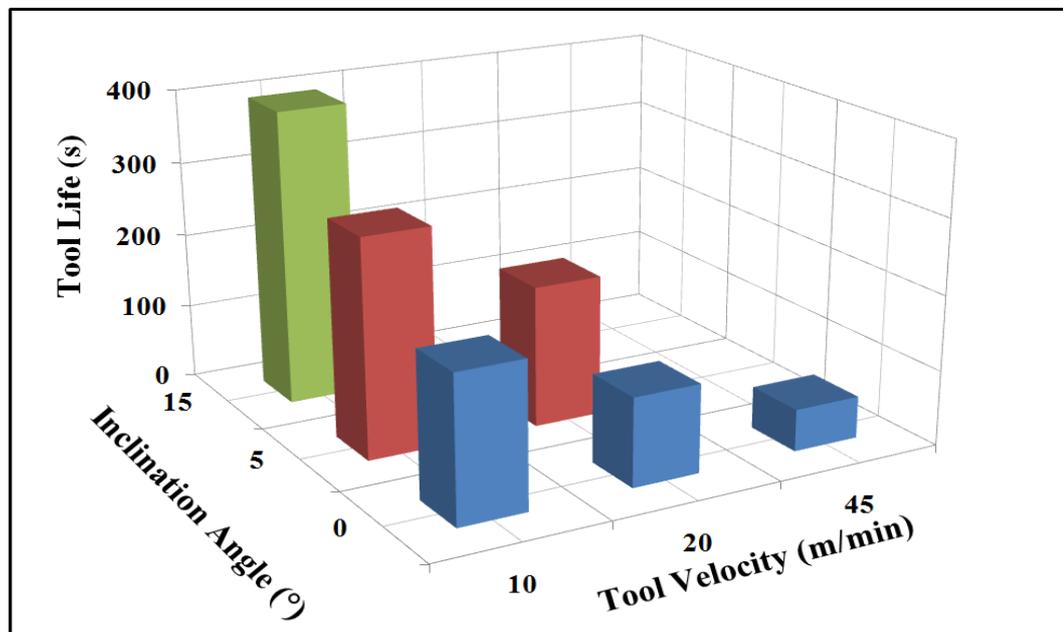
Figure 5-23: Tool life results for different inclination angles and for different tool velocities for dry cutting of Inconel 718.
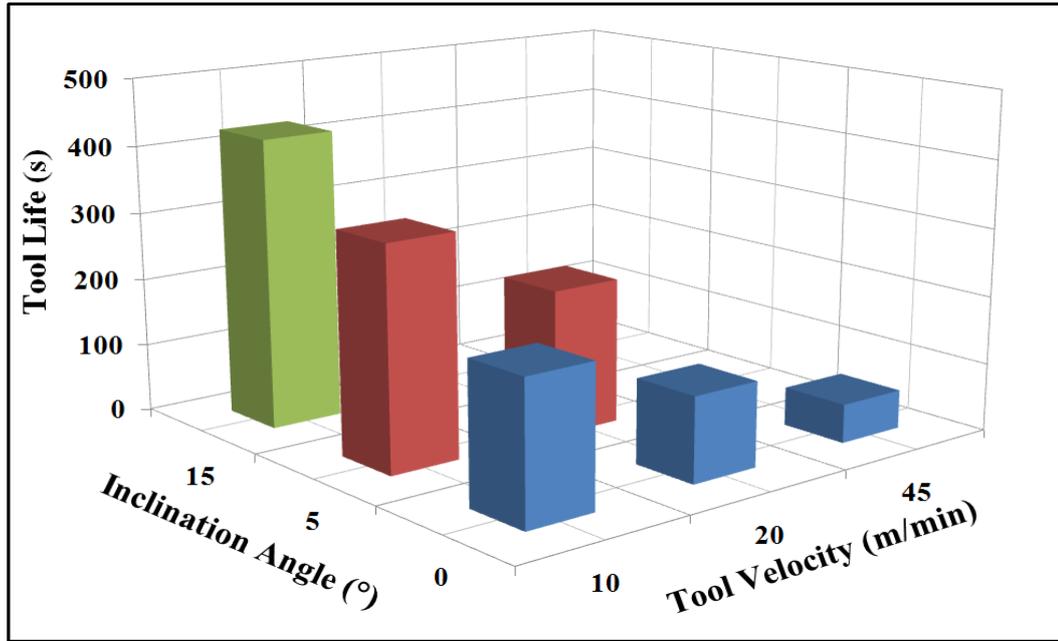
Figure 5-24: Tool life results for different inclination angles and for different tool velocities for coolant cutting of Inconel 718.
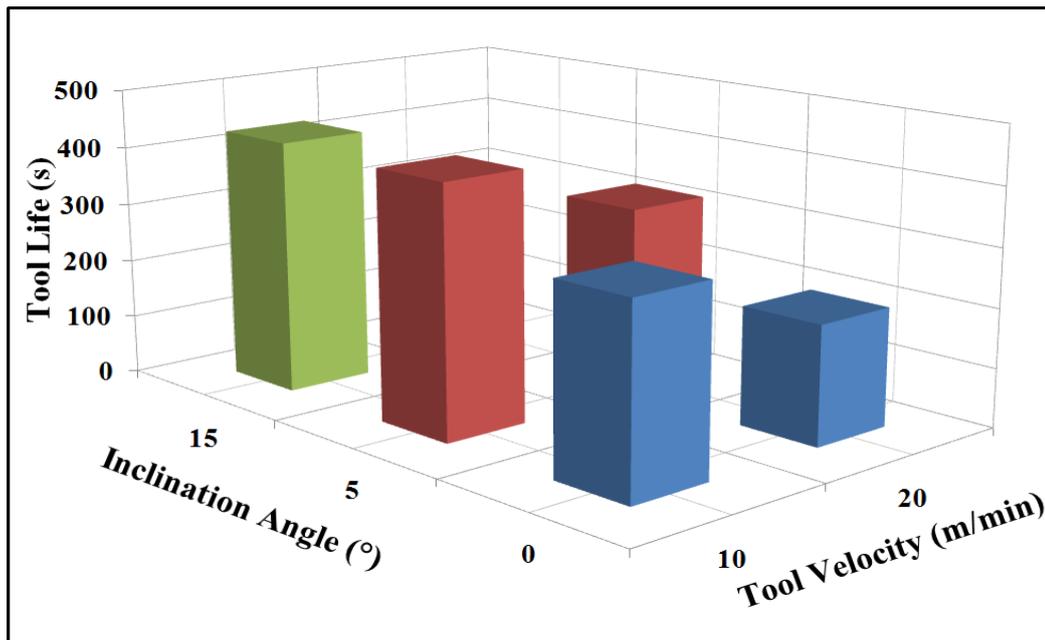
Figure 5-25: Tool life results for different inclination angles and for different tool velocities for MQL cutting of Inconel 718.

Effective transportation of cutting fluids to cutting zone improves the performance of cutting insert as seen from the figures. Lowering tool velocity results higher tool lives for all inclination angles and cooling conditions. 62% and 65% achievements in tool life are observed when cutting with 10 m/min tool velocity compared to 20 m/min at 0° inclination angle for dry and coolant cutting conditions, respectively. Using 20 m/min tool velocity instead of 45 m/min doubles the tool life for all cooling conditions at 0°

inclination angle. When 5° inclination angle tool life results are examined, cutting with MQL gives the best solution. 10 m/min tool velocity prolongs tool life 55%, 52% and 32% compared to 20 m/min for dry, coolant and MQL cutting conditions, respectively. At 15° inclination angle, coolant and MQL show similar tool life results that are slightly better than dry cutting condition.

It is found that increasing tool inclination angle yields an improvement in tool life in all cooling conditions. When tool rotates at 10 m/min, increasing inclination angle from 0° to 15° has a progress in tool life 93% and 107% for dry and coolant cutting conditions, respectively. When MQL cutting condition is considered, similar tool wear behaviors are observed for both 5° and 15° inclination angles. For 20 m/min tool velocity, to increase inclination angle to 5° results significant changes in tool life such that 60%, 72% and 59% improvements in tool lives are achieved for dry, coolant and MQL cutting conditions, respectively. It is seen that cutting insert reaches its end of life very rapidly even in cooling cutting condition when tool rotates at 45 m/min. As a result, it is meaningless to machine Inconel 718 at that tool velocity in the manner of tool life.

5.4.2 SEM Analysis of Worn Tools

In this section, SEM analyses of wear zones on cutting edge for a number of samples are presented in order to inspect the cutting inserts in detail for different cutting conditions of Inconel 718 cutting tests. Acceleration voltage used for SEM analyses is 10 kV for each sample. Figure 5-26 shows the SEM image of worn zone of cutting edge of 10 m/min tool velocity for 0º of rotary tool inclination angle for MQL cutting.
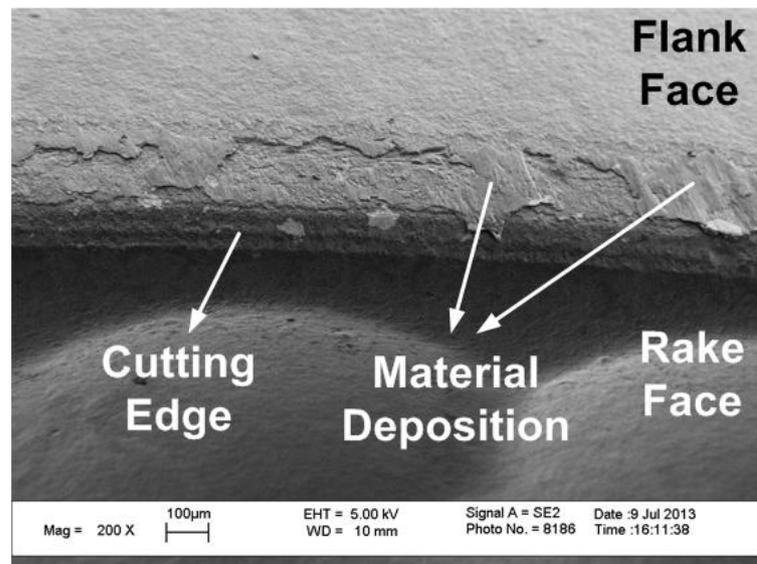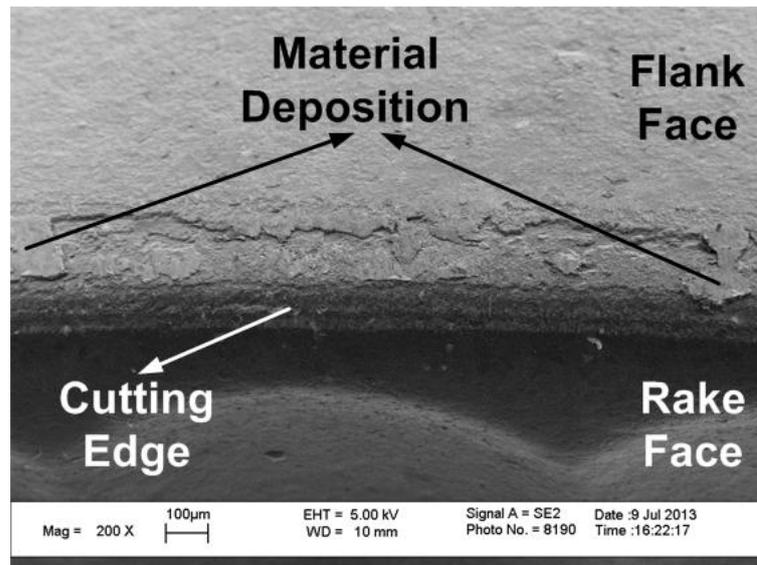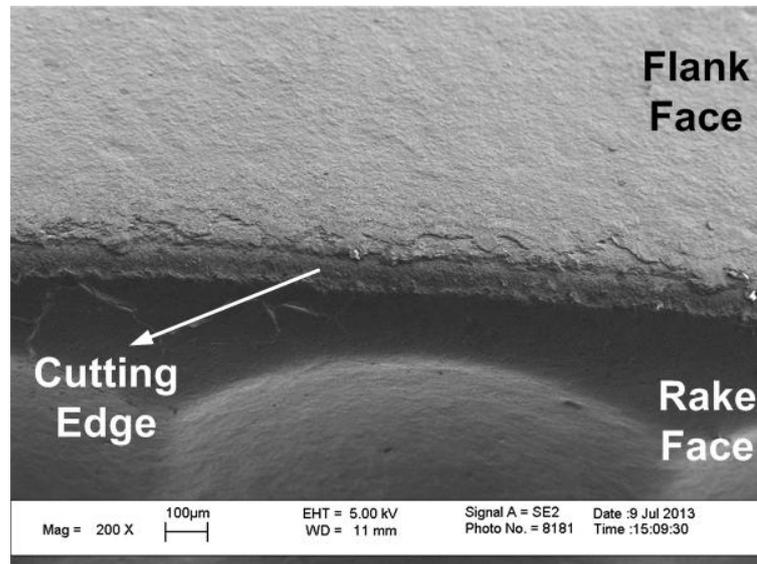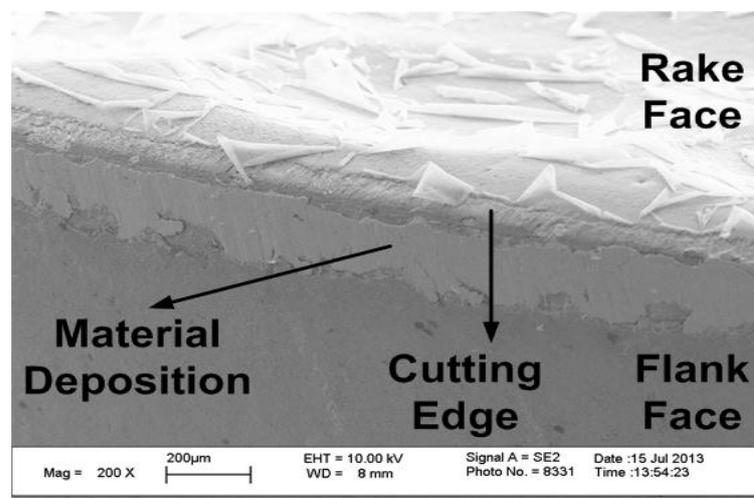

Figure 5-26: SEM image of cutting edge with 200X magnification for 10 m/min tool velocity for 0º of rotary tool inclination angle for MQL of Inconel 718.

SEM images of cutting edge for 10 m/min tool velocity for MQL cooling condition for 5º and 15º of rotary tool inclination angle are shown in Figure 5-27 and Figure 5-28, respectively.
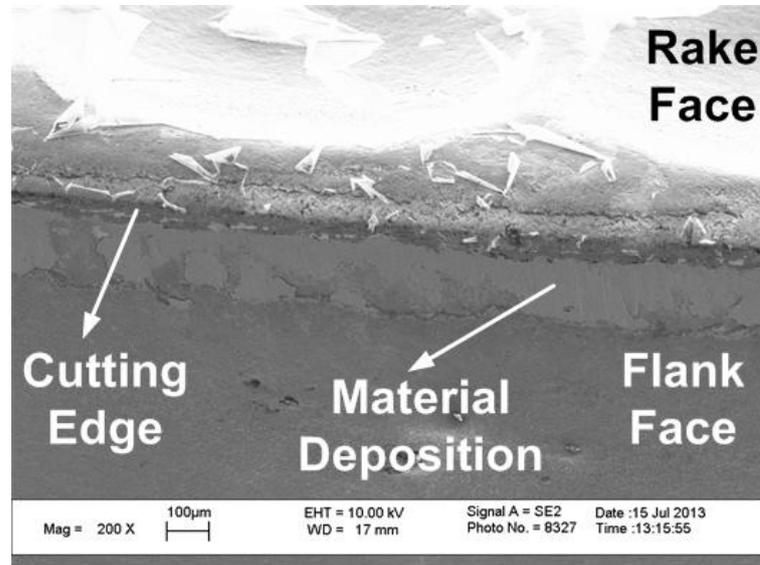
Figure 5-27: SEM image of cutting edge with 200X magnification for 10 m/min tool velocity for 5º of rotary tool inclination angle for MQL of Inconel 718.
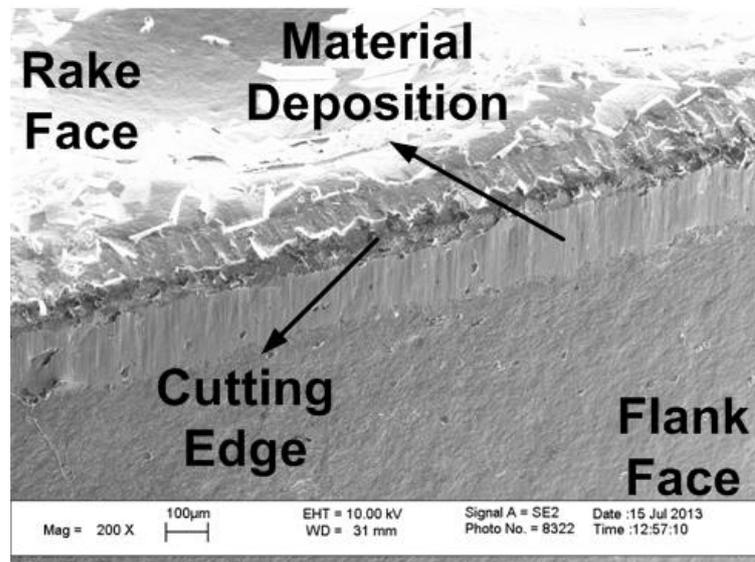
Figure 5-28: SEM image of cutting edge with 200X magnification for 10 m/min tool velocity for 15º of rotary tool inclination angle for MQL of Inconel 718.

SEM images of worn areas of inserts used for Inconel 718 tests for 10 m/min tool velocity for MQL cooling condition for difficult tool inclination angle are shown in figures. Folded and broken carbon film parts on tool rake face are seen due to high rate of carbon coating on sample. Uniformly distributed flank wear on tool edge is observed for all different tool inclination angles. Crater wear is not dominant wear mechanism.

High rate of material deposition on worn areas is observed for all samples. When samples are examined carefully, the directions of grooves on deposited material can be distinguished. These different groove directions are formed due to different tool inclination angles.

5.5   Summary

ADRT cutting tests are conducted for various tool materials and various cutting conditions to clarify the performance of process. It is seen that at the same cooling conditions and tool inclination angles, as tool velocity decreases, tool wear rate generally reduces with increasing tool life, yet, there are some exceptions in Waspaloy and Ti6Al4V. When tool velocity and cooling conditions are kept constant, higher inclination angles usually improve tool lives except a few examples in AISI 1050 steel and Waspaloy. It is also observed that interestingly dry cutting gives the best tool life results in AISI 1050 steel tests while coolant and MQL are effective for difficult to cut alloys. For surface quality, reducing tool inclination angle improves surface in both feed and circumferential directions while deteriorating circularity of machined part. Increasing tool velocity causes a rise in roughness in both feed and circumferential directions up to 125 m/min. SEM images show that adhesion of workpiece material to worn area in dry cutting is found to be more compared to coolant and MQL conditions while tool inclination angle almost no effect on amount of workpiece adhesion.

CHAPTER 6 TOOL TEMPERATURE RESULTS FOR ADRT PROCESS

Test plan given in Chapter 3 for ADRT operation for cutting temperature distribution was carried out. Temperature distribution of tool rake face is recorded by FLIR A325 SC infrared thermal camera and the results are analyzed by ThermaCAM software.

The position of thermal camera with protective window on Mori Seiki NTX2000 Mill-Turn machining center is seen in Figure 6-1.
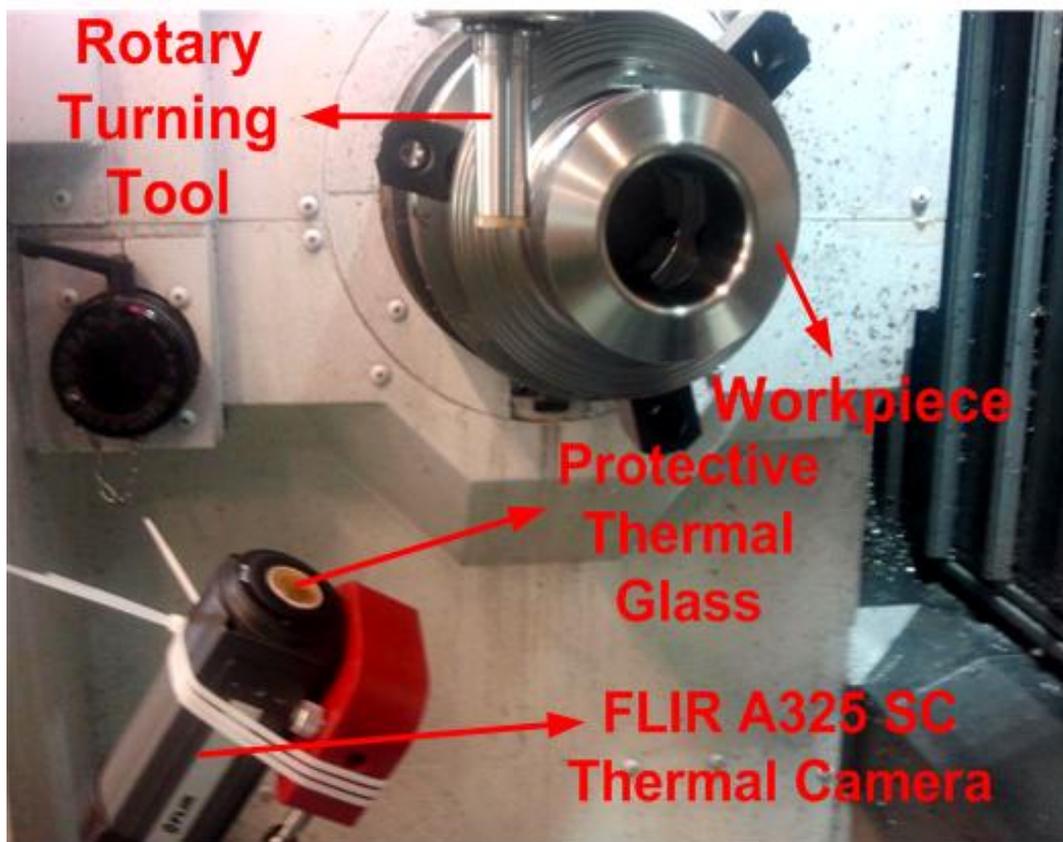
Figure 6-1: Temperature measurement set-up for ADRT cutting tests.

As stated earlier, chip motion between cutting zone and thermal camera prevents taking a clear image. In this section, the obtained best images and results will be presented. Figure 6-2 shows an example of thermal image during cutting. These images are obtained after the tool reaches the steady-state during cutting.
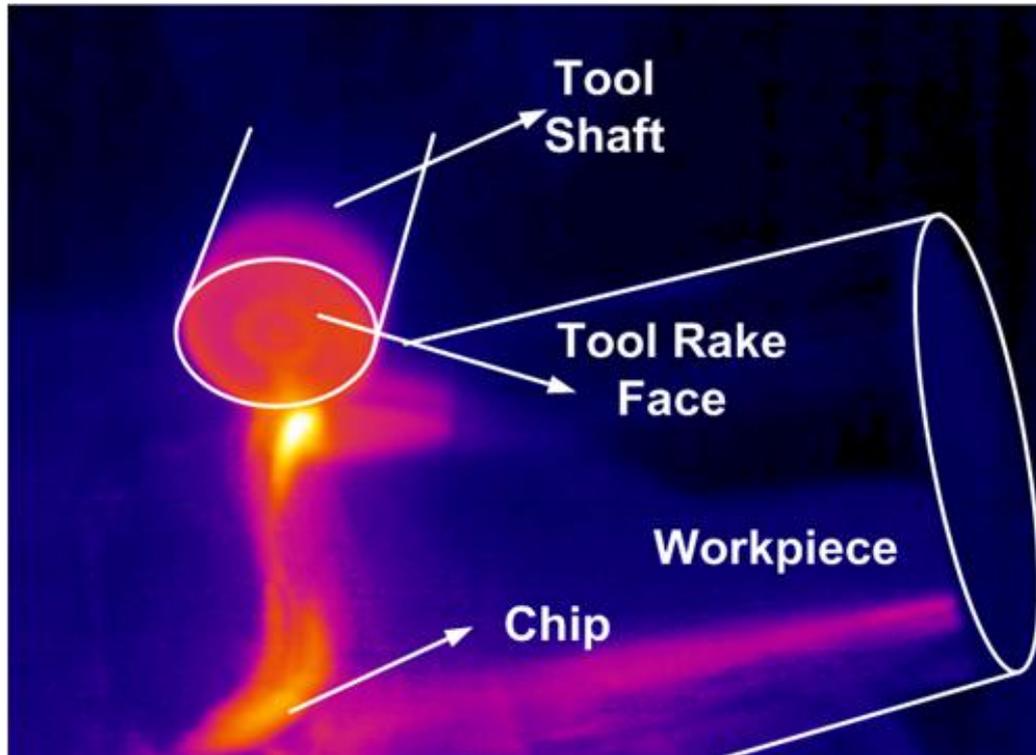
Figure 6-2: An example thermal imaging of rotary cutting.

6.1 AISI 1050 Steel

The AISI 1050 steel cutting test conditions for temperature measurements are explained in Chapter 2 in detail in Table 3-24. The used workpiece material has 80 mm diameter with 150 mm cutting length. The obtained results are presented as follows.

6.1.1 Tool Rake Face Temperature Distribution

In this section, tool rake face temperature distributions for AISI 1050 steel for different rotary tool velocities and rotary tool inclination angles are presented. During experiments, both rotary tool and workpiece rotate in CW direction.

6.1.1.1 0º Rotary Tool Inclination Angle

In this section, best thermal images for different rotary tool velocities at 0º rotary tool inclination angle are presented. Figure 6-3 shows the image for 10 m/min tool velocity.
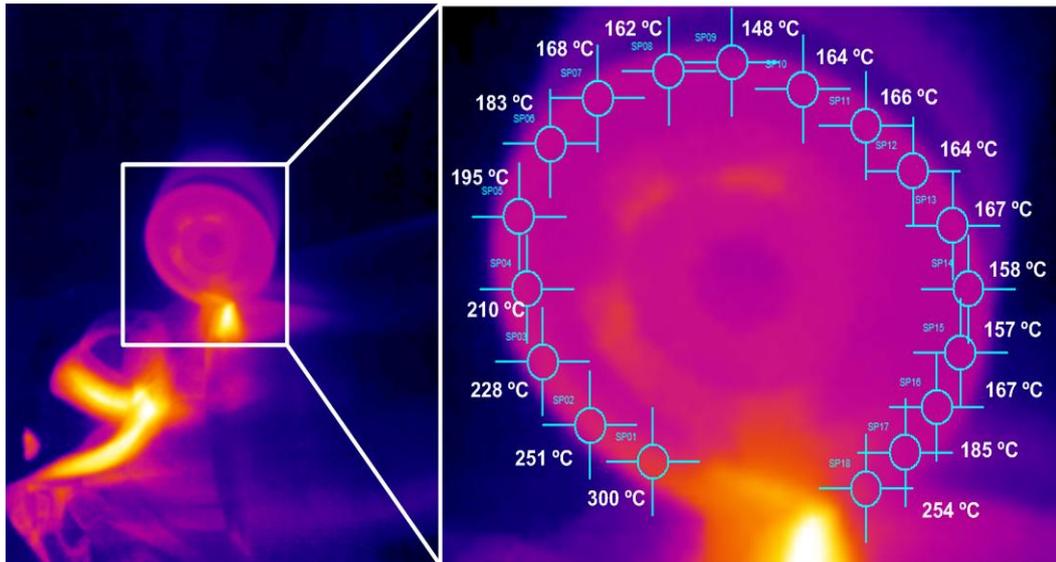
Figure 6-3: Thermal image of tool rake face temperature distribution for 10 m/min tool velocity, 0° of rotary tool inclination angle of AISI 1050 steel cutting.

Close-up views of tool rake face temperature distributions for 25 m/min and 50 m/min tool velocities are seen in Figure 6-4.
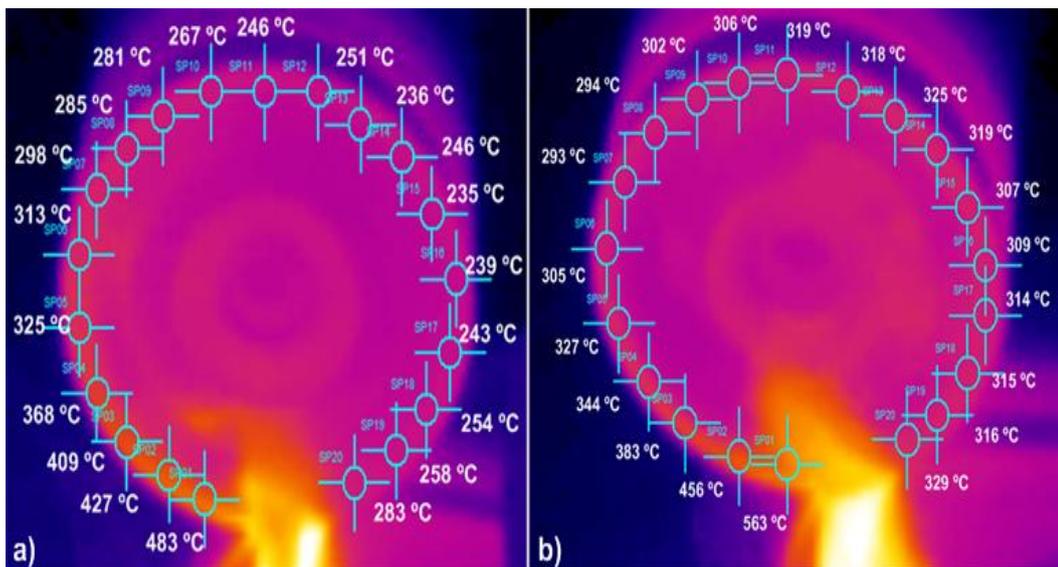
Figure 6-4: Thermal image of tool rake face temperature distribution for a) 25 m/min b) 50 m/min tool velocity for 0° of rotary tool inclination angle of AISI 1050 steel cutting.

Close-up views of thermal images obtained from 150 m/min and 250 m/min tool velocities are shown in Figure 6-5.
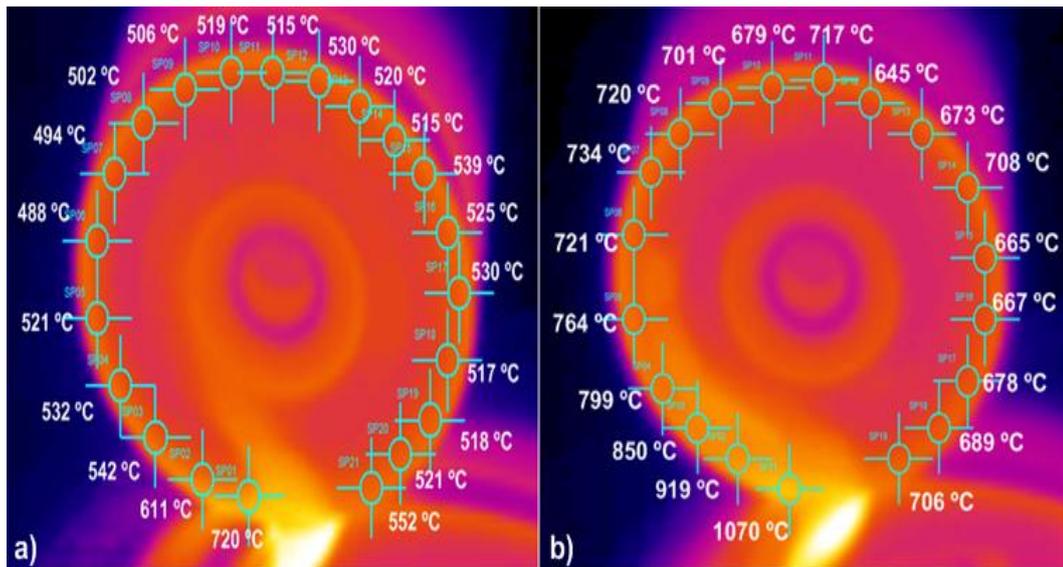
Figure 6-5: Close-up view of thermal image for tool rake face temperature distribution for a) 150 m/min b) 250 m/min tool velocity for 0º of rotary tool inclination angle of AISI 1050 steel cutting.

Temperature distributions on the tool rake face for different tool velocities are presented in the figures above. Although the temperature of the contact zone of tool with chip after leaving cutting region is expected to decrease gradually until re-entering cutting region, the results are not line in that way. Thermal fluctuations on the cutting edge are observed for all tool velocities. Contact zone temperature begins decreasing after the edge leaves cutting region and then a sudden jump to higher temperature is observed. After the jump, the temperature of the contact zone again cools down to a minimum value. Due to rotary tool motion, when the tool contact is near the cutting zone, the temperature again rises to higher temperatures close to cutting temperature. It is also seen from figures that as the tool velocity increases, higher tool temperatures are attained.

6.1.1.2   5º of Rotary Tool Inclination Angle

In this section, the best thermal images for different rotary tool velocities at 5º of rotary tool inclination angle are presented. Figure 6-6 shows the close-up view of the image obtained from cutting tests for 25 m/min tool velocity.
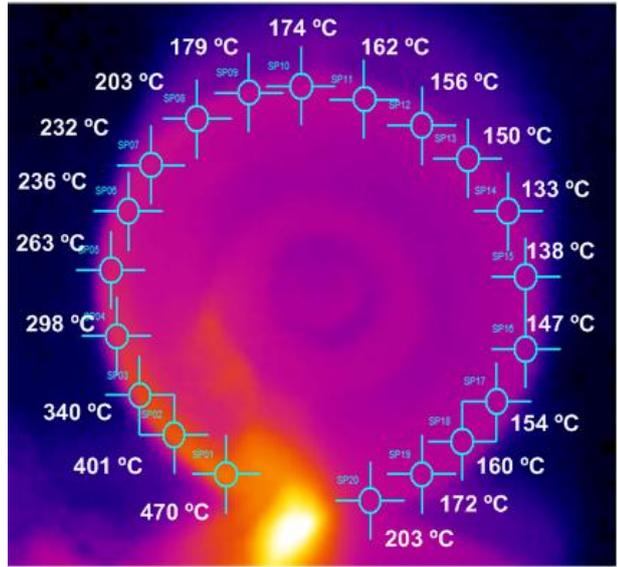
Figure 6-6: Close-up view of thermal image for tool rake face temperature distribution for 25 m/min tool velocity for 5º of rotary tool inclination angle of AISI 1050 steel cutting.

Figure 6-7 exhibits the temperature distribution on tool rake face obtained from thermal images of 50 m/min and 150 m/min tool velocities, respectively.
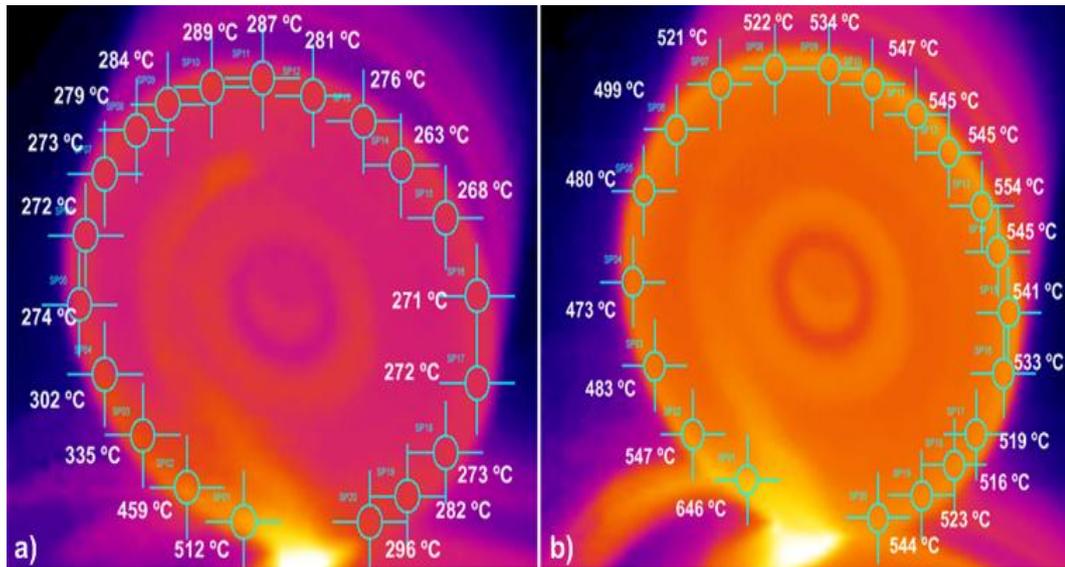
Figure 6-7: Close-up view of thermal image for tool rake face temperature distribution for a) 50 m/min and b) 150 m/min tool velocity for 5º of rotary tool inclination angle of AISI 1050 steel cutting.

For 5° of tool inclination angle, similar tool temperature distribution results are observed with 0° of that. Increasing tool velocity results an increase in temperature at leaving and entering zone of contact region of tool. At 25 m/min tool velocity, fluctuation of temperature on cutting edge is not seen, however, as tool velocity increases, temperature fluctuation rises.

6.1.2 Generated Cutting Temperatures

During temperature measurements, the chip covers the cutting zone and consequently the measured temperature is not the generated cutting temperature but that of the chip. On the other hand, in this study, chip thickness is very small, as a result, the measured temperature is assumed to be equal to or slightly lower than generated cutting temperature.

Figure 6-8 presents the generated cutting temperatures for different rotary tool velocities and for different tool inclination angles of AISI 1050 steel.
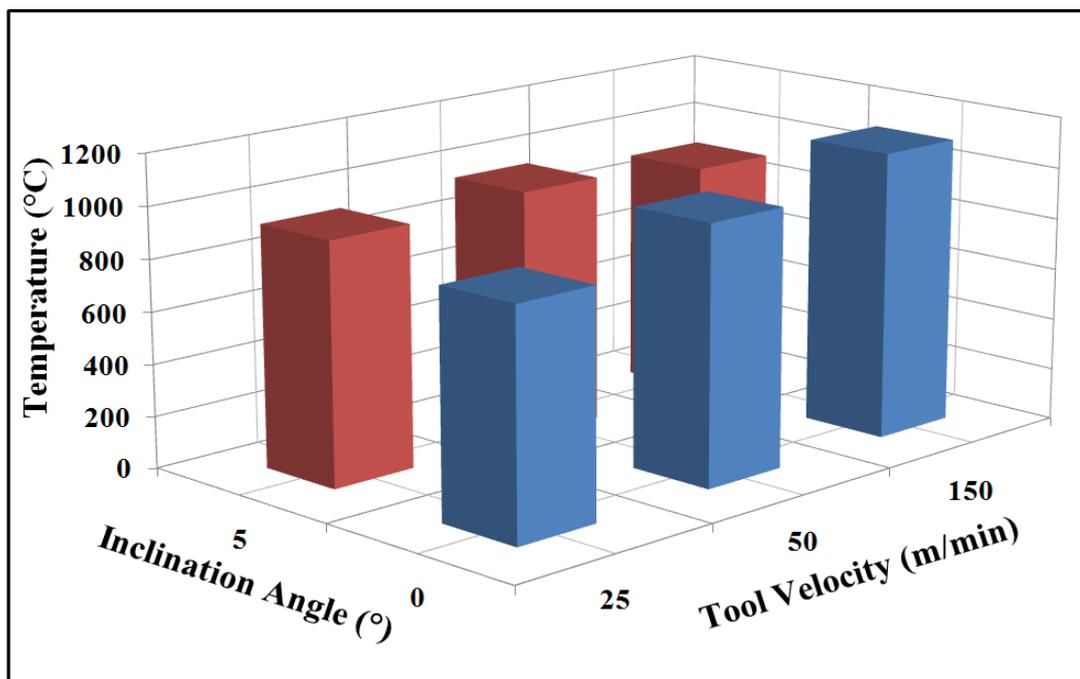
Figure 6-8: Generated cutting temperature variation with tool velocity for 0º and 5° tool inclination angles for AISI 1050 steel.

For 0° of tool inclination angle, at 25 m/min tool velocity, the minimum cutting temperatures are observed. Doubling the tool velocity to 50 m/min, results 15 % increase in cutting temperatures. As tool velocity increases further, the cutting temperature seems to exceed 1100°C. When 5° of tool inclination angle is considered, all temperature results seem to be close to each other. In the case of 50 m/min tool velocity, highest temperature is observed. When tool rotates at 50 m/min, 4% temperature rise is attained compared to half velocity. However, further increase in tool velocity causes reduction in temperature results such that in the case of 150 m/min tool velocity maximum temperature decreases 3% and 6% compared to 25 m/min and 50 m/min, respectively. It is seen from Figure 6-8, in the case of 25 m/min tool velocity,

when tool inclination angle increases from 0° to 5°, 7% decline in maximum temperature is observed. For higher tool velocities the situation changes and lower temperatures are obtained. Rising tool inclination angle causes reduction 4% and 18% in temperature for 50 m/min and 150 m/min tool velocities, respectively.

6.1.3   Cutting Temperature-Tool Life Relation

It is well known that tool wear is generally thermal base and the relation between cutting temperature and tool life is critical. Figure 6-9 shows the relation between cutting temperature and tool life for various tool velocities for 0° inclination angle.
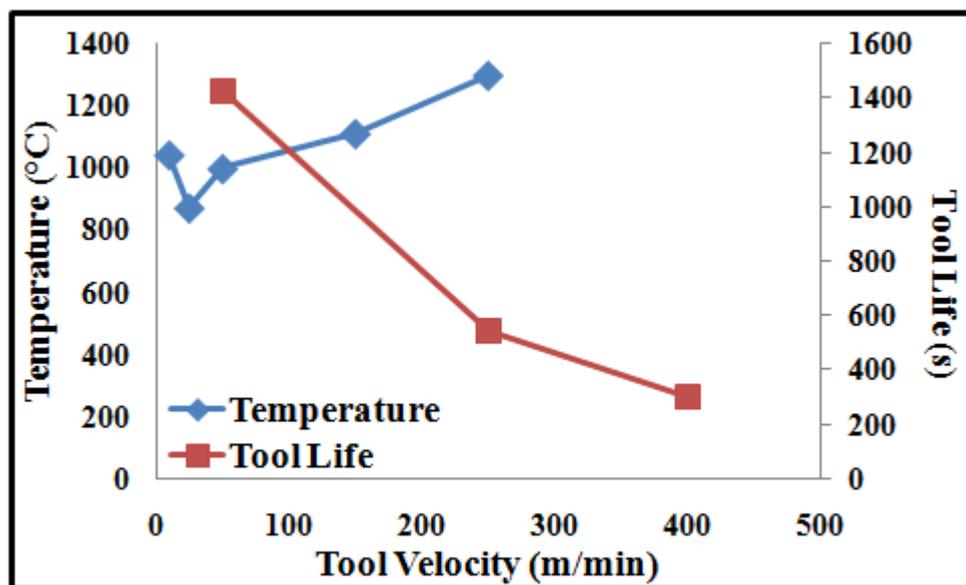
Figure 6-9:   Cutting temperature and tool life variation with tool velocity for 0° inclination angle for AISI 1050 steel.

As stated before, temperature measurements are conducted under dry cutting conditions, as a result tool life results of dry cutting conditions are used for comparison. The correlation between cutting temperatures and tool life is observed as expected such that as tool velocity increases beyond the optimum one cutting temperatures start to increase and thermally induced wear mechanism becomes active. Increasing cutting temperature cause a rise in tool wear rate with reducing tool life. It is seen from Figure 6-9 that when tool velocity is increased from 50 m/min to 250 m/min, cutting temperature also rises from 1000°C to 1270°C due to reduced cooling time of cutting insert resulting almost 60 % reduction in tool life.

6.2 Ti6Al4V

The Ti6Al4V cutting test conditions for tool rake face temperature distribution and generated cutting temperatures are explained in Chapter 3 in detail in Table 3-25. The used workpiece material has 110 mm diameter with 50 mm cutting length. The obtained results are presented as follows.

6.2.1 Tool Rake Face Temperature Distribution

In this section, tool rake face temperature distributions for Ti6Al4V for different rotary tool velocities and rotary tool inclination angles are presented. During experiments, both rotary tool and workpiece rotate in CW direction.

6.2.1.1 0º of Rotary Tool Inclination Angle

In this section, obtained best images for different rotary tool velocities 0º of rotary tool inclination angle are presented. Figure 6-10 shows the image obtained from cutting tests for 3 m/min tool velocity.

Figure 6-10: Thermal image for tool rake face temperature distribution for 3 m/min tool velocity for 0º of rotary tool inclination angle of Ti6Al4V cutting.

Thermal image with close-up view for 5 m/min tool velocity is presented in Figure 6-11.

Figure 6-11: Thermal image for tool rake face temperature distribution for 5 m/min tool velocity for 0º of rotary tool inclination angle of Ti6Al4V cutting.

Close-up views of thermal images obtained from 10 m/min, 15 m/min, 20 m/min and 25 m/min tool velocities are seen in Figure 6-12.

Figure 6-12: Close-up view of thermal image for tool rake face temperature distribution for a) 10 m/min b) 15 m/min c) 20 m/min and d) 25 m/min tool velocity for 0º of rotary tool inclination angle of Ti6Al4V cutting.

For 0° of tool inclination angle, temperature distributions on tool rake face are seen in figures for different tool velocities. Thermal fluctuations on tool cutting edge are observed in all tool velocities. It is seen that higher tool velocity cases cause more irregular thermal fluctuations compared to lower ones. Moreover, as tool velocity increases, the leaving and re-entering temperatures of contact zone seems to be much higher.

6.2.1.2   5º of Rotary Tool Inclination Angle

In this section, obtained best images for different rotary tool velocities 5º of rotary tool inclination angle are presented. Figure 6-13 shows the image obtained from cutting tests for 5 m/min tool velocity.
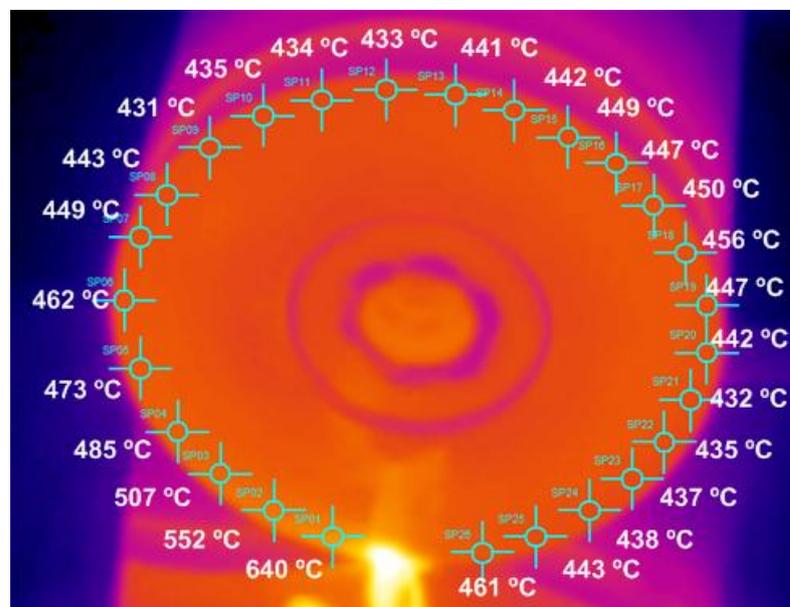
Figure 6-13: Close-up view of thermal image for tool rake face temperature distribution for 5 m/min tool velocity for 5º of rotary tool inclination angle of Ti6Al4V cutting.

Tool rake face temperature distributions for 10 m/min and 20 m/min tool velocities are seen in Figure 6-14.
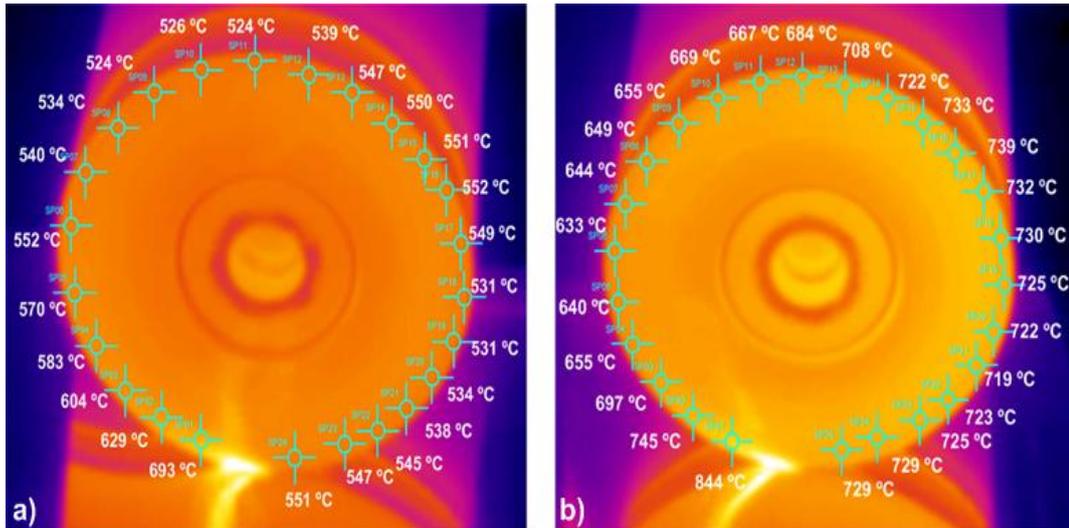
Figure 6-14: Close-up view of thermal image for tool rake face temperature distribution for a) 10 m/min b) 20m/min rotary tool velocity for 5º of tool inclination angle of Ti6Al4V cutting.

When 5° of tool inclination angle is considered, almost similar temperature behaviors are observed with 0° of that. An increase in tool velocity causes higher irregular thermal fluctuations. It is noticed from figures that the effect of tool velocity on process to rise tool temperature during operation.

6.2.1.3 10º of Rotary Tool Inclination Angle

Figure 6-15 shows the image obtained from cutting tests for 5 m/min and 10 m/min tool velocities.
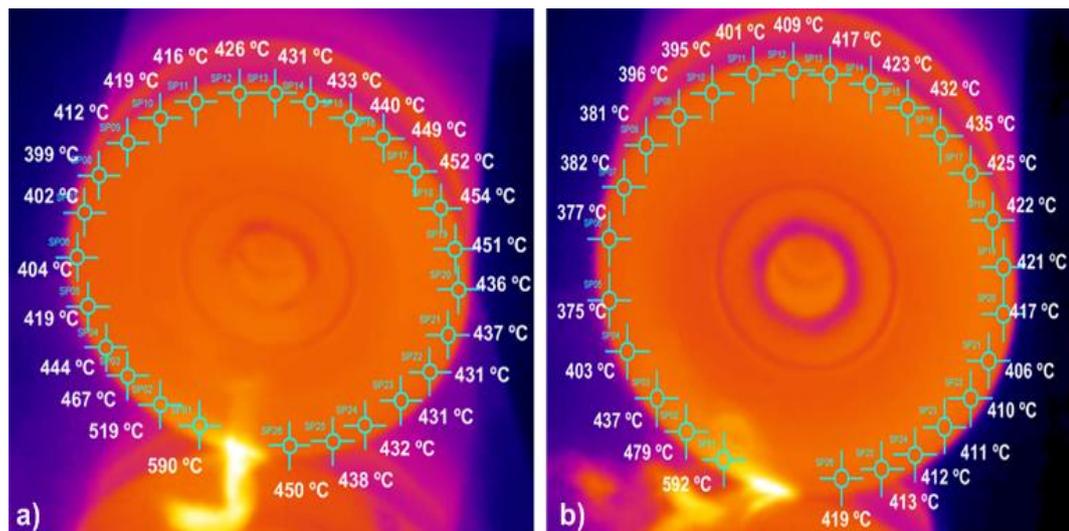
Figure 6-15: Close-up view of thermal image for tool rake face temperature distribution for a) 5 m/min and b) 10 m/min tool velocity for 10º of rotary tool inclination angle of Ti6Al4V cutting.

Close-up views of thermal images obtained from 15 m/min and 20 m/min tool velocities are seen in Figure 6-16.
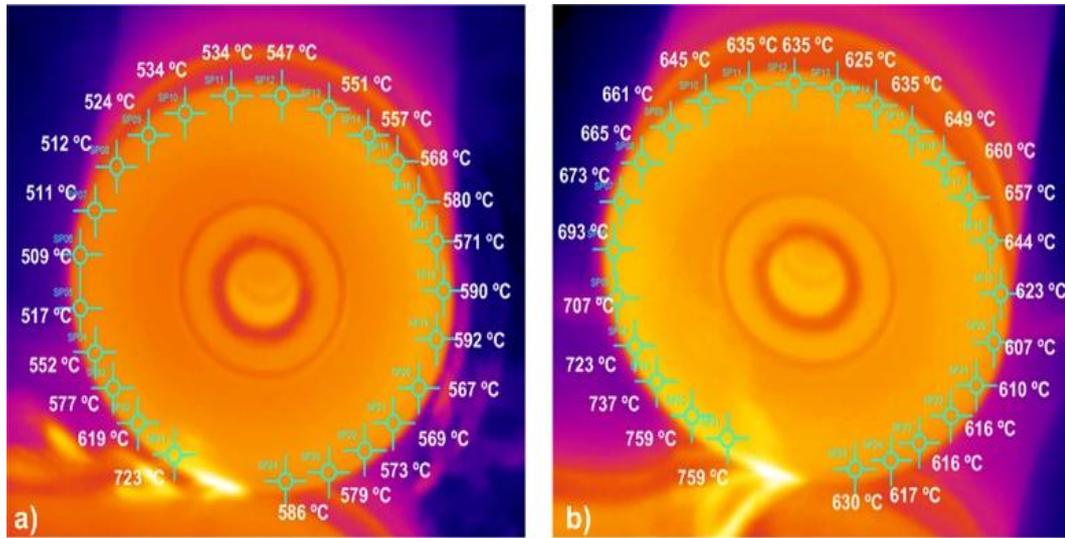
Figure 6-16: Close-up view of thermal image for tool rake face temperature distribution for a) 15 m/min and b) 20 m/min tool velocity for 10º of rotary tool inclination angle of Ti6Al4V cutting.

When temperature distribution on tool cutting edge for 10° of tool inclination angle is examined, irregularity in temperature fluctuation on tool cutting edge seems to be increased. As tool velocity increased, temperature on tool rake face rises. At 10° of tool inclination angle, the amount of change in temperature as tool velocity increases is not high as much as at lower tool inclination angles.

6.2.1.4   15º of Rotary Tool Inclination Angle

In this section, obtained best images for different rotary tool velocities and 15º of rotary tool inclination angle are presented. Figure 6-17 shows the image obtained from cutting tests for 5 m/min and 10 m/min tool velocities.
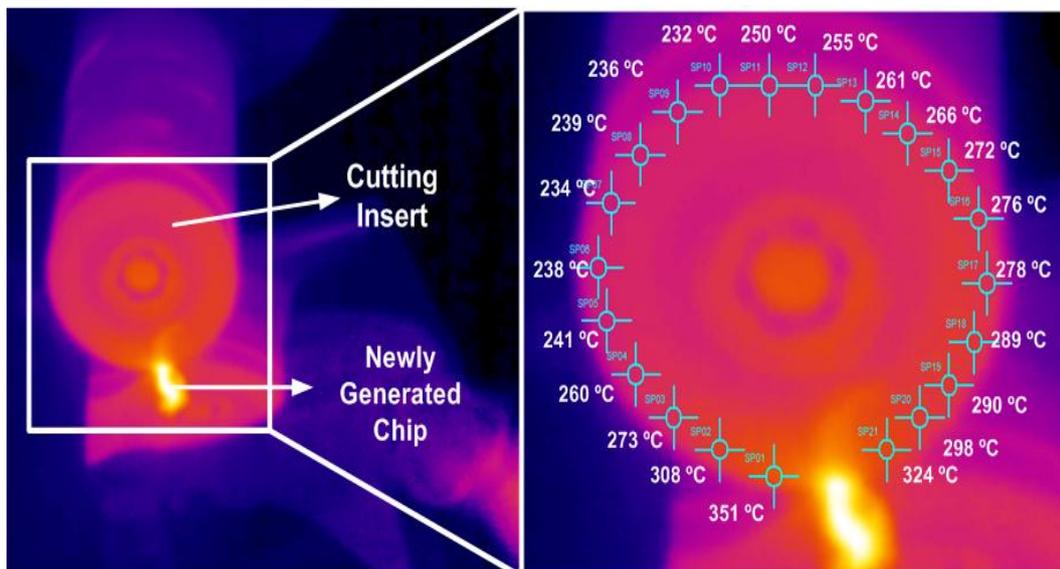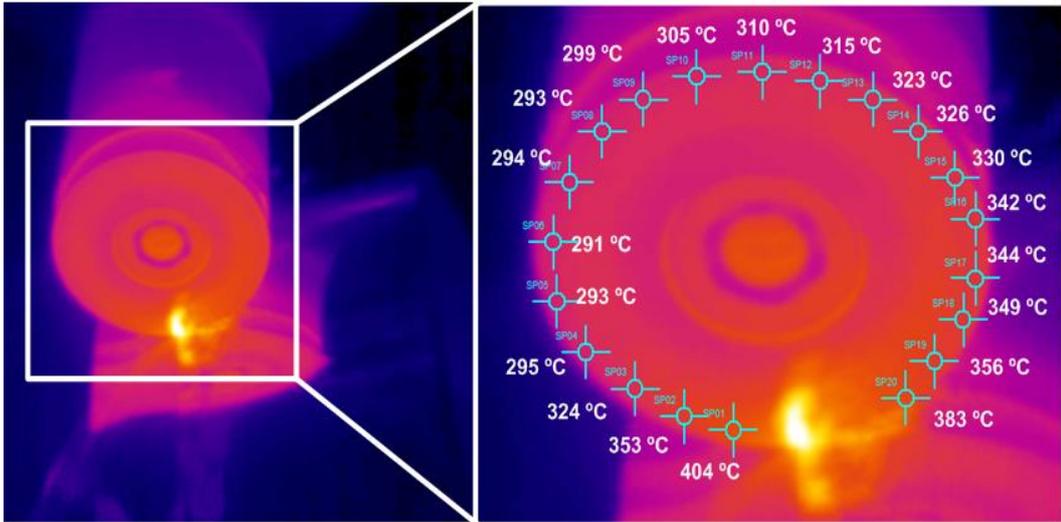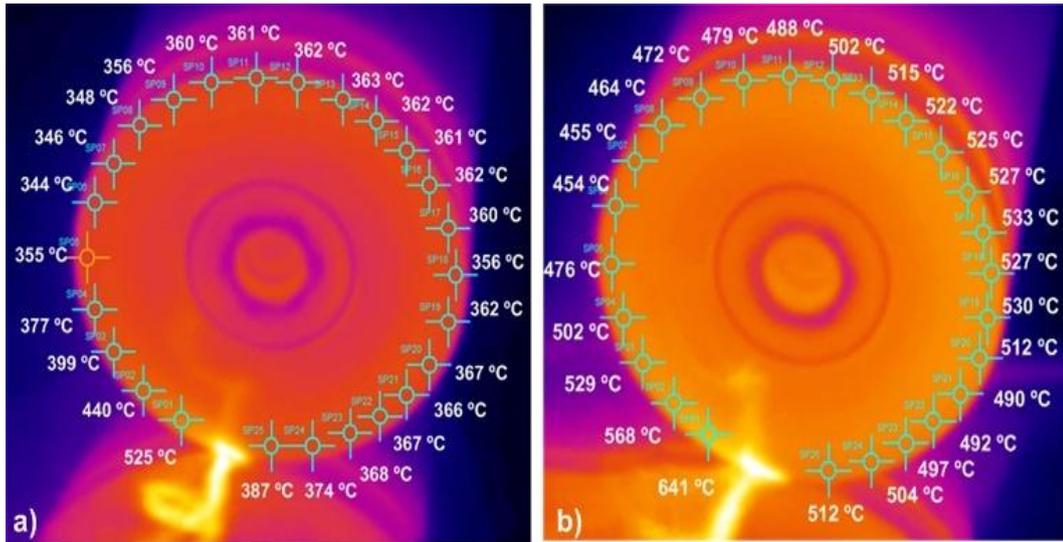
Figure 6-17: Close-up view of thermal image for tool rake face temperature distribution for a) 5 m/min and b) 10 m/min tool velocity for 15º of rotary tool inclination angle of Ti6Al4V cutting.

Close-up views of thermal images obtained from 15 m/min and 20 m/min tool velocities are seen in Figure 6-18.

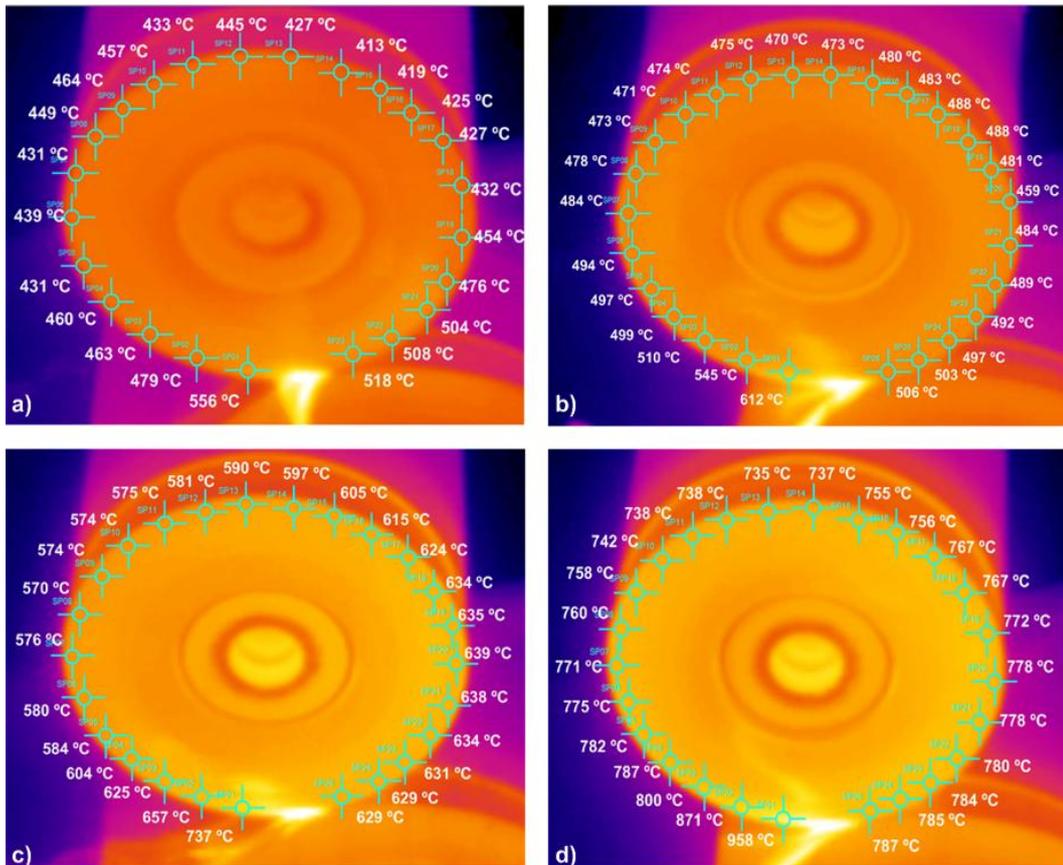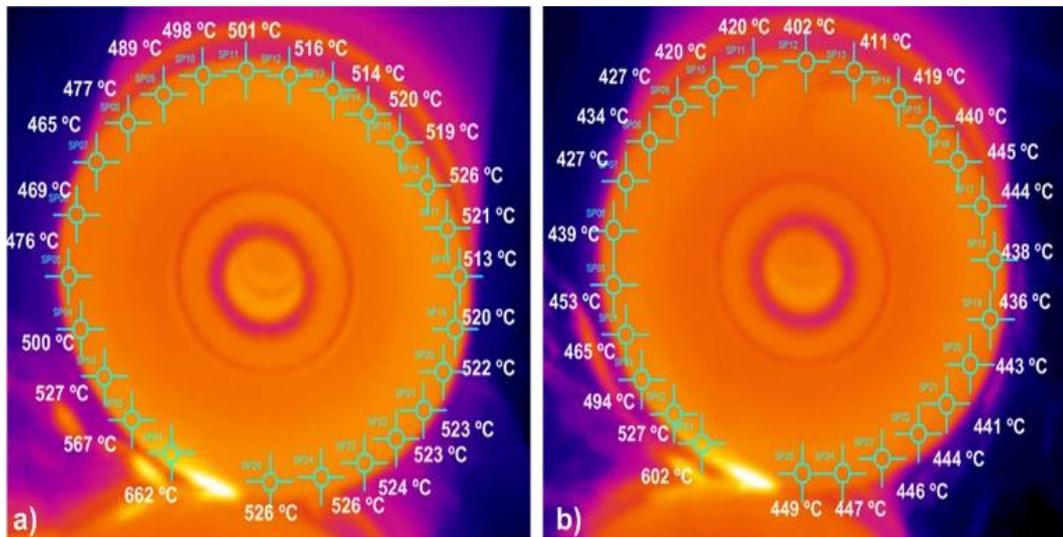Figure 6-18: Close-up view of thermal image for tool rake face temperature distribution for a) 15 m/min and b) 20 m/min tool velocity for 15º of rotary tool inclination angle of Ti6Al4V cutting.

From figures for 15° of tool inclination angle it is easily understood that increasing tool velocity up to 20 m/min causes higher tool temperatures. At 20 m/min tool velocity, almost 10% reduction in temperature is found compared to 15 m/min tool velocity. However, thermal fluctuation on tool cutting edge at that inclination angle shows similar behavior with lower tool inclination angle such that as tool velocity increases, irregularity on thermal fluctuation seems to be rise significantly.

6.2.2   Generated Cutting Temperatures

As in AISI 1050 steel, during cutting tests, the measured temperature is not the generated cutting temperature due to chip preventing of good image. Measured chip temperature is close to generated cutting temperature since chip thickness is very small.

Figure 6-19 presents the generated cutting temperatures for different rotary tool velocities and for different inclination angles of Ti6Al4V.
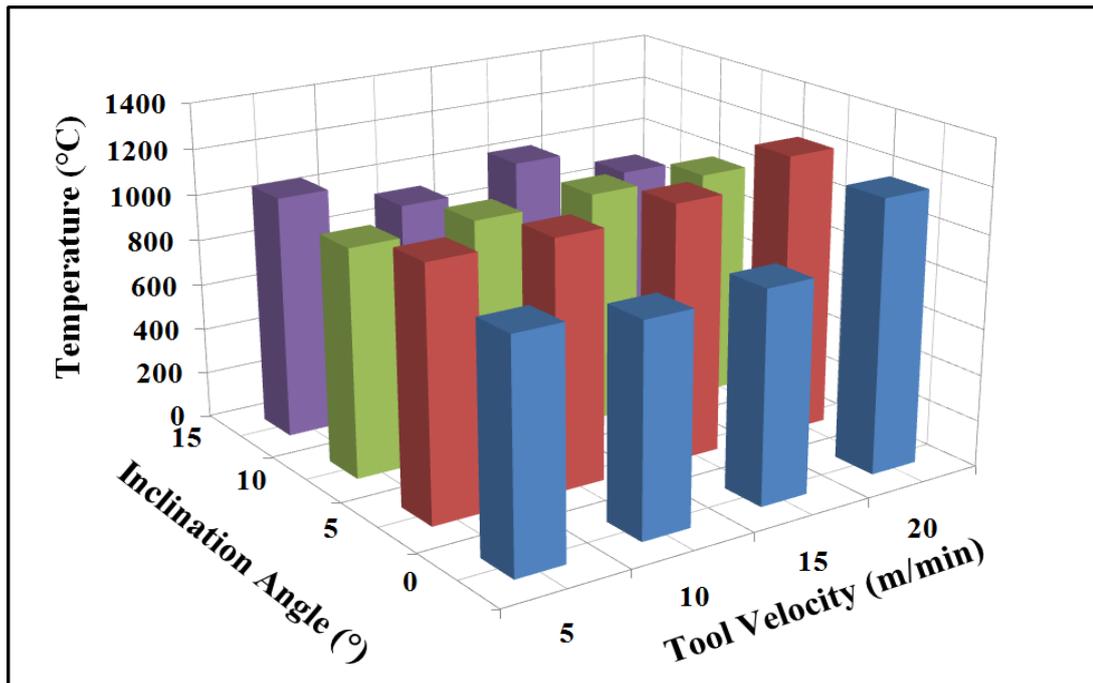
Figure 6-19: Generated cutting temperature variation with tool velocity for 0º, 5°, 10° and 15° tool inclination angles for Ti6Al4V.

Almost similar tool temperature trends are observed for both 0° and 5° inclination angles. Lowest tool temperatures are found at 10 m/min tool velocity for both 0° and 5° inclination angles, then, as tool velocity increases further, temperature seems to be rise gradually. Cutting with 10 m/min provides 27% and 12% reduction in temperature compared to highest temperatures for 0° and 5° of tool inclination angles, respectively. For 10° of tool inclination angle, highest temperatures are attained at 15 m/min tool velocity. Decreasing tool velocity to one third of 15 m/min results in 7% reduction in the generated temperature. When 15° of tool inclination angle results are examined, temperature variation with tool velocity seems to be irregular. When tool rotates at 10 m/min, 13% progress in generated temperatures is achieved compared to 5 m/min tool velocity. Lowest temperatures are found when tool velocity is 20 m/min. at that velocity, improvements in temperature are 4% and 14 % compared to 10 m/min and 15

m/min tool velocities, respectively. From Figure 6-19, it is seen that at 5° of tool inclination angle, all tool velocities result in higher temperatures. Beyond that inclination angle, for 10 m/min and 20 m/min tool velocities, a decreasing trend for cutting temperatures are observed. For 5 m/min tool velocity, 9% and 4% improved cutting temperature results are attained for 10° and 15° of tool inclination angles compared to 5° of tool inclination angle.

6.2.3 Cutting Temperature-Tool Life Relation

The relation between cutting temperature and tool life for Ti6Al4V for different cutting conditions is also examined. Figure 6-20 and Figure 6-21 show the relation between cutting temperatures and tool life for various tool velocities for 0° and 5° inclination angles, respectively.
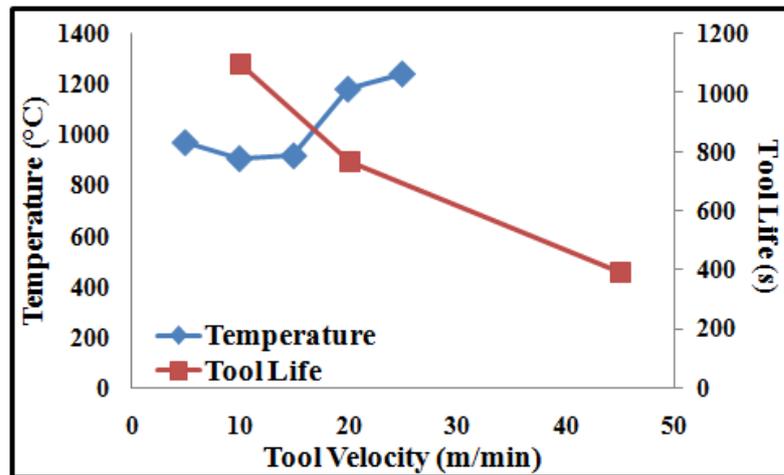
Figure 6-20: Cutting temperature and tool life variation with tool velocity for 0° inclination angle for Ti6Al4V.
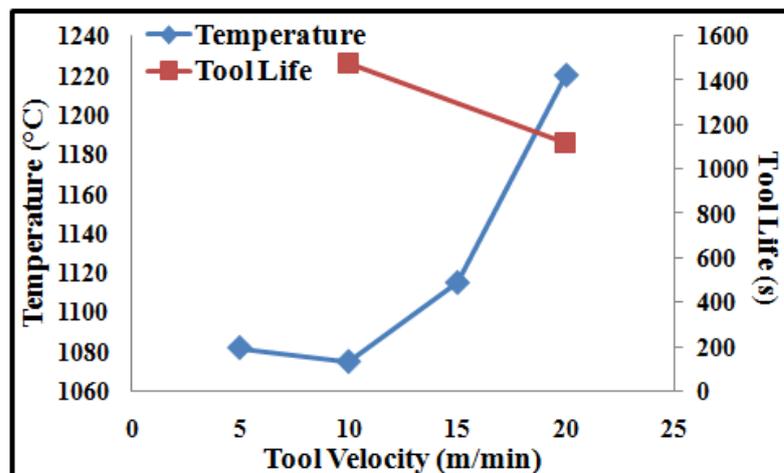
Figure 6-21: Cutting temperature and tool life variation with tool velocity for 5° inclination angle for Ti6Al4V.

All cutting tests for temperature measurement and tool life are conducted under dry cutting conditions. It is seen from figures that at lower cutting temperatures longer tool lives are observed for both inclination angles. Lower cutting temperature suppresses thermally induced wear mechanism and reduces tool wear rate. Generally, as tool velocity increases beyond optimum value, cutting temperatures increase resulting lower tool life. At 0° tool inclination angle and at 10 m/min tool velocity, cutting temperature is measured almost 900°C. When tool velocity is doubled, generated cutting temperature increases up to 1180°C and 30% reduction in tool life is obtained due to high wear rate. Similarly, at 5° inclination angle, increasing tool velocity from 10 m/min to 20 m/min causes 14% increase in cutting temperature and 24% decline in tool life for Ti6Al4V cutting tests.

6.3   Summary

Temperature measurements are done for different materials and for different cutting parameters under dry cutting condition. It seen from results that increasing tool velocity causes an increase in thermal fluctuations on tool rake face. At the same tool velocities, an increase in inclination angle causes reduction in cutting temperatures except lower velocities. At the same inclination angles, the effect of tool velocity is not same for all conditions. For AISI 1050 steel, at low inclination angle, increasing velocity results higher cutting temperatures while at higher inclination angle, moderate tool velocity shows maximum cutting temperature. When Ti6Al4V tests are considered, at lower inclination angles, increasing tool velocity results higher cutting temperatures, yet, at higher inclination angles, fluctuations at cutting temperatures are observed as tool velocity varies.

CHAPTER 7 DISCUSSIONS

In this thesis, conventional turning, SPRT and ADRT cutting tests are conducted for different workpiece materials and cutting conditions. The tool wear, cutting force, surface quality and temperature measurements obtained from cutting tests are given in Chapters 4-6. In this chapter, a comprehensive summary of cutting test results are discussed.

7.1 Conventional Turning and SPRT Cutting Tests

Different workpiece materials with different cutting conditions are used to investigate the performance of SPRT compared to conventional turning tool. For proper comparison in tool life, insert normalization is done on the conventional turning tool. It is found that SPRT process exhibits superior tool life compared to conventional one especially in difficult to cut alloys. For AISI 1050 steel, similar tool life results are observed for SPRT and conventional turning processes in dry cutting conditions. In Waspaloy tests, an improvement of achieved 9 folds in achieved compared to conventional turning in dry cutting conditions. When Ti6Al4V tests are considered, SPRT tool improves tool life 6.5 folds compared to conventional turning tool in dry cutting condition. The effect of coolants on tool life cannot be disregarded. Coolant has positive effect in tool life such that 14 % achievement in tool life compared to dry cutting condition is observed. When coolant and MQL are used in Waspaloy tests, tool life is at least doubled compared to dry cutting condition. In Ti6Al4V tests, 114 μm and 124 μm tool wear are measured after 150 154 minutes cutting with coolant and MQL, respectively, while 153 μm flank wear is observed in 74 seconds in conventional turning tests with using coolant. Uniformly distributed flank wear over entire cutting edge with no crater wear is the main tool deformation mode for SPRT process. In addition to flank wear, crater wear is also observed in conventional turning tests especially for difficult to cut alloys. The prolonged tool life in SPRT is attributed to the use of entire perimeter of circular insert as well as cooling period during cutting. In conventional turning, the same portion of tool is engaged with workpiece while in SPRT, tool rotation provides the fresh portions of the tool continuously to engage the

workpiece. This situation reduces the insert- workpiece contact time for SPRT process, and as a result, heat accumulation at the same portion of tool reduces. This is to say that the generated heat dissipated to all over the circular cutting edge. The work done for chip formation is reduced compared to conventional turning, and furthermore the friction condition on tool rake face is easier. Low cutting temperatures are achieved in SPRT reducing the thermally activated tool wear mechanism on the cutting edge.

When cutting force results are considered, SPRT process provides lower forces compared to conventional turning tool except in radial direction. In SPRT, the reduction in the tangential and feed forces are not less than 17% in all cutting conditions compared to conventional turning process. This reduction is attributed to easier chip shearing with reduced work done resulting in lowered specific cutting energy in SPRT process. Moreover, lower cutting forces are observed due to reduced friction conditions in SPRT process. In SPRT, radial forces are found to be higher than conventional turning. This is because of the rotary motion of the insert which causes changes in the cutting velocity direction due to process kinematics resulting process to be more oblique compared to conventional turning.

After the cutting tests with the SPRT, marks on the surface are analyzed. These are caused by the rotary motion of tool. This motion changes the direction of cutting and the marks on the surface are found to be parallel to this direction. Chip adhesion to workpiece reduces surface quality, too. This can be attributed to the smearing action. Chip swirls around the tool and squeezes between the tool and workpiece. Moreover, in the SPRT process the surface roughness in the circumferential direction is found to be better than conventional turning. Low rigidity is an important problem in the SPRT process as it increases tool run-out and tendency to chatter during cutting. Worse roughness values in feed direction and worse circularity values can be explained by this.

It is seen that at lower cutting velocities, theoretical and experimental tool velocity (rotation speed) results show good agreement. However, when cutting velocity increases the difference between the predicted and measured tool speeds increases. This can be attributed the reduced friction conditions between chip and tool at higher cutting velocities. Moreover, friction in bearing system of rotary shaft is also another factor effecting tool velocity.

7.2   ADRT Cutting Tests

The performance of ADRT process is tested for different workpiece materials and cooling conditions with various tool velocities and inclination angles. When tool inclination angles and cooling conditions are kept constant, it is seen that reduction in tool velocity results longer tool lives in all cutting materials. Tool life is improved at least 2 folds when tool velocity is 50 m/min compared to other tool velocities for every cooling and inclination angles in AISI 1050 steel. When Waspaloy tests are examined, cutting with 10 m/min achieves tool life at least 60% higher compared to other velocities while other cutting conditions are kept constant. The only exception is 20 m/min tool velocity with 0º of tool inclination angle for cutting with coolant. 10m/min and 20 m/min tool velocities show promising results in Ti6Al4V tests. It is obvious from Inconel 718 test results that minimum tool velocity reduces tool wear rate. For instance 35% and 31% improvements in tool life is achieved when tool velocity is 10 m/min compared to 20 m/min in MQL cutting for 0º and 5º of tool inclination angles.

It is also found that when tool velocity and cooling condition are kept constant, increasing tool inclination angle generally results lower tool wear rates and longer tool lives. When AISI 1050 steel tests are considered, at higher tool inclination angles, tool life performance is achieved at least 20% compared to lower ones. However, lower inclination angle tested for 50 m/min and 400 m/min tool velocities for dry cutting condition shows better tool life results compared to higher one. Similar results are observed in Waspaloy tests where higher tool inclination angle provides prolonged tool life. 5º of inclination angle at 10 m/min tool velocity in dry cutting is the only exception to this situation by providing slightly better tool life compared to 15º of that. Similarly, improvement in tool life by increasing tool inclination angle in Ti6Al4V tests is evidential. For example, 15º of inclination angle achieves tool lives 41 %, 72% and 192% compared to 0º of inclination angle for dry, coolant and MQL cutting conditions respectively. Similar results are observed in Inconel 718 tests, too. Increasing inclination angle to 15º improves tool life 93% and 107% for dry and coolant cutting conditions, respectively, for 10 m/min tool velocity. However, increasing inclination angle to 5º does not have considerable effect such that only 5% and 4% improvements are achieved in tool life for coolant and MQL conditions, respectively.

As expected, coolant and MQL generally show promising tool life results in cutting tests especially in difficult to cut alloys. In Waspaloy, at 10 m/min tool velocity, dry cutting improves tool life at least 11% compared to coolants in 0º and 5º of tool inclination angles. Interestingly, dry cutting condition provides longer tool lives in all cutting conditions in AISI 1050 steel.

It is essential to discuss the material machinability for the same cutting conditions. Figure 7-1, Figure 7-2 and Figure 7-3 show some examples for Waspaloy, Ti6Al4V and Inconel 718 tests for various conditions.
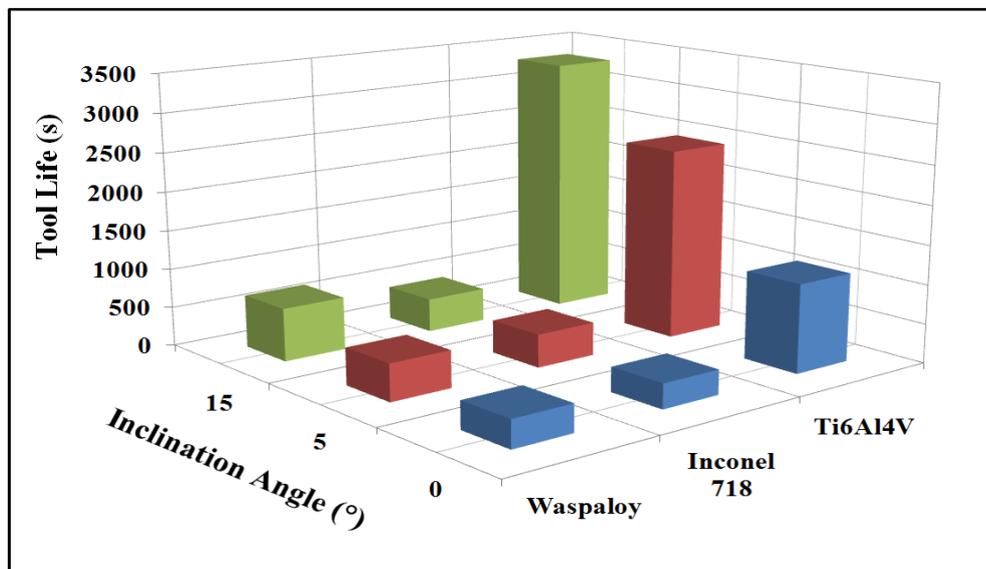
Figure 7-1: Tool life variation with different rotary tool inclination angles for 10 m/min rotary tool velocity for MQL cutting of Waspaloy, Ti6Al4V and Inconel 718.
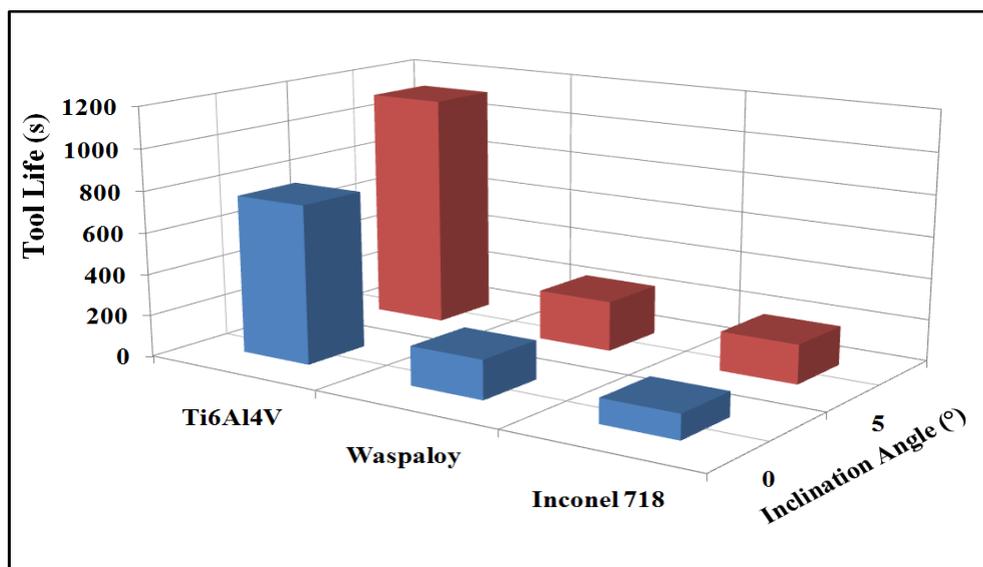
Figure 7-2: Tool life variation with different rotary tool inclination angles for 20 m/min rotary tool velocity for dry cutting of Waspaloy, Ti6Al4V and Inconel 718.
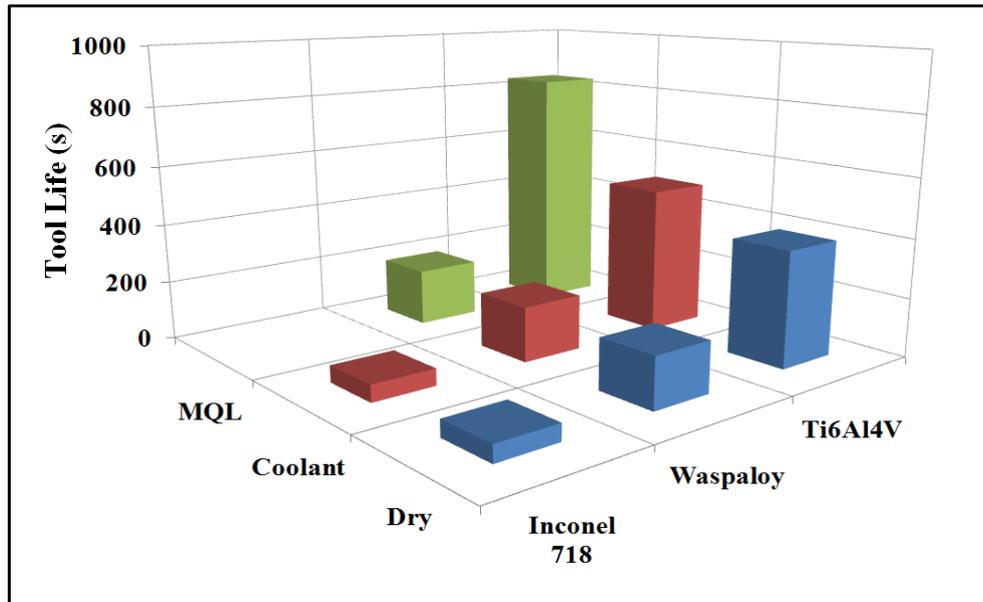
Figure 7-3: Tool life variation with different cooling conditions for 45 m/min tool velocity for 0° inclination angle of Waspaloy, Ti6Al4V and Inconel 718 cutting.

It is seen from figures that machinability of Ti6Al4V is better compared to nickel-base alloys in all conditions. Although thermal properties of Ti6Al4V is limited compared to nickel-base alloys, owing to lower mechanical properties, chip formation is easier compared to nickel-base alloys resulting longer tool lives. Moreover, hard carbide particles in microstructure of nickel-base alloys results higher tool wear rates. Lower tool velocities should be selected for prolonged tool life. Increasing inclination angle is effective in all testing materials. Coolants and MQL generally improves tool performance during cutting.

When the surface quality of machined parts is examined it is found that marks on the surface are in the direction close to effective cutting velocity owing to tool rotational motion. Cutting at 0° of tool inclination angle shows better results in both feed and circumferential directions compared to 5° of that except 125 m/min tool velocity. The change in tool velocity has little effect on surface quality in feed direction at 5° of tool inclination angle. On the other hand, at 0° of inclination angle, as tool velocity increases, the roughness in feed direction increases up to 3.2 μm at 125 m/min. In circumferential direction, an increase in tool velocity deteriorates surface quality for both tool inclination angles. Increasing tool velocity up to 150 m/min results 1.99 μm in surface roughness for 5° of tool inclination angle. On the other hand, at 0° of tool inclination angle, surface roughness rises gradually up to 125 m/min tool velocity then for further velocities it starts to decrease. When circularity of machined workpiece is

taken into consideration, it is seen that 5º of tool inclination angle shows better results than 0º of that. At 0º of tool inclination angle, as tool velocity increase, circularity reduces from 61.33 μm to 18.5 μm at 100 m/min then rises up to 54.5 μm at 150 m/min tool velocity. At 5º of inclination angle, except 50 m/min, the trend of circularity tend to decrease as tool velocity increases up to 125 m/min.

SEM images show that uniformly distributed flank wear with no crater wear is observed in ADRT tools for all testing materials. Higher rate of material adhesion to worn area is observed in dry cutting of Waspaloy tests. In Ti6Al4V tests, little or no material adhesion is observed such that especially in MQL condition, almost clear worn land is seen. In Inconel 718 tests, the effect of inclination angle is examined and deposited material is observed in all cases. However, due to different inclination angles, various adhesion directions are observed for all cases.

7.3   Comparison of Different Inserts

In this part, the different insert performances on machinability of difficult to cut alloys are examined. The Insert-1, used in SPRT tests, and Insert-2, used in ADRT tests are compared for tool wear behaviors. Coolant and MQL conditions with two different inclination angles are tested for Waspaloy, Ti6Al4V and Inconel 718 alloys.

Figure 7-4: Tool flank wear comparisons for two different inserts for Waspaloy for a) coolant cutting b) MQL cutting.

Figure 7-5: Tool flank wear comparisons for two different inserts for Ti6Al4V for a) coolant cutting b) MQL cutting.
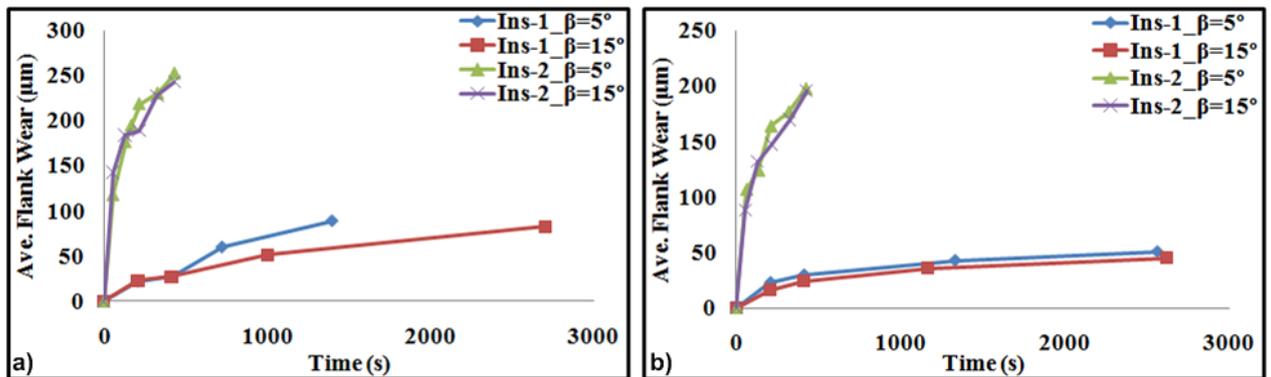
Figure 7-6: Tool flank wear comparisons for two different inserts for Inconel 718 for a) coolant cutting b) MQL cutting.

It is seen that Insert-1, used in SPRT tests, exhibits better tool wear results than Insert-2, used in ADRT tests, in all testing materials and cutting conditions. Increasing tool inclination angle has positive effect on Insert-1 tool life as expected. The considerable difference between tool wear rates can be explained by the different coating types of inserts. Insert-1 has a special coating called Alcrona has superior hot hardness and oxidation resistance compared to conventional coating types. Moreover, the diameter of Insert-1 (27 mm) is larger than Insert-2 (25mm) but this situation is not effective as the influence of coating type.

7.4 Comparison of SPRT and ADRT

ADRT process is more flexible compared to SPRT process such that tool inclination angle and tool velocity can be arranged by user. On the other hand, it would be worthless unless this flexibility has an advantage on SPRT process concerning machinability and productivity of alloys. In this purpose, the performance comparison of SPRT and ADRT is very essential. For proper comparison, same insert, MU23-

PN1.5A is used for both processes. Waspaloy and Ti6Al4V alloys are tested for coolant and MQL conditions. The results are shown in Figure 7-7 and Figure 7-8.
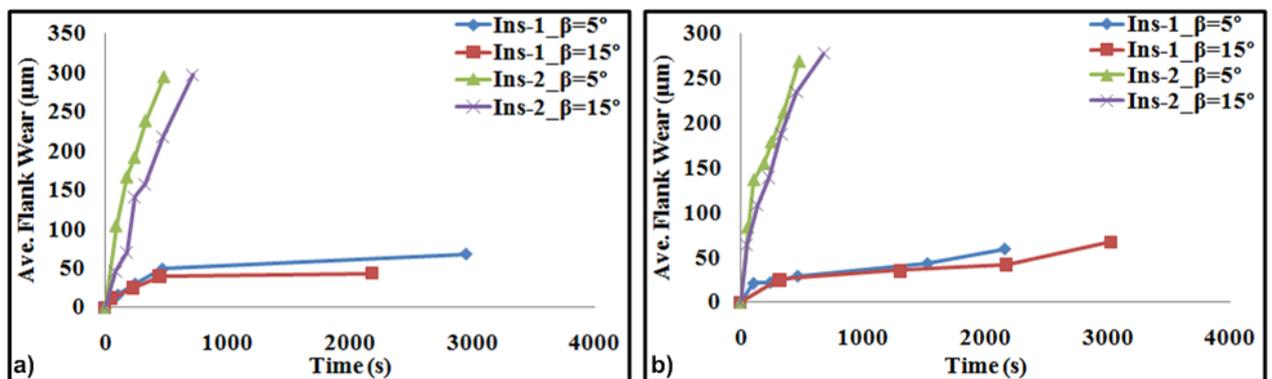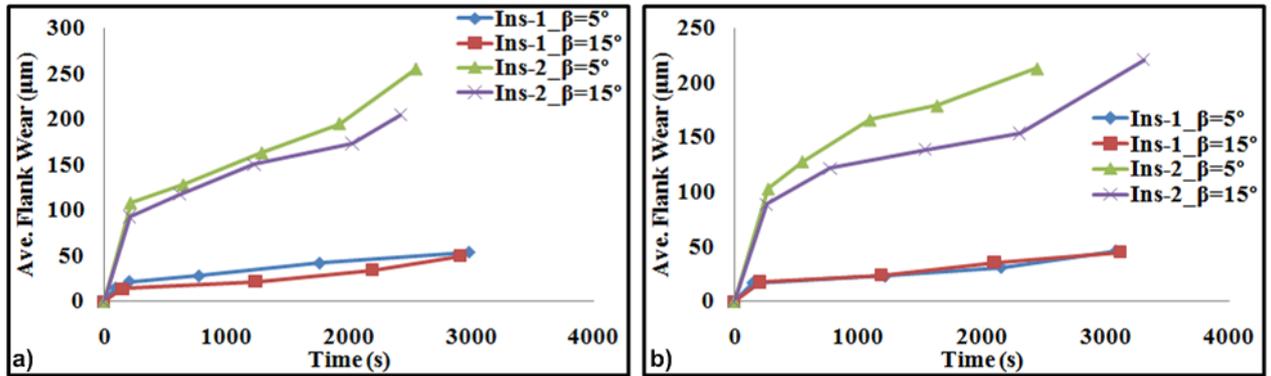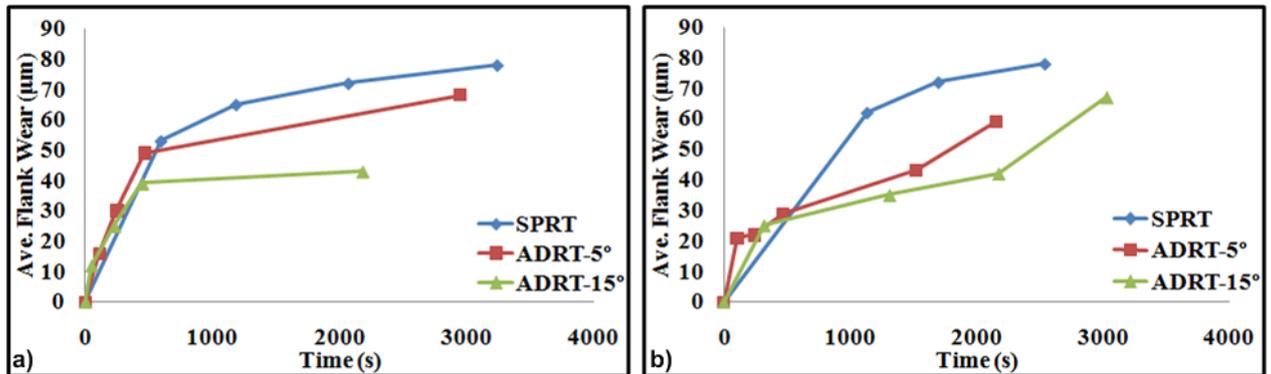

Figure 7-7: Tool flank wear comparisons of SPRT and ADRT for Waspaloy for a) coolant cutting b) MQL cutting.
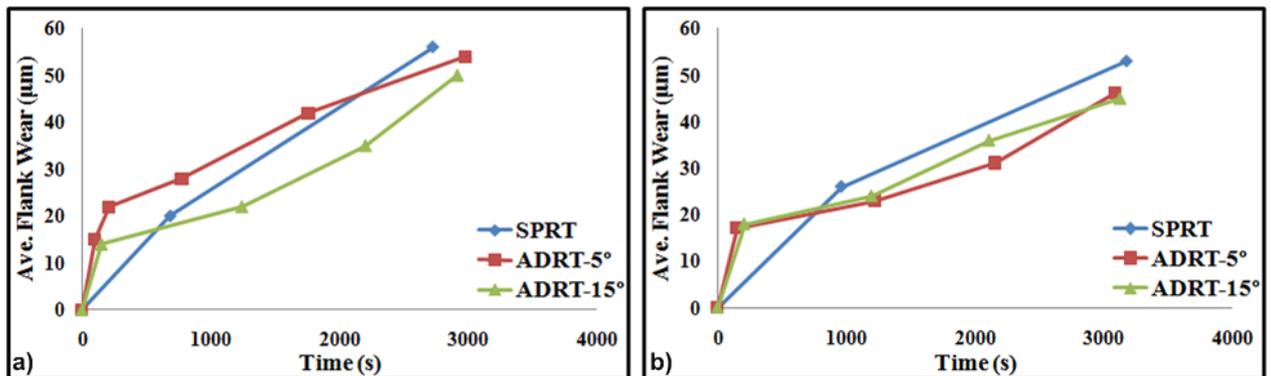
Figure 7-8: Tool flank wear comparisons of SPRT and ADRT for Ti6Al4V for a) coolant cutting b) MQL cutting.

It should be mentioned that tool velocities are 9.5 m/min and 10 m/min for SPRT and ADRT processes, respectively. It is seen from graphs that ADRT gives better tool lives than SPRT for Waspaloy for both inclination angles and for both cooling conditions. Increasing tool inclination angle also improves tool life in ADRT. When Ti6Al4V results are considered, ADRT exhibits slightly better tool lives for both inclination angles for MQL cutting. For coolant cutting, similar tool wear rates are observed for both processes. This can be attributed the low supporting rigidity of SPRT process. Lower rigidity of SPRT tool can cause chatter resulting higher tool wear rate and chipping of insert.

7.5 Temperature Measurements

Temperature measurements are conducted for two different materials and for various cutting conditions. It is seen that as tool inclination angle is constant and the tool velocity increases, the tool temperature tends to increase for all inclination angles and for all testing materials. Fluctuations on tool rake face become irregular when tool velocity increases. It can be explained by the change in convection conditions of air on tool rake face during cutting and change in the cooling time contact zone of insert due to change in tool velocity.

Optimum tool velocities for minimum generated temperatures are observed in some cases such that 0º of inclination angle of AISI 1050 steel and Ti6Al4V. At velocities lower than optimum one higher temperature is attained mainly owing to longer contact time between the tool engagement zone and workpiece. On the other hand, further increase in tool velocity results higher temperatures due to shortened cooling time of this intermittent cutting process. Apart from these cases, increasing tool velocity results in higher temperatures except at 15º of tool inclination angle for Ti6Al4V. It is also seen that increasing tool inclination angle generally suppresses the temperature rise. Increasing inclination angle from 0º to 5º, in AISI 1050 steel, causes 4% and 18% reduction in temperatures. When Ti6Al4V is considered, 5º of tool inclination angle presents higher temperatures. Further increase in inclination angle results lower temperatures.

7.6 Summary

In this chapter, all cutting tests results are examined. In addition to concluded results of previous sections, this chapter brings some conclusions. Ti6Al4V shows superior machinability in all cutting conditions compared to nickel-base alloys due to lower mechanical properties. Moreover, it is found that coating type of insert has a great influence on tool wear rate. Increasing hot hardness and oxidation resistance of insert lowers tool wear rate. When ADRT and SPRT are considered using the same insert and keeping other cutting parameters constant, ADRT is found to have low wear rate for all testing materials and cooling conditions compared to SPRT. This is mainly due to rigidity of SPRT tool.

CHAPTER 8 CONCLUSIONS

The objective of this thesis is to understand the performance of rotary turning processes on especially difficult to cut alloys with different cutting parameters and cooling conditions. As an important indication of the performance, tool wear measurements are done at varying time intervals where VB=0.2 mm is considered as the end of tool life criteria. In addition, cutting forces in three directions are measured in these tests. Furthermore, surface roughness and circularity of machined workpiece are examined. Temperature distributions on tool rake face for various materials are also analyzed using a thermal camera.

Based on the results obtained from the cutting tests, some conclusions are derived and listed below.

- The development of tool wear of SPRT is lower than conventional turning for difficult to cut alloys due to effective self-cooling of rotary tool.
- Coolant and MQL improve tool life in both conventional and SPRT process owing to effective heat removal from the cutting zone in addition to the lubrication effects.
- Lower cutting forces in tangential and feed direction are observed in SPRT compared to conventional turning due to increased effective rake angle and oblique angle reducing cutting energy.
- Machined surface marks are found to be at an angle to feed direction in SPRT.
- SPRT deteriorates surface quality in feed direction. Also, slightly worse circularity results are observed in SPRT compared to conventional turning.
- There is an optimum tool velocity minimizing tool wear rate and cutting temperatures in ADRT. The velocities apart from this optimum one results higher wear rates and cutting temperatures.
- At high tool inclination angles, ADRT shows better performance in tool life for every tested material.
- Coolant and MQL show promising results for difficult to cut alloys while dry cutting is the best choice for AISI 1050 steel for ADRT process.

- SEM images show that material adhesion is observed on worn land of the flank face in most cases of ADRT. High rate of material deposition is found at dry cutting for difficult to cut alloys.

- At 0° tool inclination angle, increasing tool velocity deteriorates surface roughness in both feed and circumferential direction. At 5° tool inclination angle, change in tool velocity does not have any significant effect on roughness in feed direction. However, in circumferential direction, increasing tool velocity deteriorates surface quality.

- Higher tool inclination angle shows better circularity of workpiece in ADRT. There is an optimum tool velocity, 125 m/min, beyond that circularity of part begins to deteriorate.

- Increasing tool velocity in ADRT, causes irregular thermal fluctuations on tool rake face. Moreover, increasing tool velocity results in higher generated temperatures during cutting.

- Increasing tool inclination angle results lower temperatures except low tool velocities.

8.1   Suggestion for Rotary Turning Applications

The rigidity of SPRT tool should be increased. It reduces process chatter preventing chipping on cutting edge and surface deterioration. Cutting with coolant and MQL should be preferable for removing heat from cutting zone for SPRT. Optimum tool velocity should be selected for ADRT process to provide longer tool life and lowering thermal fluctuations on tool rake face. Tool inclination angle should be increases as much as possible without exposing to chatter for increasing tool life. For better surface quality, lower tool inclination angle with lower tool velocity should be selected, but it should be keep in mind that lowering inclination angle causes worse workpiece circularity. As a result, higher inclination angles could be used for roughing operations. Coolant and MQL should be used during cutting for difficult to machine materials while dry cutting is the best option for AISI 1050 steel.

8.2   Original Contributions of the Thesis

For SPRT process, due to lots of studies in literature about tool life, component forces and surface quality, showing the increment in machinability of one of the difficult to

alloys, Waspaloy, with using SPRT for various conditions with prolonged tool life and lowered component forces is one of the additive features of this thesis. Contributions of this thesis to ADRT are more essential than that of SPRT. The effects of tool inclination angle and tool velocity on tool life, surface quality and circularity of workpiece are investigated for various difficult to cut alloys and various cooling conditions. In addition, better thermal images of ADRT tool are observed with thermal fluctuation on tool rake face using thermal camera. Furthermore, the result of the performance comparison of SPRT and ADRT for the same workpieces and for the same cutting conditions is another implication of thesis.

8.3   Future Work

As a future work, more rigid and stiff SPRT and ADRT tools can be designed and produced as chatter stability is one of the most important limiting factors for rotary turning. The cutting parameters such as cutting velocity, feed rate and depth of cut which are kept constant during cutting tests would be changed for further tests in order to see their effects on performance of process. The performance of rotary turning would be tried on other difficult to machine materials such as cobalt-base alloys, structural ceramics, composite materials and hardened steels. In addition to tool inclination angle, tool offset height with respect to workpiece axis can be incorporated in order to evaluate performance of process for various conditions for further studies. Various cooling systems like cryogenic cooling and CO_2 spray cooling could be tried for rotary processes. Modeling of tool temperature can be another issue in order to understand the mechanism behind rotary tool wear. Correlation of model results with tool rake face temperature measurement results would be useful for optimization process. A proper set-up for thermal camera could be produced to see only the cutting insert rake face temperature without influenced from environmental effects. The results which are obtained from these long tests will be used to create a database for future works.

REFERENCES

[1] Ezugwu, E.O., Wang, Z.M., 1997, Titanium Alloys and Their Machinability - A Review, Journal of Materials Processing Technology, 68, 262-274.

[2] Ezugwu, E.O., Wang, Z.M., 1999, The Machinability of Nickel-Based Alloys: A Review, Journal of Materials Processing Technology, 86, 1-16.

[3] Che-Haron, C.H., 2001, Tool Life and Surface Integrity in Turning Titanium Alloy, Journal of Materials Processing Technology, 118, 231-237.

[4] Nabhani, F., 2001, Machining of Aerospace Titanium Alloys, Robotics and Computer Integrated Manufacturing, 17, 99-106.

[5] Choudhury, I.A., El-Baradie, M.A., 1998, Machinability of Nickel-Base Super Alloys: A General Review, Journal of Materials Processing Technology, 77, 278-284.

[6] Costes, J.P., Guillet, Y., Poulachon, G., Dessoly, M., 2007, Tool Life and Wear Mechanism of CBN Tools in Machining of Inconel 718, International Journal of Machine Tools & Manufacture, 47, 1081-1087.

[7] Zoya, Z.A., Krishnamurthy, R., 2000, The Performance of CBN Tools in the Machining of Titanium Alloys, Journal of Materials Processing Technology, 100, 80-86.

[8] Rahman, M., Seah, W.K.H., Teo, T.T., 1997, The Machinability of Inconel 718, Journal of Materials Processing, 63, 199-204.

[9] Kamata, Y., Obikawa,T., 2007, High Speed MQL Finish-Turning of Inconel 718 with Different Coated Tools, Journal of Materials Processing Technology, 192-193, 281-286.

[10] Hong, S.Y., Markus, I. Jeong, W.C., 2001, New Cooling Approach and Tool Life Improvement in Cryogenic Machining of Titanium Allay- Ti-6Al-4V, International Journal of Machine Tools & Manufacture, 41, 2245-2260.

[11] Shaw, M.C., Smith, P.A., Cook, N.H., 1952, The Rotary Cutting Tool, Transaction of ASME, 74, 1065-1076.

[12] Armarego, E.J.A., Karri, V., Smith, A.J.R., 1994, Fundamental Studies of Driven and Self-Propelled Rotary Tool Cutting Processes-1: Theoretical Investigation, International Journal of Machine Tool and Manufacture, 34/6, 785-801.

[13] Armarego, E.J.A., Karri, V., Smith, A.J.R., 1994, Fundamental Studies of Driven and Self-Propelled Rotary Tool Cutting Processes-2: Experimental Investigation, International Journal of Machine Tool and Manufacture, 34/6, 803-815.

[14] Venuvinod, P.K., Lau, W.S., Reddy, P.N., 1981, Some Investigations into Machining with Driven Rotary Tools, Journal of Engineering for Industry, 103, 469-477.

[15] Venuvinod, P.K., Rubenstein, C., 1983, The Principle of Equivalent Obliquity and its Application to Rotary Turning, CIRP Annals-Manufacturing Technology, 32/1, 53-58.

[16] Choi, G.I.H., Dornfeld, D., 1990, Analytical Predictions of Rotary Cutting Processes, Transactions of NAMRI/SME, 146-153.

[17] Armarego, E.J.A., Katta, R.K., 1997, Predictive Cutting Model for Forces and Power in Self-Propelled Rotary Tool Turning Operations, Annals of the CIRO, 46/1, 19-24.

[18] Li, L., Kishawy, H.A., 2006, A Model for Cutting Forces Generated During Machining with Self-Propelled Rotary Tools, International Journal of Machine Tools and Manufacture, 46, 1388-1394.

[19] Hao, W., Zhu, X., Li, X., Turyagyenda, G., 2006, Prediction of Cutting Force for Self-Propelled Rotary Tool using Artificial Neural Networks, Journal of Materials Processing Technology, 180, 23-29.

[20] Kishawy, H.A., Li,L., El-Wahab, E.L., 2006, Prediction of Chip Flow Direction During Machining with Self-Propelled Rotary Tools, International Journal of Machine Tool & Manufacture, 46, 1680-1688.

[21] Chang, X., Chen, W., Pang X., Zhong G., 1995, Selection of cutting regime for self-propelled rotary cutting tools, Procedings of the Institution of Mechanical Engineers, Part B, 209(B1), 63-66.

[22] Harun, S., Shibasaka, T., Moriwaki, T., 2008, Cutting Mechanics of Turning with Actively Driven Rotary Tool, Journal of Advanced Mechanical Design, Systems and Manufacturing, 214, 579-586.

[23] Kishawy, H.A., Pang, L., Balazinski, M., 2011, Modeling of Tool Wear during Hard Turning with Self-Propelled Rotary Tools, International Journal of Material Sciences, 53, 1015-1021.

[24] Joshi, S.S., Ramakrishnan, N., Nagarwalla, H.E., Ramakrishnan, P., 1999, Wear of Rotary Carbide Tools in Machining of Al/SiCp Composites, Wear, 230, 124-132.

[25] Chen, P., 1992, High Performance Machining of SiC Whisker-Reinforced Aluminium Composite by Self-Propelled Rotary Tools, Annals of the CIRP, 41/1, 59-62.

[26] Wang, M., Ezugwu, E.O., Gupta, A., 1998, Evaluation of a Self-Propelled Rotary Tool in the Machining of Aerospace Materials, Tribology Transactions, 41/2, 289-295.

[27] Ezugwu, E.O., Olajire, K.A., Wang, Z.M., 2002, Wear Evaluation of a Self-Propelled Rotary Tool When Machining Titanium Alloy IMI 318, Proceedings of the Institution of Mechanical Engineers, Part b: Journal of Engineering Manufacture, 216, 891-897.

[28] Kuroda, M., Myoji, T., Itani, H., Itakura, K., 2000, Improvement of Cutting Efficiency by Rotary Tool, Mitsubishi Heavy Industries Ltd. Technical Review, 37/1, 24-28.

[29]Manna, A., Bhattacharyya, B., 2002, A Study on Different Tooling Systems during Machining of Al/SiC-MMC, Journal of Materials Processing Technology, 123, 476-482.

[30] Kishawy, H.A. Becze, C.E., McIntosh, D.G., 2004, Tool Performance and Attainable Surface Quality During the Machining of Aerospace Alloys using Self-Propelled Rotary Tools, Journal of Processing Technology, 152, 266-271.

[31] Ezugwu, E.O., 2007, Improvements in the Machining of Aero-Engine Alloys using Self-Propelled Tooling Technique, Journal of Materials Processing Technology, 185, 60-71.

[32] Kossokowska, J., Jemielniak, K., 2012, Application of Self-Propelled Rotary Tools for Turning of Difficult to Machine Materials, Procedia CIRP 1, 425-430.

[33] Lei, S., Liu, W., 2002, High Speed Machining of Titanium Alloys using the Driven Rotary Tool, International Machine Tools & Manufacture, 42, 653-661.

[34] Nakajima, H., Kato, A., Sasahara, H., Yamamoto, H., Muraki, T., Tsutsumi, M., 2008, Effect of Rotary Cutting Tool Posture on Machining Performance utilizing Multi-Tasking Lathe, Journal of Advanced Mechanical Design, Systems and Manufacturing, 2/4, 532-539.

[35] Hosokawa, A., Ueda, T., Onishi, R., Tanaka, R., Furumoto, T., 2010, Turning of Difficult to Machine Materials with Actively Driven Rotary Tool, CIRP Annals - Manufacturing Technology, 59, 89-92.

[36] Chen, P., 1992, Cutting Temperatures and Forces in Machining of High-Performance Materials with Self-Propelled Rotary Tool, The Japan Society of Mechanical Engineers, 35/1, 180-185.

[37] Dessoly, V., Melkote, S.N., Lescalier, C., 2004, Modeling and Verification of Cutting Tool Temperatures in Rotary Tool Turning of Hardened Steel, International Journal of Machine Tools and Manufacture, 44, 1463-1470.

[38] Sasahara, H., Satake, K., Nakajima, H., Yamamoto, H., Muraki, T., Tsutsumi, M., 2008, High-Speed Rotary Cutting of Difficult to Cut Materials on Multi Tasking Lathe, International Journal of Machine Tools and Manufacture, 48, 841-850.

[39] Harun, S., Shibasaka, T., Moriwaki, t., 2009, Cutting Temperature Measurement in Turning with Actively Driven Rotary Tool, Key Engineering Materials, 389, 138-143.

[40] Yamamoto, H., Sataki, K., Narita, T., Sasahara, H., Tsutsumi, M., Muraki, T., 2010, Thermal Behavior and Chip Formation on Rotary Cutting of Difficult to Cut Materials Utilizing Multi Tasking Lathe and MQL, Key Engineering Materials, 447-448, 806-810.